

**UNIVERSITÀ DEGLI STUDI DI PADOVA**  
**Dipartimento Ingegneria Civile Edile ed Ambientale**

**Master's Degree Thesis in**  
**Environmental Engineering**

**THE SCROVEGNI CHAPEL IN PADUA:  
FLOODING CAUSES AND  
COUNTERMEASURES**

***Supervisor: Prof. Paolo Salandin***

***Graduate student: Valentina Scarpa Bandelloni***

ACADEMIC YEAR 2014/2015



# Contents

1. Introduction: brief history of Scrovegni Chapel structure.....	6
2. Status of the Cenobio .....	13
3. Suggested countermeasures .....	19
4. S.W.M.M.: Storm Water Management Model.....	38
4.1 Software .....	38
4.2 Short description of the SWMM blocks.....	41
4.3 Structure and operation of hydraulic routine .....	43
4.3.1 Fundamental equations of SWMM code .....	43
4.3.2 Flow Routing .....	45
4.3.2.1 Steady Flow Routing.....	46
4.3.2.2 Kinematic Wave Routing .....	46
4.3.2.3 Dynamic Wave Routing.....	47
4.4 Schematization of the drainage area .....	47
4.5 Hydrological elements.....	50
4.5.1 Subcatchments description.....	50
4.5.2 Rainfall representation .....	51
4.5.3 Surface runoff.....	52
4.5.4 Hydrological losses .....	53
4.5.5 Infiltration.....	53
4.5.5.1 Green-Ampt method.....	54
4.5.5.2 SCS method .....	55
4.5.5.3 Horton method .....	57
5. Rainfall characterization.....	60
5.1 Comparison of historical rainfall data of Padua .....	61
5.2 Analysis of data .....	64
5.2.1 Analysis of 1 hour precipitations.....	66
5.2.2 Analysis of 3 hours precipitations .....	69
5.2.3 Analysis of 6 hours precipitations .....	70

5.2.4	Analysis of 12 hours precipitations .....	71
5.3	Validation of results.....	72
5.4	Extraction of pluviometric possibility curve .....	73
5.4.1	Pluviometric curve for TR = 5 years.....	74
5.4.2	Pluviometric curve for TR = 10 years.....	74
5.4.3	Pluviometric curve for TR = 20 years.....	75
5.4.4	Pluviometric curve for TR = 50 years.....	75
5.4.5	Pluviometric curve for TR = 100 years .....	76
5.5	Rainfall analysis results.....	76
6.	Preliminary design of the network with rational method .....	79
6.1	Description of method.....	79
6.2	Design of the network.....	82
7.	S.W.M.M. analysis.....	86
7.1	Rainfall event design .....	93
7.1.1	Constant intensity rain of project .....	97
7.1.2	Sifalda rain of project .....	98
7.1.3	Chicago rain of project.....	99
8.	S.W.M.M. results.....	102
8.1	Nodes analysis.....	102
8.2	Links analysis .....	104
8.3	Subcatchments analysis .....	10600
8.4	Graphical elaboration.....	109
8.5	Museum confluence analysis.....	113
8.6	Graphical elaboration.....	116
8.7	Return period of 20 years.....	120
9.	CONCLUSIONS .....	124
	ANNEX I – Rainfall data.....	125
	ANNEX II - Rainfall data analysis .....	129
	ANNEX III - Rainfall-intensity curves.....	133
	ANNEX IV - Pearson test .....	136



BIBLIOGRAPHY ..... 138

# 1. Introduction: brief history of Scrovegni Chapel structure

The Scrovegni Chapel was dedicated to St. Mary of Charity, was painted between 1303 and 1305 by Giotto, who was commissioned by the wealthy banker Enrico Scrovegni in Padua, who erected the chapel for the benefit of his family and the entire population of the city.

Enrico Scrovegni, in February 1300 purchased the entire area of the ancient Roman arena of Padua and there erected a sumptuous palace, of which the chapel was the private oratory and future family mausoleum.

Dante placed the father of Enrico Scrovegni, Rainaldo, among the damned who are in Hell, branding him as a usurer. For a long time this sentence led believe that the son had erected the chapel to atone for the sins of wear, and those of the parent.



*Figure 1.1 Giotto painting cycle in the Scrovegni chapel.*

Through the beautiful frescoes, Enrico Scrovegni wanted to set up a continuous conversation with his city and show up himself with a different the profile of a patron, in fact he used the accumulated wealth and remitted it in a circle, as a spiritual gift to his people.

The dating of the frescoes is deductible to a good approximation by a series of news of the time: over the purchase of land in 1300, in 1303 there was the first foundation (or at least the consecration of the soil). On 1 March 1304, Benedict XI granted indulgence to those who would visit the chapel and a year later, on 25 marzo1305, the chapel was consecrated.

The frescoes are traditionally dated to this final phase, between 1304 and 1306. The narrative stories of the Virgin and Christ completely cover the walls, while in the counter the magnificent Last Judgement is painted, to conclude the story of human salvation. Enrico Scrovegni didn't enjoy it for a long time because the political events forced him to emigrate as an exiled in Venice, from which he returned only dead: he was buried in the chapel, at the bottom of the apse, in a tomb canopy.



*Figure 1.2 Scrovegni chapel and palace in an ancient representation.*



*Figure 1.3 The chapel nowadays.*

Through ancient documents the history of ownership succession of the Arena is well known, including the history of chapel and the palace: Scrovegni palace was object of a lot of transformations to adapt the architecture to the visual pleasure of the Renaissance, up to arrive under authority of the Gradenigo family in the nineteenth century.

The structure was in bad conditions due to the lack of maintenance: in 1817 the porch fell down, so that the City urged the Gradenigo family to reconstruct the porch because of the danger of deterioration of the frescoes. The Gradenigo family did not adjust the structure, indeed, continued in 1827 the demolition of the building next to the church without taking the necessary precautions for the demolition of the walls that were adjacent to the chapel, as evident in Figure 1.2.

The demolition of such structure, in contact with the north side of the church, may have been the primary cause of injury between the vault and the wall of the facade: in any case, the demolition of the building, leaving exposed the northern wall of the oratory to moisture and the rain, could cause damage to the famous frescoes.

Antonio Tolomei, Mayor of the city from 1881 to 1885, was the promoter of the purchase of the Chapel by the City of Padua. The first resolution of the Municipality for the purchase was adopted in 1880, and after long negotiations and legal disputes the City of Padua acquired the Arena for the sum of 54 921 L with the burden of payment of perpetual L. 253.95 per year to the vestry of the church of the Hermits.

Since the Chapel was acquired by the city of Padua, in 1880, the frescoes have been continuously subject of special attention and, in the nineteenth and twentieth century, various conservation projects were promoted. From the seventies to the present day, thanks to close cooperation between local government, Superintendents and Central Institute for Restoration, accurate studies and monitorings have been made to preserve the status of the building and the state of conservation of paintings, on the air quaeven improving air quality by reducing pollutants.

Checks at the structure performed in the last decade showed a stabilization of the situation, and permitted to run a restoration program that ended in 2002 and was carried out by the Central Institute for Restoration: thanks to the protocol agreement signed between the City and the Ministry of Heritage and Activities cultural, and after twenty years of experiments and studies, the Chapel was clean from moisture condensation caused by perspiration of the hundreds of thousands of visitors that crowded it, but especially from the dangerous transformation of plaster in gypsum, due to sulfation.

A series of research and measurements of environmental parameters has led the construction of a technological equipped body (CTA) to filter and break down the most aggressive atmospheric pollutants, and this countermeasure has been paired with the regulation of visitors flow: the construction of the new access body, along with installation of an air treatment system, allows managing the strong flow of visitors to foster the conservation of frescoes.

In the nineteenth century when the church was privately owned by the city, the chapel was in danger of collapse as a result of the actions of the last heirs, the nobles Gradenigo. They did not hesitate to demolish the magnificent palace of Enrico Scrovegni, adjoining the chapel, because in need of restoration, and and to make matters worse in 1829 after the huge

damages in the roof of the chapel, they wanted to crumble the masterpiece of Giotto to excavate building material.

The attack on this artistic masterpiece was foiled by strong negotiations from the municipality and citizens, lasted more than sixty years, involving lawyers, engineers, men of culture, and everyone who was aware of the need to preserve for posterity a heritage, that was formally private but belonging to the public.

Nowadays the problems that undermine the security of the Chapel are different, but not less dangerous than those that marked the history of the chapel in the nineteenth century.

The chapel has been long injured by time. The inspections carried out from 1998 to today are not so encouraging: from a structural point of view the Scrovegni Chapel presents lesions, mainly located along the vault, but prof. Modena stated that these injuries result from the ancient damages suffered from the chapel still between the nineteenth and twentieth centuries, when the great palace Scrovegni was demolished and the porch collapsed, and so the chapel was destabilized by the resulting adjustments. These wounds were caused by ancestral events, on the contrary earthquakes in the recent decades do not seem to have affected the structure.

The current problems to the structure arise from natural factors influenced by the human presence; in fact, the main problem encountered today is the hydrological situation, that was threatened by the project of majestic urban constructions close to the chapel.

The Chapel and the Cenobio are located near the sixteenth century city walls and the river Piovego. The floor of the Cenobio, above which there is the Chapel, has been subjected to serious and alarming floodings for years, mainly generated by the rising of the water table.

The September 16, 2009, as example, an exceptional weather event triggered the alarm for the water level in Cenobio of the Scrovegni Chapel: water table level was so high that rainwater entered through ground level and from the basement window and the entire crypt was completely flooded (17 cm were recorded in a single day).

The Culture Committee in October 2009 dealt with the problem of flooding that happened in the crypt of the Scrovegni Chapel, and asked the Mayor of Padua to establish a technical and independent scientific committee, composed of distinguished experts, aimed at assessing the hydrogeological situation in the area around the chapel, with a focus on the right and left banks of the canal Piovego, to get the possible proposition of technical solutions to protect the Chapel itself.

The delicate hydro-geological situation was likely to be modified by the construction of an Auditorium less than 200 meters from the chapel. In the same area was also proposed the construction of a 104 meters high skyscraper, and was really built a parking garage.

In 2011 the City commissioned to three engineers, D'Alpaos, Salandin, Simonini, professors from the University of Padua, an investigation into the possible consequences that the construction of the Auditorium could have on the surrounding area, and in particular on the Chapel.



Due to the implications for the foundation, stability of the monumental building, the delicate structural equilibrium of the famous Giotto's frescoes may be altered by the variations of the water table.

For this reason, a relatively large number of piezometers and wells (16) were drilled in an area of approximately 8 ha, within two aquifers characterizing the subsurface medium down to a depth of 30 m. Topographic studies were made by this expert committee, many piezometers were installed to observe the behavior of the aquifer in the Scrovegni Chapel and also in the neighboring area. Control wells were also made, to experimentally assess what was happening if stressing water table in certain positions. Starting from the experimental data that were obtained by the commission, the hydrogeological system that affects the Scrovegni Chapel and the surrounding areas were mathematically modeled, in order to simulate a hypothetical future evolution to lead feedbacks in perspective to perform interventions in Boschetti area [Camporese et al., 2012].

The team decreed the existence of two aquifers, analyzing results provided by pumping tests conducted after the drilling of piezometers and wells, through which water was pumped and extracted, both interesting the deepest aquifer and the shallow one.

Superficial and deep aquifers have been demonstrated not to be divided in a clear way in the area of the Chapel, even if the answer to the dynamic solicitation inducted by variations in the Piovego level results more pronounced in the deep aquifer.

The first aquifer is located between 4 e 12 m and the deeper aquifer between 17 e i 28 m and they are weakly unbalanced.

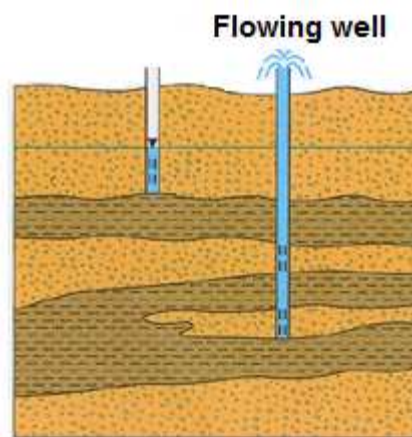


Figure 1.4 Representation of aquifer situation under Arena gardens

The pumping tests, performed to define the hydraulic behavior of these two distinct but interconnected aquifers were continued for a limited time because there was a great fear that a possible disaster would happen by a continuous pumping in defined positions: during tests, the Scrovegni Chapel was instrumented to observe if there were movements caused by the operations that were carried out. No damages were produced by testing the hydrological situation, and interesting results were determined.

The commission demonstrated that if water is pumped out in certain positions, especially from the deep aquifer, the effects can be felt under the Scrovegni Chapel, even if pumpings continued for a relatively short time (the longer test was 48 hours long).

Even a test for investigate level changes in Piovego was conducted to see the response to these changes in the aquifers under Scrovegni Chapel. This has permitted to study the general behavior of the whole hydrological system, with the aim of translating it into mathematical model. From these tests a connection between the deeper aquifer and the more superficial deeper aquifer was found, and a role of Piovego on changes in groundwater level was revealed [D'Alpaos et al., 2011].

If the deeper aquifer is depressed in the area surrounding the Arena gardens, in particular where the Auditorium should be built, the aquifers in the area of the Scrovegni Chapel suffers and can react by changing water pressure in the soil.

By lowering effective stress, positive pore pressure reduces the available shear strength within the soil mass thereby decreasing the slope stability and this situation may represent a danger for the mechanical stability of the structure.





## 2. Status of the Cenobio

The floor of the Cenobio has the same level of the surface aquifer: in case of heavy rainfall events repeated in a short time, the raising of the water table immediately reach the crypt and water enters the structure through the floor and the walls.

The problem occurs when the shallow aquifer is quickly saturated because of huge rainfall events and additionally the inadequacy of the system for the disposal of meteoric water.

The media attention to this issue arose in 2009 after an important flood that affected the crypt of the Scrovegni Chapel following the rainfall event of 16 September 2009.



*Figure 2.1 Area next to the church in September, 2009*

The crypt has the same dimensions of the central nave of the Chapel and the floor (8.91 m.a.s.l.) is 4.63 m lower than the floor of the church as seen in Figure 2.4.

Water that enters the chapel is coming from groundwater: in old studies conducted by prof. geologist Illiceto, he hypothesized that the Piovego influence the level of groundwater, but more recent studies have observed that is the rainfall water that represents the greatest contribution to the rapid growth of the aquifers [Illiceto, 2002].

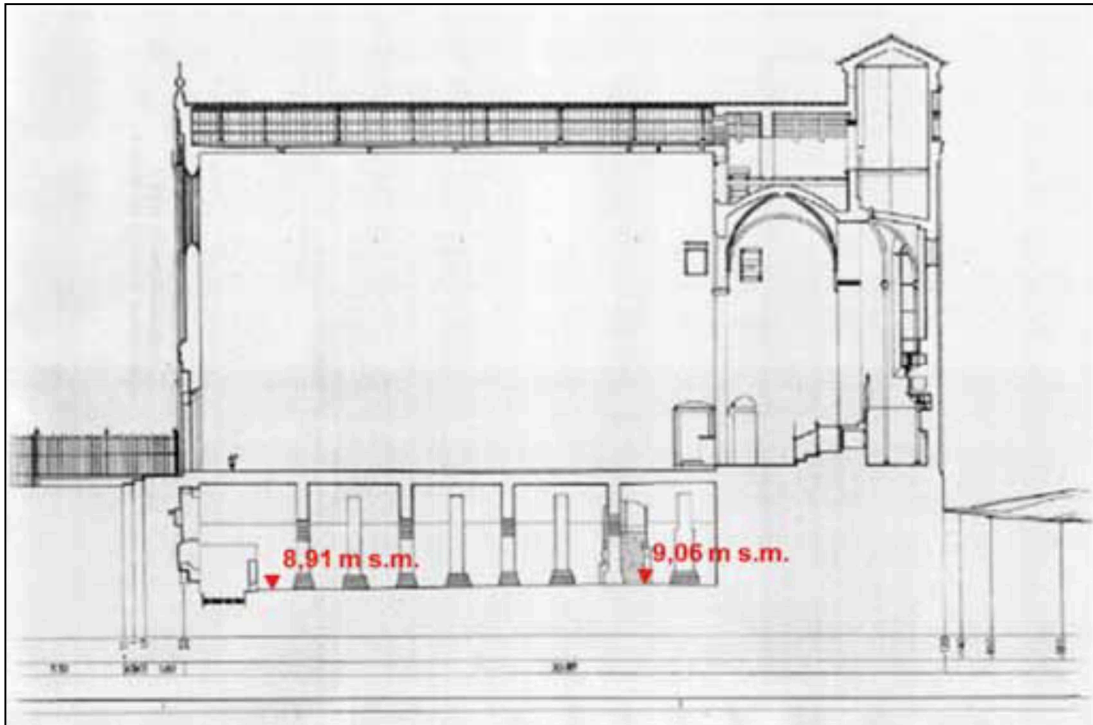


Figure 2.4 Section of Chapel and Cenobio, with the level of the floor in m.a.s.l, detected in 2013.



Figure 2.5 Pump station installed inside the Cenobio.



*Figure 2.5 Tank containing pumps installed in the cenobio.*

Water that enters the chapel is coming from groundwater: in old studies conducted by prof. geologist Illiceto, he hypothesized that the Piovego influence the level of groundwater, but more recent studies have observed that is the rainfall water that represents the greatest contribution to the rapid growth of the aquifers [Illiceto, 2002].

Lowering the water table in the area surrounding the church seems an immediate solution, but historically the water has always been high (about 8.9 m.a.s.l.) and a sudden drop of the water table could create structural problems, which must be doubtless avoided.

A water pressure drop is translated into a corresponding increase in effective stress state in the ground accompanied by vertical movements of the land that may affect the delicate structural balance of Scrovegni Chapel. The aim of this study is to avoid flooding in the Chapel by reducing the water table level in the area, but in the same time is fundamental to avoid any intrusive action that can modify the balance between nature and structure.

A solution to adopt is to limit the infiltration of water into the groundwater through the construction of a new drainage network in the entire area: the best action to undertake will be to reduce the possible meteoric contribution in groundwater, and the control of these outflows can only be done through the implementation of an appropriate structure, that quickly removes the water that arrives from rainfall.

The study conducted in this area by the Department an Hydraulic Engineering, maritime, environmental and geotechnical engineering, in 2001, was aimed at defining the hydraulic and geotechnical scenarios related to the construction an an auditorium in Piazzale Boschetti, near the Gardens Arena: in this occasion analyzes were performed to evaluate changes in underground aquifers.

The measure of the aquifer during the whole 2004 in two piezometers (A near the chapel and B 200 m far from the first one) showed that the groundwater is influenced by the level of the Piovego river and also by the weather events that cause two different hydrologic problems. Firstly the rainfall water flows into the Piovego channel and increase the water table level, and secondly the high permeability of the subsoil of the Chapel promotes deep drainage of leaks that arise both from drainage system and also stagnation in the surrounding area, especially behind the apse of the chapel where the morphology of the gardens is depressed due to the need to access the underpass connecting the two areas of the gardens.

The level measured at the points A and B is different during important rainfall events, while it tends to settle on the same value during stationary conditions. In 2009, the maximum excursion of the aquifer was +/- 20 cm (max = -4.48 m, min = -4.91 m value relative to the floor of the Chapel), the height measured at point A is almost always lower than that measured the point B of a quantity that varies between 10 and 20 cm [D'Alpaos et al., 2011]. For both aquifers values specific storage and hydraulic conductivity were measured.

Specific storage  $S_s$  [ $m^{-1}$ ] is the volume of water released by a unit volume of the porous medium for a unit change of pressure head, and the value of hydraulic conductivity [ $m/s$ ] is the reciprocal of resistance to motion, that despite the extreme heterogeneity of soils in the area, is quite significant:

*Table 2.1 Aquifer parameters.*

<i>Upper groundwater</i>		<i>Lower groundwater</i>	
<b>K</b>	<b>S<sub>s</sub></b>	<b>K</b>	<b>S<sub>s</sub></b>
$1,3 \times 10^{-3}$	$1,1 \times 10^{-2}$	$2,3 \times 10^{-4}$	$5,6 \times 10^{-4}$

The measurements performed in the study indicate that the level of Piovego, in the period considered, is always lower than the level of the groundwater, therefore groundwater, both shallow and deep, responds quickly and appreciably to forcing weather, and employs a long time to be naturally rebalanced. It is reasonable to assume that this behavior is influenced by losses, also consistent, in the drainage network that covers the area [D'Alpaos et al., 2011].

The data obtained from investigations in the area Scrovegni allowed the reconstruction of the stratigraphic profile below the Chapel of up to 20 m deep.

Five different layers are continuously present, although with slightly varying thickness from point to point:

- Layer 1: bricks, mortar and rubble in silty-sandy matrix (land retriever) from pc to - 1.30 m
- Layer 2: sandy silt and clay from -1.3 to -1.5 m
- Layer 3: coarse sand with gravel levels from -5.00 to -12.50 m
- Layer 4: clayey silt alternating silty sand from -12.50 to -16.50 m
- Layer 5: medium-fine sand from -16.50 to -20 m.



The units are referred to the floor of the Scrovegni Chapel [D'Alpaos et al., 2011].

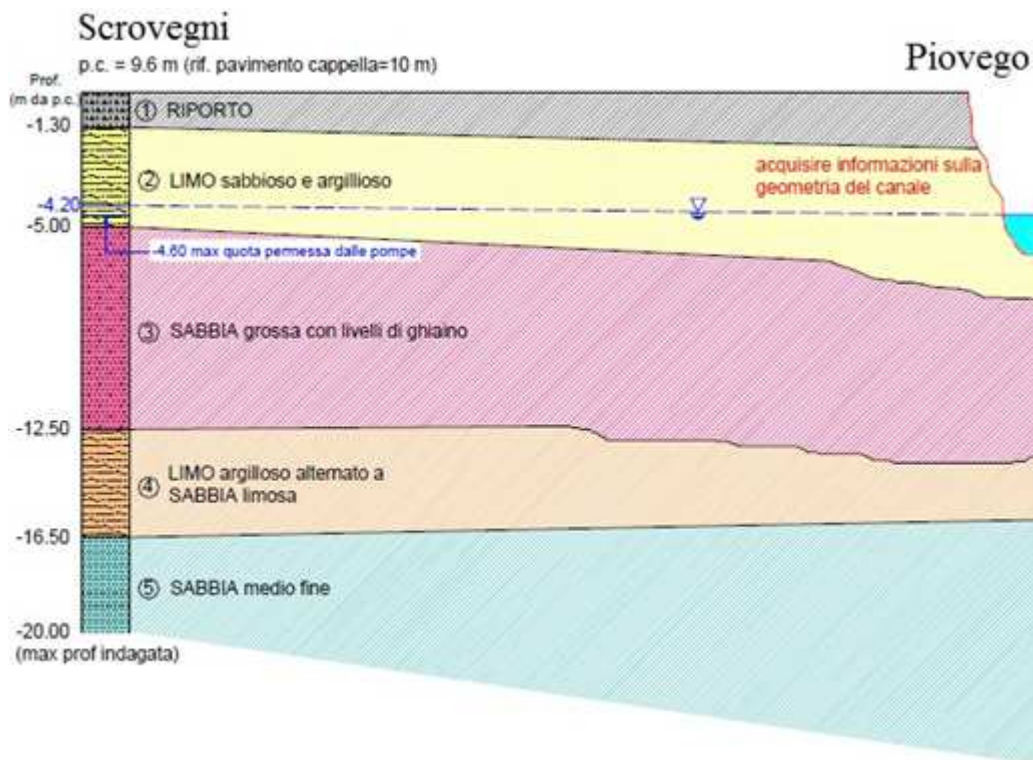


Figure 2.6 Soil stratigraphy of the Scrovegni area

The geographical location of the Chapel directly promotes the infiltration of rainwater into the ground because it is located in a park where the soil, as just described weakly silty sand, represents a preferential access to groundwater, and tall trees are losing leaves clog the drains worsening the already unstable situation.

Besides the constant monitoring and continuous maintenance, continuously perpetuated, it is necessary to expand the sewer in the area, which dates back to the early '900.



### 3. Suggested countermeasures

In December 2014 an inspection to the Arena drainage system was conducted by the Municipality of Padua with the supervision of the University. This drainage system inspection tried to understand how the drains in the area arena are linked together, and where they discharge the collected water.

The current functioning of the network is fundamental to understand where there are problems and where actions must be taken to improve the drainage conditions in the area.

A technical inspection highlighted that no attention was posed on the status of the network system because the manholes had no maintenance and they were totally clogged, so that they could not perform their daily function.

The municipality, after the inspection, has provided the correct maintenance to stem the problem of rainfall leakage in the soil.

The following images have been captured during the recognition of the area.



*Figure 3.1 Manhole in front of the Chapel, totally clogged by sludge.*





*Figure 3.2 Manhole in the Scrovegni totally clogged by sludge*



*Figure 3.3 Reconstruction of the trend of the network by utilizing a probe.*





*Figure 3.4 Visual inspection of a conduit that results interrupted.*

The drainage network in Arena actually is not defined because the municipality has no database file with all the drainage system data.

The purpose of the inspections was to trace the shape of the network, to analyze the connections between the drains, and their point of water discharge.

After several attempts, the goal was ruled out for physical impossibility to achieve it. The various probes used, and also the video inspection, were not able to determine the route of pipelines, due to clogging and/or breakage: the existing pipelines and some manholes are made of stones, so they are easy to break and generally vulnerable to loss compared with new manholes, which could be achieved. To understand how the structure of the network, the arena area should be excavated, but this zone is covered by archaeological restrictions. Fundamental to stem the danger is to check that the pipes do not leak and possibly repair them, finally it is necessary to increase the network.

The solution of excavate the area and assess actual conditions of the network becomes disadvantageous in terms of time and cost, the best solution is to close the old stone pipelines, and build a new small network that fulfills the function of protecting the Scrovegni chapel from flooding.

During the inspection the pipeline track has been reconstructed with many difficulties because as visible in Figure 3.4 a main pipe is interrupted and the probe couldn't go back to the conduit.

The network in this zone is visibly insufficient and not well determined with a plan so becomes necessary to rebuild it with new proper materials, respect to dig this protected area to understand how the network behaves and restore the old conduits.

The structure and path of municipal conduits where the manholes discharge their flow, are even unknown because no documentation has been provided from municipality to understand the functioning of the network.

To analyze the problem and describe the area, in this project for simplicity Scrovegni garden is considered divided in three parts: northern, southern and arena, as described in Figure 3.5. The inspection described above has been done in the old arena zone, because is it closed to the chapel and due to a very delicate morphology, in this part is fundamental to build immediately a proper sewage system.

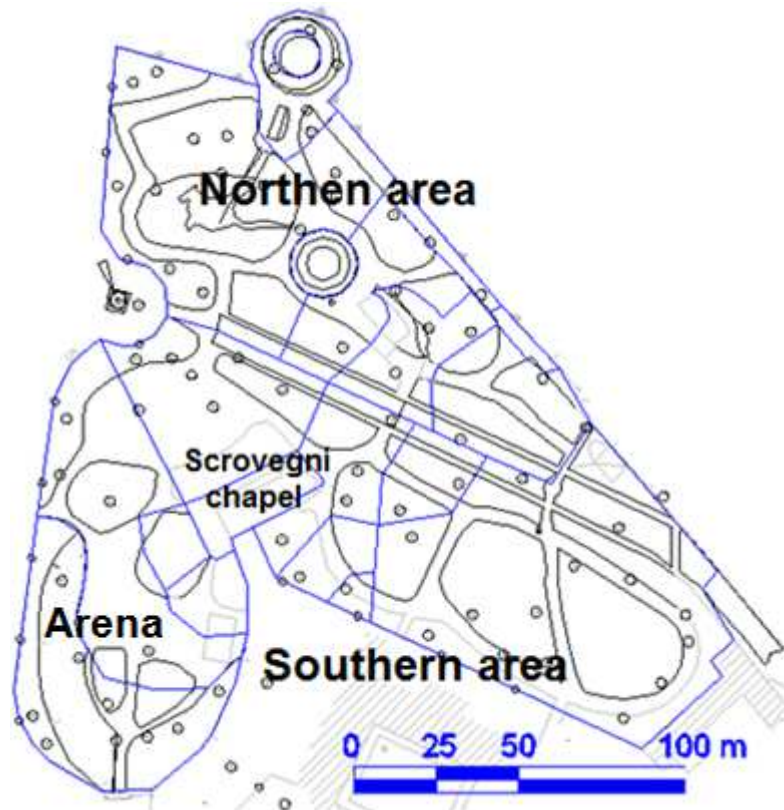


Figure 3.5 General plan of the area, subdivided in sub basins.

**NORTHEN AREA:** In the northern area of the gardens, towards the bastion, rainfall water is not efficiently collected because the drains are poorly arranged and insufficient: manholes are often bypassed, rain water has created many rills in the soil, and the amount of water is such that preferential pathways in the gravel have been naturally formed (Figure 3.8).

The water starts to accumulate in the area of the fountain, and then slide down to the most depressed part of the gardens, named S<sub>2</sub> (Figure 3.6).

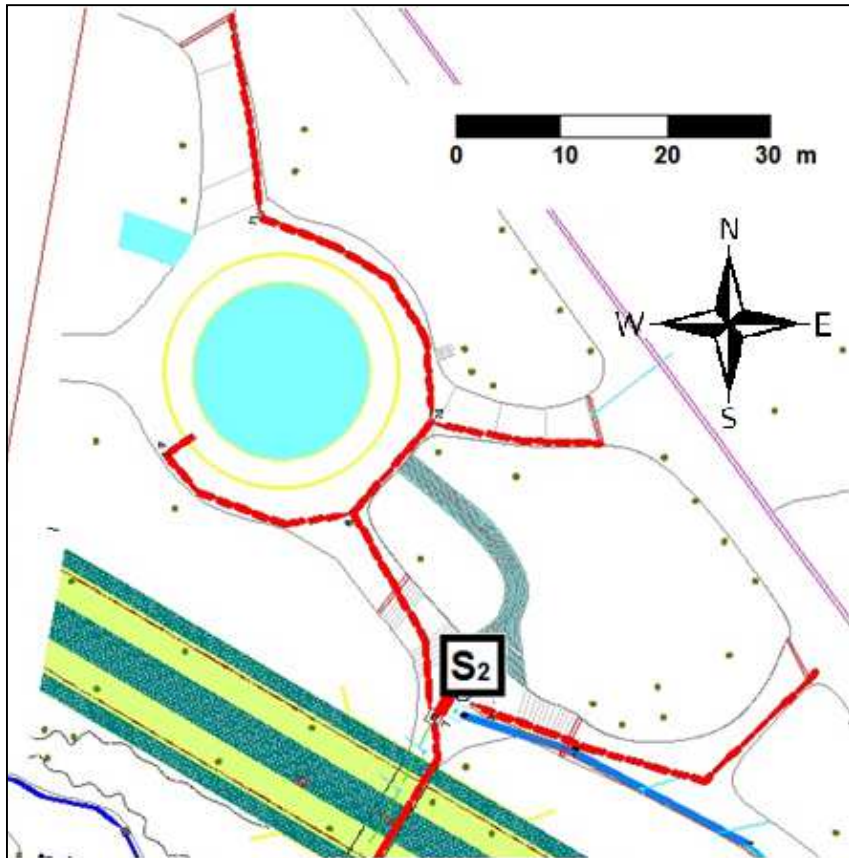


Figure 3.6 Northern part of Arena Gardens: water flows towards S2

The several stagnation areas reveal the lack of some drains and also the inadequacy of the current ones, which are badly arranged, inadequate in number, and often clogged as visible in the figures below.



Figure 3.7 Area of stagnation of rainfall water





*Figure 3.8 Bad disposal of manhole, turned around by rainfall*



*Figure 3.9 Rills in the soil due to a huge quantity of water.*





*Figure 3.10 Rills in the soil due to a huge quantity of water.*



*Figure 3.11 Bad disposal of manholes that don't work as hypothesized*

The goal in the northern part of the gardens is to improve the drainage network through the addition of manholes and to better arrange the current ones where necessary. As defined before, the whole network of the northern area collects water in S<sub>2</sub> (Figure 3.11) where there is a lifting system which discharges directly the water into Piovego river.



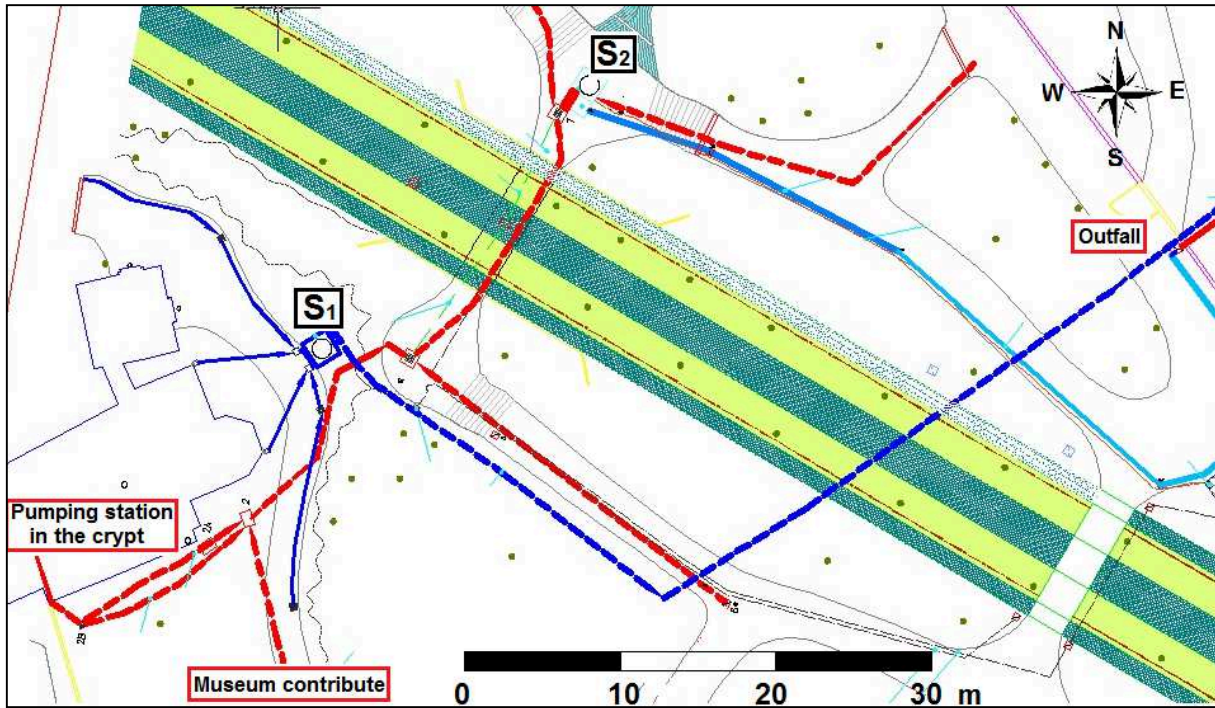


Figure 3.12 Actual drainage network in the area.

S<sub>2</sub> receives many water contributions: water that arrives from the northern area of the gardens and from P<sub>3</sub>, which collects mainly manholes that are located in the entranceway to the Scrovegni chapel. This network is represented with red color pipelines in Figure 3.11.

SOUTHERN AREA: The southern area of the garden is a natural basin because the depression of the land is significant (approximately the level is 12 m.a.s.l.) and water easily stagnate at low points: many manholes will be installed to prevent the infiltration of the entire contribution, because at present no drains exist here.

In Figure 3.13/14 is visible the huge stagnation that persists during a consistent rainfall event.



Figure 3.13 Southern part of the gardens flooded



Figure 3.14 . Southern depressed area after a huge rainfall event.

Near the chapel there is an area of 1 hectare covered by the museum: another point to analyze is that rainwater coming from the museum arrives in S<sub>2</sub>. This contribution is consistent because the museum represents a 10 000 m<sup>2</sup> almost waterproof area.

The flow rate coming from the museum is defined by the formula  $Q = \varphi * j * S$

$\varphi$  = runoff coefficient, which is assumed to be 0.1 - 0.2 for green areas, while 0.8 - 0.9 for impervious areas.

$j$  = intensity of rainfall =  $h/t_c$

$h$  = height of rain, expressed in mm, reference is made to a rain with  $T_R$  of 5 years, as defined by Italian legislation for urban sewage systems.

The height  $h$ , is defined by the rainfall intensity-duration curve  $h(\text{mm}) = at^n$ .

For this area,  $a = 38,53$  and  $n = 0,248$  (as calculated in Chapter 4).

The value  $t_c$  is considered equal to 12 minutes (720 sec).

The result of calculations is  $h = 38,53 * 0.2^{0.248} = 25,85$  mm.

$S$  = Surface area (in hectares)

$Q = \varphi * S * h/t_c = (0,8 * 10000 * 0,025) / 720 = 0,3$  cm/sec = 300 l/sec

The flow rate coming from the museum is about 300 l/s and represents a significant portion of the flow received at the booster station that is installed near the Chapel.

The status of hydraulic network near the Chapel is critical; this important contribution of water must be removed from the Scrovegni Chapel area, and not be conveyed in its vicinity as happens today.



Starting from the current situation and assuming a long shutting down of  $S_2$ , an overflowing that goes back to the area museum/chapel can be generated, and this hits the hydraulic safety of Scrovegni Chapel which is located lower than the walking path that is immediately above all the pipelines of the drainage system.

$S_2$  node also receives the water coming from the pumps of the crypt, that are estimated as a flowrate of  $40 \text{ m}^3/\text{h}$ .

The booster stations that receive many contributions and discharge them out of the area are both  $S_2$  and  $S_1$ : the most quantity of water is received in  $S_2$  but the manholes neighboring to the church discharge the water in  $S_1$ , which is the lifting system dedicated to this area only.

The solution hypothesized to avoid flooding problems in the future is to divert meteoric contribution coming from the museum in the lower part of the gardens, where new manholes will be installed connected to the same network: the largest amount of water will be carried far from the Chapel and finally will be discharged by a new lifting system that will be designed.

Following the new project, the contributions that arrives in  $S_2$  and that can become potentially dangerous to the operation of the network are reduced, and a large part of the infiltration that occurs in the lower part of the gardens is easily removed by many manholes installed along a new pipeline coming from the museum.

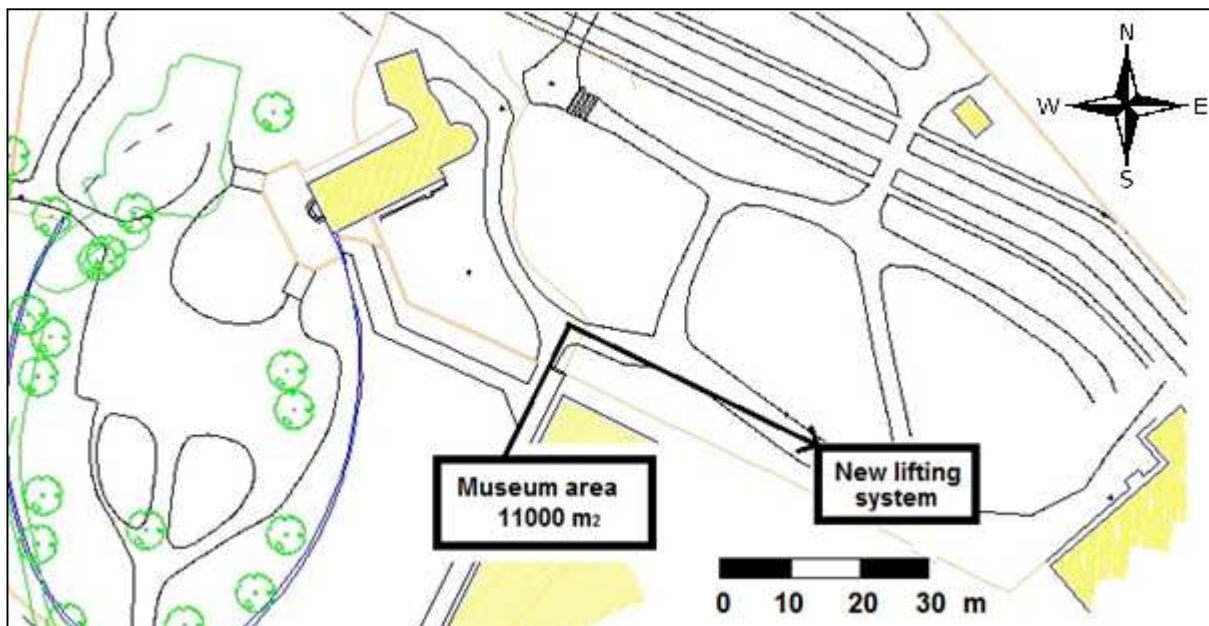


Figure 3.15 Representation of the new diversion hypothesized from the museum

According to the new hypothesis, water from the crypt will be no longer discharged in  $S_2$  (Figure 3.12) but will be directly discharged in  $S_1$ , to dedicate this lifting system only and exclusively to the area church, this system will only receive by the traps around the chapel and the water eliminated from cenoby.



If possible, to reduce the flow in  $S_1$ , the manholes in the front of the church will be discharged in Corso Garibaldi.

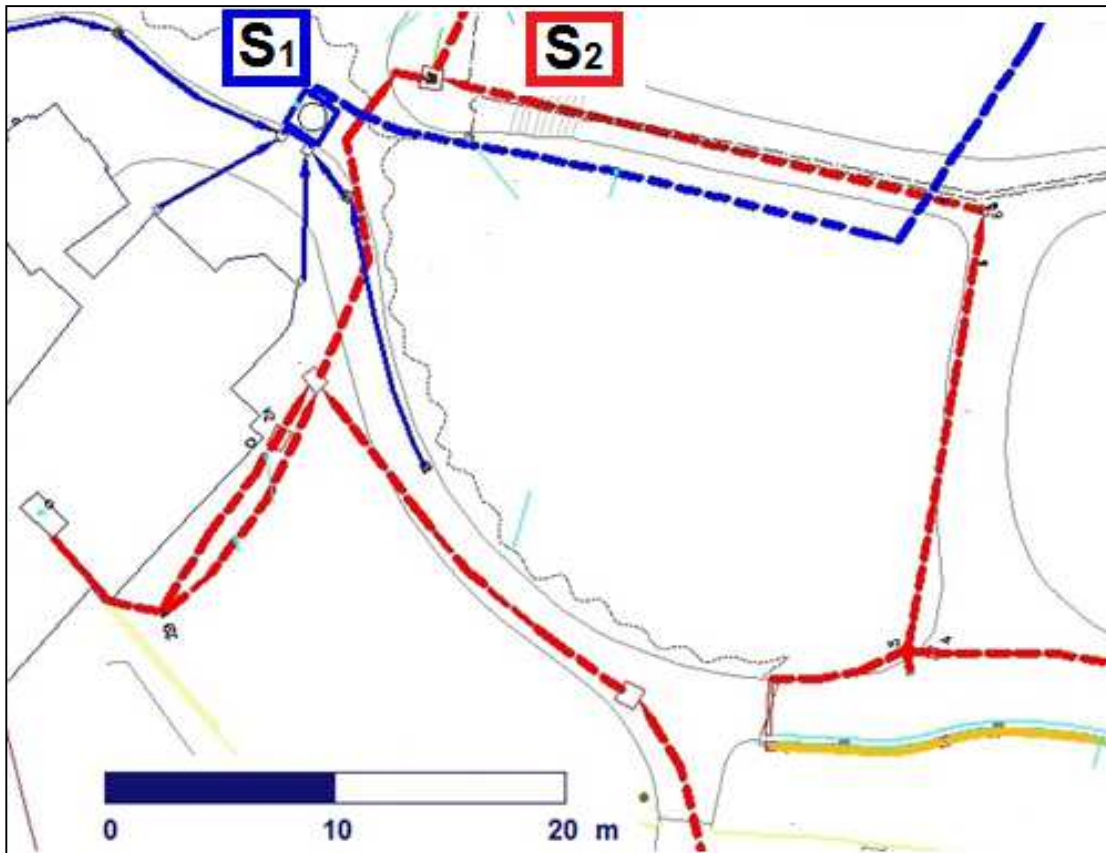


Figure 3.16 Current situation of the hydraulic network

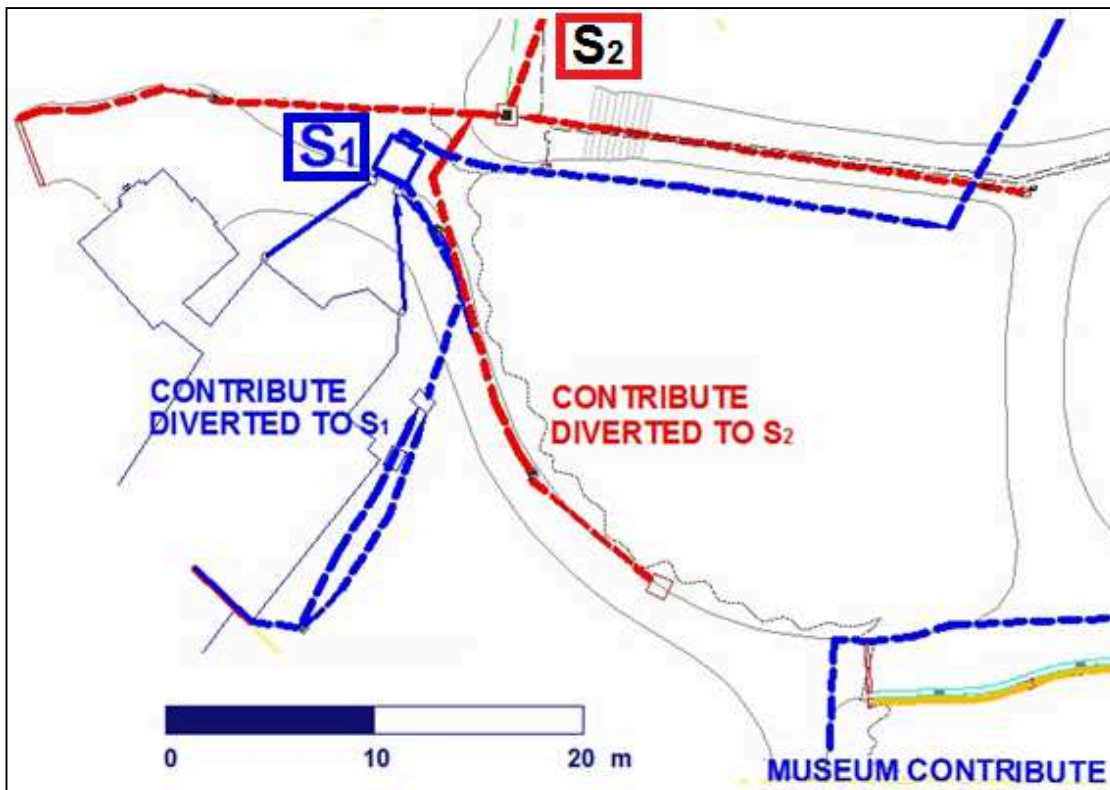


Figure 3.17 Hypothetic solution for drainage network in Arena Gardens area.

ARENA: The area of Arena, closed to Corso Garibaldi, lacks of an efficient drainage system, considering the natural slope of the soil there are lots of depressions that during rain become preferential points for the infiltration of rainwater into the groundwater.

Well point drains installation, to pump groundwater if water table level grows until flowing into the Cenobio, seems a simple way of resolving the problem but this solution is not possible in practice because a meter below the level of the land there is a slab dating back to Roman times, and for archaeological restrictions it can not be interrupted. Moreover, the presence of two aquifers, both shallow and deep, produces a particular effect because even if the superficial layer is lowered, the one below has high piezometric levels that pushes on the states above and cause the same penetration in the crypt.

Currently the archaeological excavations to unearth Scrovegni palace are opened, and represent a preferential way for rainwater to infiltrate (Figure 3.18), as the excavation is several meters deep.



*Figure 3.18 Ponding zone in archeological excavation.*

The primary objective of the municipal administration will be to cover the excavation, if possible with a layer of 30 cm of impermeable material, creating gradients such that the rain water is conveyed towards the manholes to the drainage system.

In the arena are two large valleys along the perimeter, but these have always existed and will be maintained as such: reshaping the contours of the area should be avoided to let water in these, as far as possible.

Around the Scrovegni Chapel, in the side that is entirely located in the arena gardens, there is a wall with narrow manholes below that is evidently saturated by water and demonstrates a huge presence of water in the soil near the church.



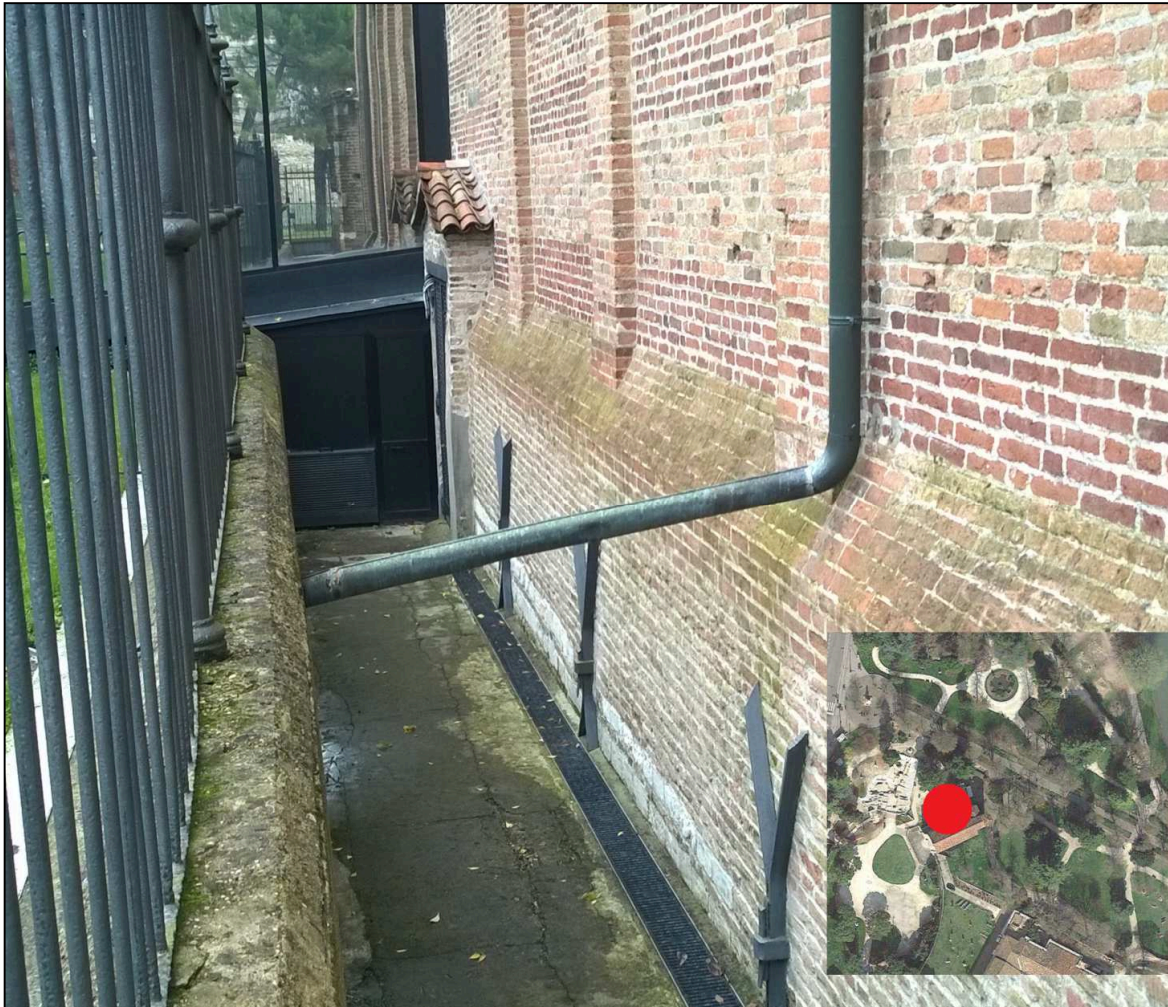


*Figure 3.19 Wall that surround the Scrovegni Chapel.*



*Figure 3.20 Clear level of humidity in the wall around the chapel*

After an inspection of the wall, it appears completely saturated with water that comes from deeper layers of the soil, as visible in Figure 3.20. At this exact point it is difficult to operate due to the presence of the ancient slab 1 m below the ground level, and then the only possible solution assumed is to install a drainage pipe of 300 mm diameter to collect meteoric contribution of water that infiltrates into the ground. The drain will be placed around the long side of the chapel and will be discharged, if possible, in the municipal network of Corso Garibaldi.

The solution provided is to increase the number of manholes: two items will be inserted in the most depressed part of the gardens, paired with other two manholes already existent, and another solution to apply will be to create a new slope in the area to as to facilitate the natural drainage of water towards the manholes.

It is sufficient that the new slope was between 0.5% and 1%: the outlines of flower beds will be kept fixed because they were designed by Jappelli, an architect from Padua. According to an analysis of the level curves, the slope required to allow water already exists but this should be regularized because it is not homogeneous. The analysis of Arena section is described in Figure 3.21/23/24 and the final redrawing of this area in represented in Figure 3.24. This process has been done by analyzing the level curves in AutoCAD: the curves have been rearranged following the natural slope of the soil but considering the future drainage system: most of rain must be conducted in the pipeline network.

The material used to realize the new slope will be waterproof to facilitate the flow of water and prevent this to pond in the soil, infiltrating. In this part only 4 manholes exist: two in the most depressed part, in front of the church, and other two in the higher part, next to Corso Garibaldi. The manholes existing in the lower area will be connected to other two to increase the drainable surface (about 100 square meters for caditoia).

The 300 mm diameter drain will be installed in the side of the chapel that looks into the excavations. Is important to notice that the water that enters the Chapel flows from the norther wall to the southern part of the crypt: the presence of the drain is fundamental to collect a huge quantity of water that makes the soil completely saturated in the northen part (Figure 3.17). Two caption grids will be added in the access ramps from the street to the arena, the ground is very steep in the ramps and water flows down so quicky and then stagnate. All contributions originating in the zone of the arena, if possible, will be discharged to municipal network in in Corso Garibaldi, to avoid an overloading of the pumping plant that is near the church. Given the lack of detailed data of the connection with the municipal network, the main solution adopted is to collect all the contributes and then discharge them into Piovego through a pumping station, that is already in the design phase with other aims.



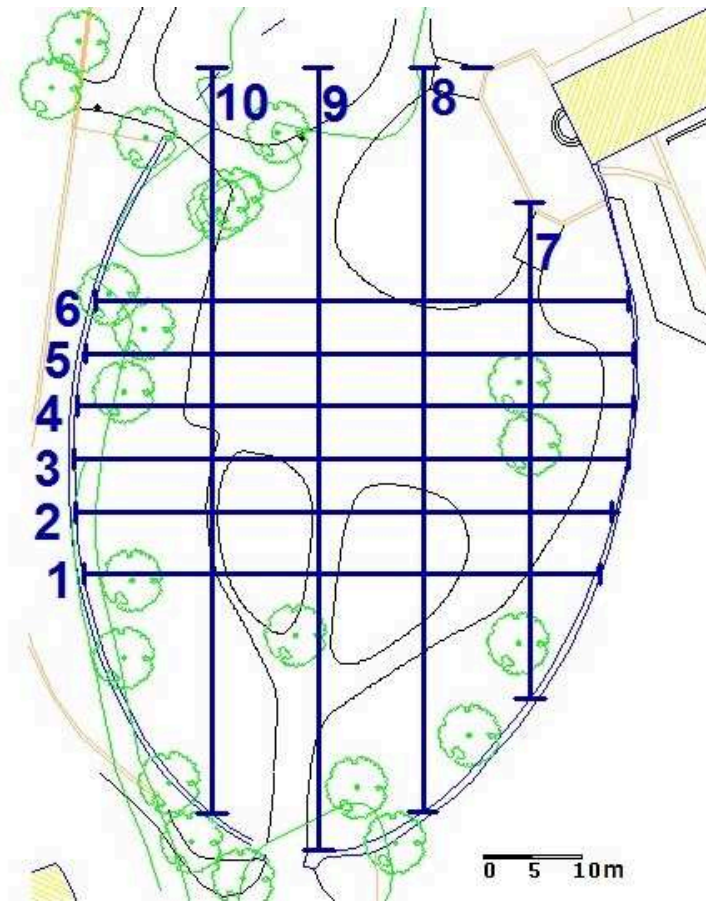


Figure 3.21 Sections, Arena.

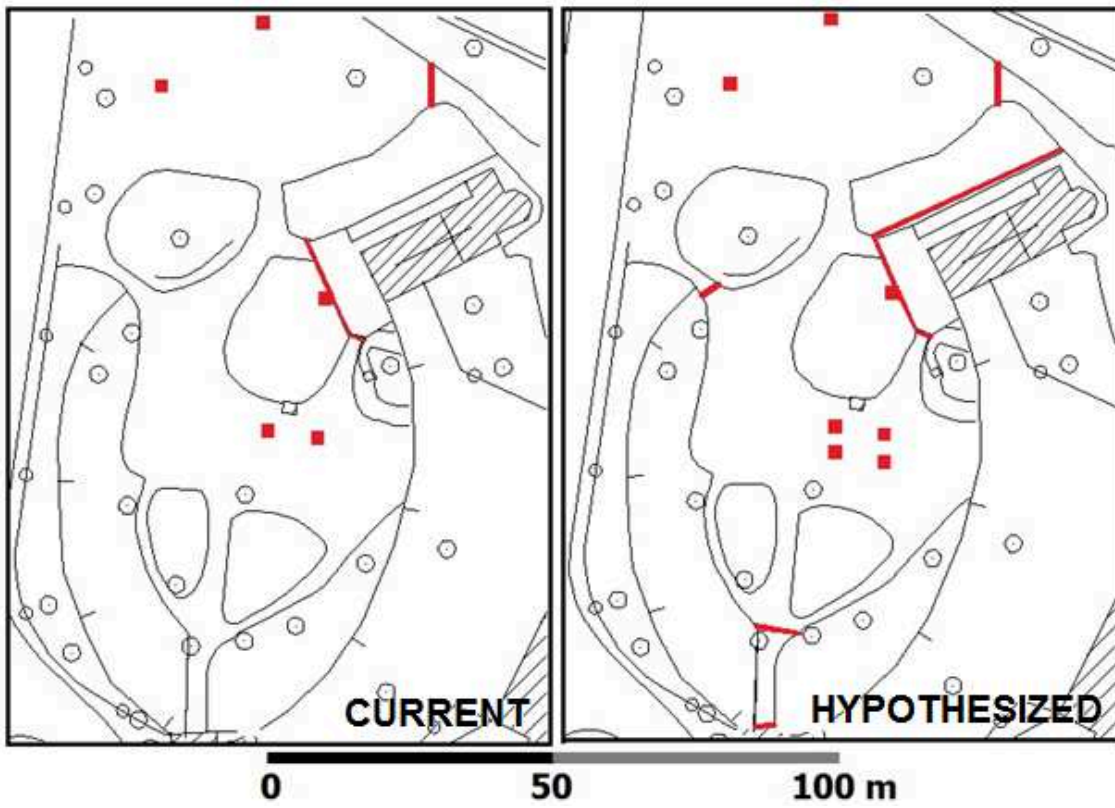


Figure 3.22 Current situation and network hypothesized, Arena.

## TRANSVERSE SECTIONS (m.a.s.l.)

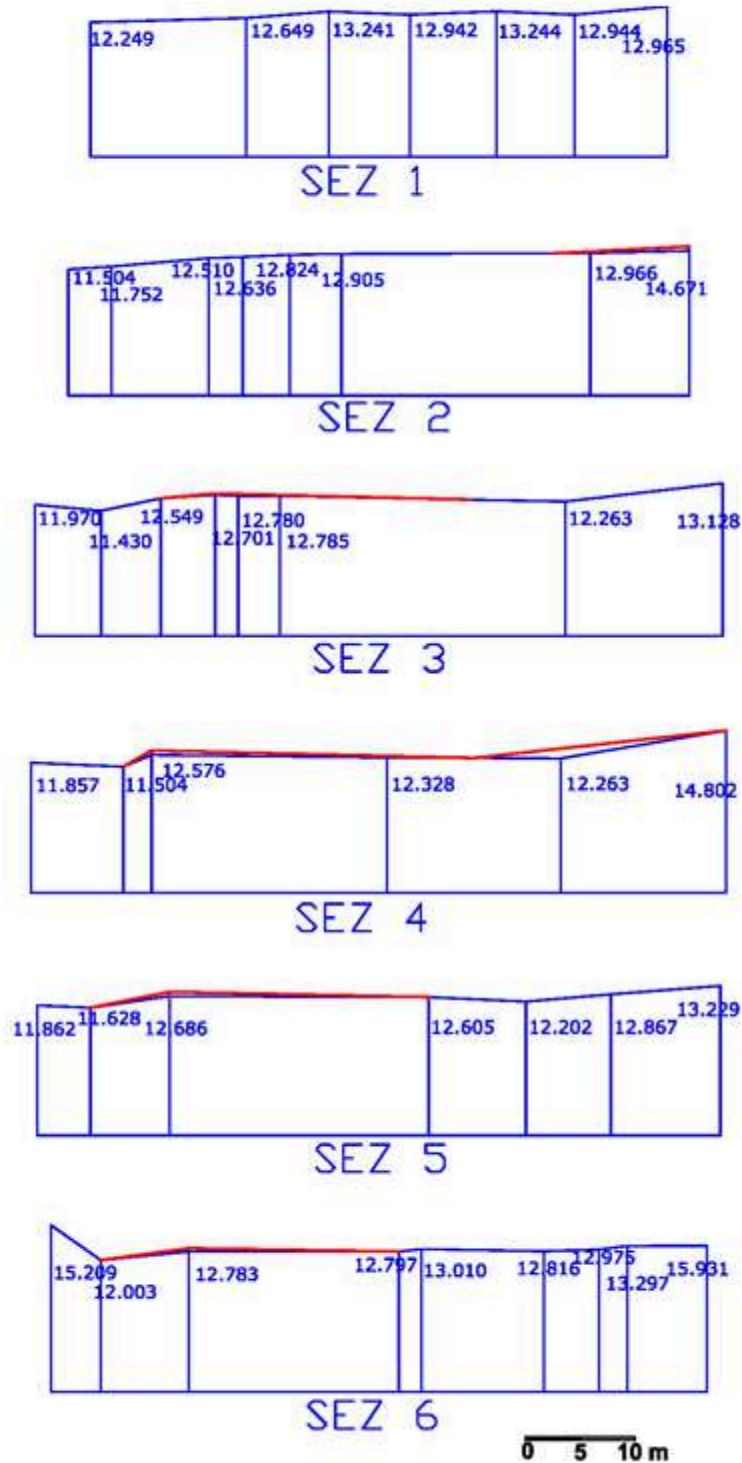
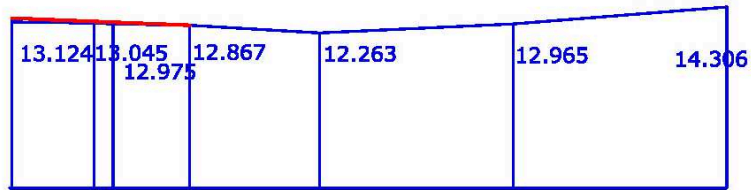
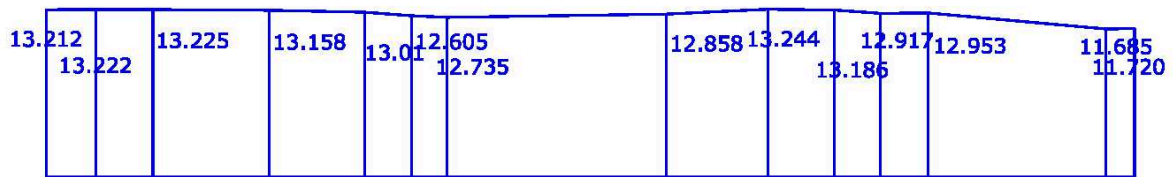


Figure 3.22 Transversal sections of Arena garden

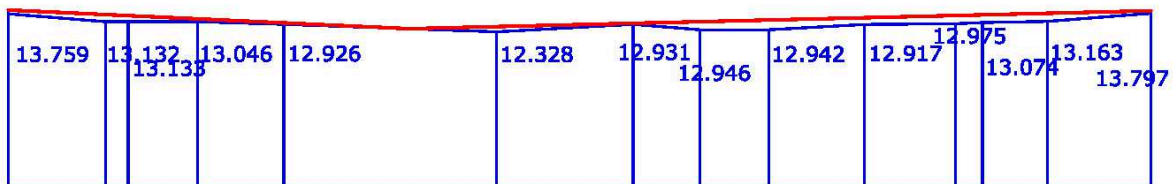
# LONGITUDINAL SECTIONS (m.a.s.l.)



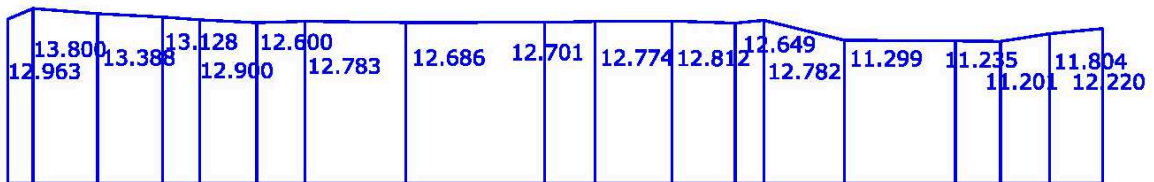
SEZ 7



SEZ 8



SEZ 9



SEZ 10

0 5 10 m

Figure 3.23 Longitudinal sections of Arena gardens

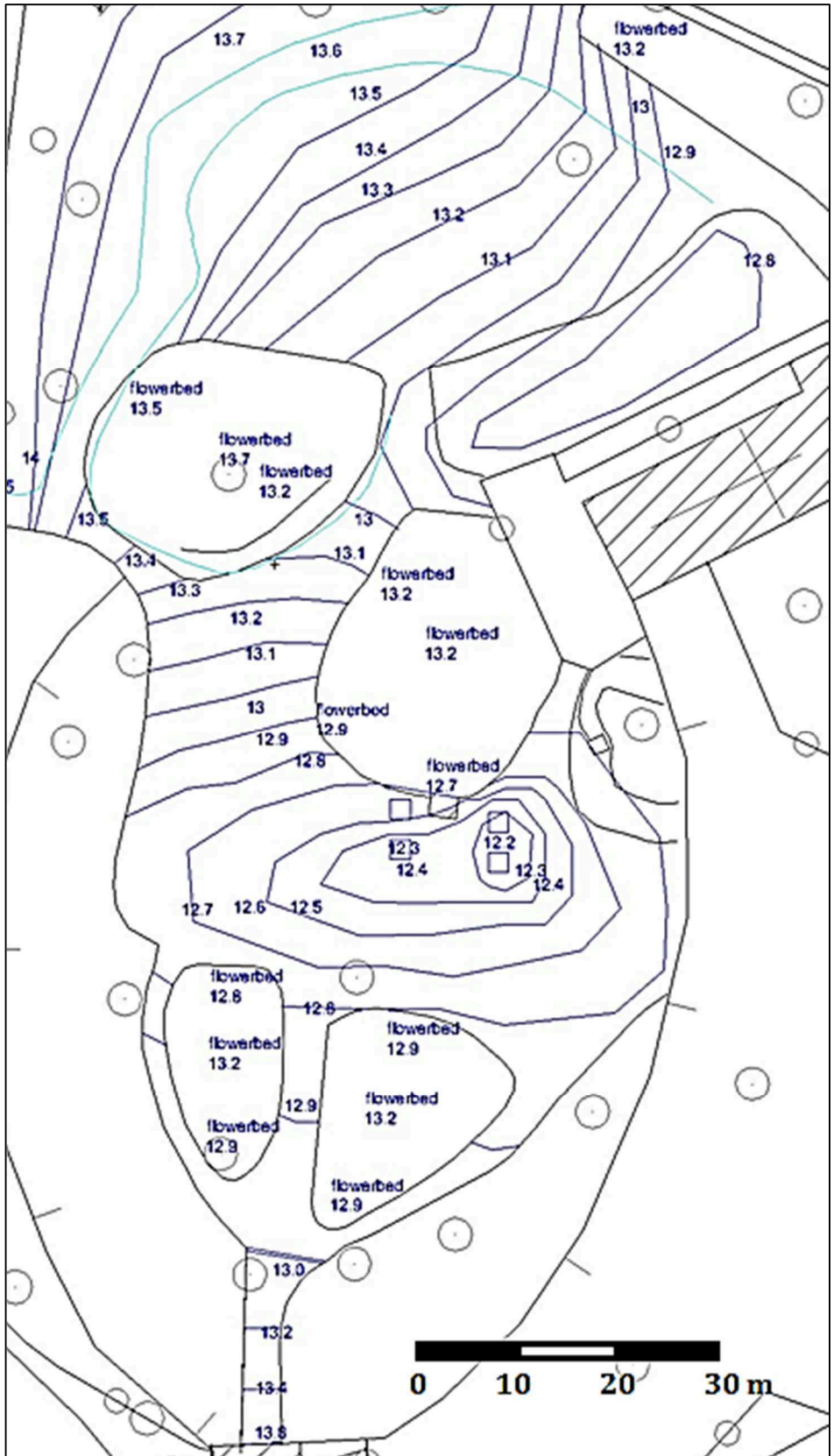


Figure 3.24 Redrawing of slopes in the area of Arena with proper level curves





# 4. S.W.M.M.: Storm Water Management Model

## 4.1 Software

A new drainage network has been designed to solve flooding problem around Scrovegni Chapel: the system is designed with Rational method, that is the most suitable method to estimate urban watersheds. The software used to verify the effectiveness of the study is the EPA Storm Water Management Model (SWMM), produced and developed by the Water Supply and Water Resources Division of the Environmental Protection Agency (EPA).

SWMM was developed in 1971 and over the years it has undergone continuous development and improvement up to the version that is used in this study, the 5.0.

It continues to be widely used throughout the world for planning, analysis and design related to storm water runoff, combined sewers, sanitary sewers, and other drainage systems in urban areas, with many applications in non-urban areas as well. The current edition, Version 5, is a complete re-write of the previous release. Running under Windows, SWMM 5 provides an integrated environment for editing study area input data, running hydrologic, hydraulic and water quality simulations, and viewing the results in a variety of formats. These include color-coded drainage area and conveyance system maps, time series graphs and tables, profile plots, and statistical frequency analyses.

This latest version is a rewrite of the previous version using a different programming language (from the old Fortran77 to the latest C ++), but it is always based on the same computational structure.

SWMM offers the possibility of performing hydraulic calculations and simulations on a network of channels or pipes, which is stressed by meteoric phenomena or inputs from different sources.

The use of this model requires an integral description of the analyzed area: the program by modeling many parameters only checks the truthfulness of calculations in retrospect.

The transport flow is generated through a system which is composed of channels, pipes, pumps, pumping stations and storage units. The program is estimated as the flow of water into the sewer system varies according to the variation of rainfall and its duration, considering all the possible variables: evaporation of surface water that is not subject to runoff, infiltration of rain in unsaturated soil, leaching of infiltrated water into groundwater, any accumulation of snow on the surface and its subsequent dissolution.

The use of S.W.M.M. is useful for assessing whether the sizing of a drainage system is precautionary (flooding should be avoided, even in case of critical conditions), but can also be used to estimate the propagation of pollutants, in order to predict and size the plants involved in the treatment of harmful substances. The results provided by the program are available in both graphical and tabular form [U.S. EPA, 1992].

SWMM conceptualizes a drainage system as a series of water and material flows between several major environmental compartments. These compartments and the SWMM objects they contain include:

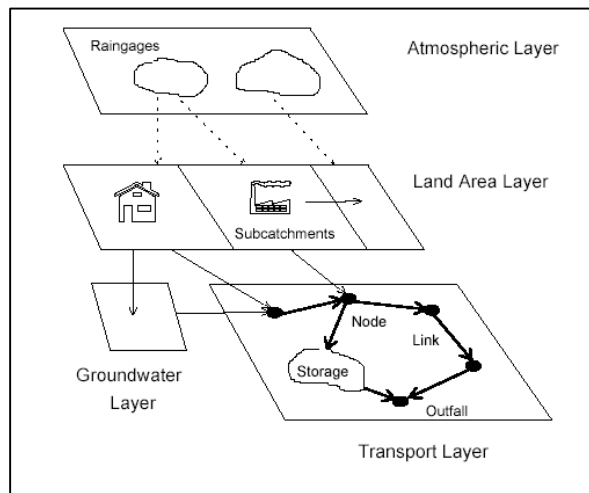


Figure 4.1 Layers in SWMM

**ATMOSPHERE:** from which precipitation falls and pollutants are deposited onto the land surface compartment. SWMM uses Rain Gage objects to represent rainfall inputs to the system. In atmosphere the values of rainfall simulation uses for precipitation on the basin are defined. It is possible to run simulations of critical events ranging from rain to urge the catchment studied:

- A "single event", ie simulations lasting a few hours;
- "Continuous" or simulations lasting several days or months.

**TERRITORY:** Land Surface compartment, which is represented through one or more Subcatchment objects. It receives precipitation from the Atmospheric compartment in the form of rain or snow; it sends outflow in the form of infiltration to the Groundwater compartment and also as surface runoff and pollutant loadings to the Transport compartment.

**GROUNDWATER:** receives infiltration from the Land Surface compartment and transfers a portion of this inflow to the Transport compartment. This compartment is modeled using Aquifer objects.

*TRANSPORT*: This layer contains the network of channels, pipelines, artifacts. SWMM uses a topological description of the network based on a geometry created from branches and nodes: they have specific properties which combined together are used to represent the entire network of hydraulic flow.

In this area the computation of the network propagation is done by choosing between different forms: steady state flow or dynamic flow that is based on the complete resolution of the equations of De Saint Venant. In the second case the program allows you to make more accurate calculations, also phenomena such as backwater, free surface and pressurized state, and reversion of the flow are modeled.

As can be seen from Figure 4.2, the calculation program appears to be basically structured in a modular manner, made up of individual blocks with a specific function and calculation routines.

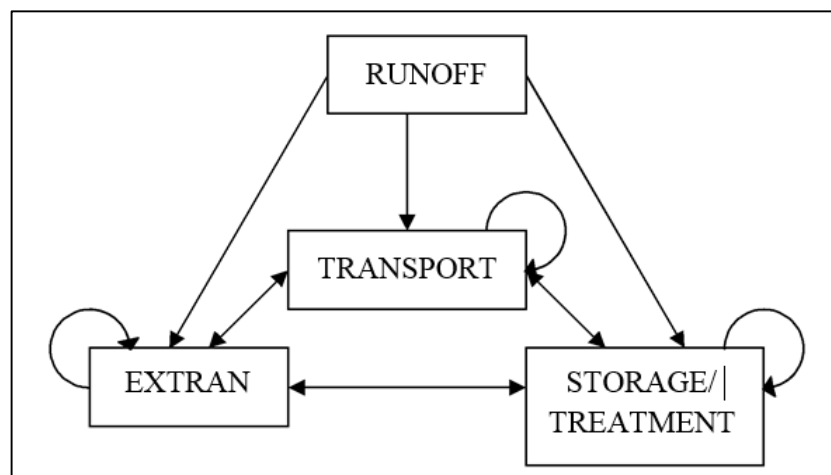


Figure 4.2 Possible relations between the different SWMM blocks

Each block can be used individually or in cascade (Figure) so that the result can be seen as a start point for the use of the subsequent block with the exception of the block Runoff which admits as inputs only the meteorological data from the modules and Rain and Temperature.

S.W.M.M. is able to represent the various hydrological processes that produce runoff both from urban areas and not. These processes include:

- precipitation;
- evaporation of water;
- accumulation and snowmelt;
- infiltration of rain in the layers of the unsaturated soil;
- percolation of infiltrated water into groundwater layers;
- interflow between groundwater and the drainage system;

## **4.2 Short description of the SWMM blocks**

As already mentioned the program is divided into two modules: one of service and another one Computational.

The first module contains many blocks that are used to process the results obtained; In fact you can perform statistical operations on the values obtained from the simulations (Statistic block), meteorological and climate data are managed to be included in the program, or are used in continuous type simulations (Temperature and Rain blocks), to manage the results obtained through graphics and prints (Graph block), adjust the output values in order to aggregate data that can be used as cascade blocks (Combine block).

Executive block belongs to the service module, which manipulates the interface files between the various blocks and the block, or the sequence of blocks, to be executed.

The Computational module contains four blocks with the related hydrological and hydraulic process simulators: a block for surface runoff modeling (block Runoff), one for calculation of the propagation in the network with the kinematic wave schematization (Transport), the third is a block of dynamic calculation based on the full resolution of the De Saint Venant equations that govern the hydraulic phenomenon of propagation within the network (Extran), and finally, one which describes the processes within a sewage treatment plant (Storage / Treatment).

The Runoff block is the first step of a simulation in SWMM. It receives as input any meteorological data recorded in the Rain and/or Temperature blocks, or you can enter the hyetographs (with rainfall intensity/time or total precipitation in mm/time) defined by the user.

Runoff analyzes the rainfall-runoff process using an approach based on the technique of non-linear reservoirs with an option for the calculation of water intake caused by snow melting. The processes of infiltration and evaporation are analyzed too, in order to obtain a tracked hydrograph as a result in each branch of the network studied. The block can be set to perform simulations for time periods ranging from minutes to years.

Runoff also offers the possibility of simulating the quality of water, studying the processes of moving surfaces contaminated from the draining surfaces to sewer.

As an output of this block hydrographs are obtained, they serve as input to the drainage network.

The Transport block, which can follow the launch of Runoff, goes to model the quality and quantity behavior of the system, relying on the hydraulic calculation of kinematic wave schematization. The qualitative analysis is based on first order kinetics, with Shield criteria on initialization of the motion. The results are levels, flow rates and concentrations of

contaminants for each component of the network, that is shown schematically in a system of branches and nodes.

Storage/ Treatment block is essentially a specialization of Transport; it can simulate three pollutants in a tank containing up to five units or processes. The block also simulates the decay processes of the first order, associated to a complete mixing, removal functions and sedimentation dynamic. It is also possible to calculate a prediction of starting-up, management and maintenance costs for each unit of processing.

The block Extran, Extended Transport, is basically the hydraulic "heart" of SWMM; it makes possible to model the outflows propagation within the network, using the full resolution of De Saint Venant equations. Extran turns out to be a complete module for the simulation of tree or mesh networks; also regurgitation phenomena, reversals of the flow in the branches, the motions at free surface and under pressure are modeled.

Extran uses a topological description of the network based on a branched geometry nodes; branches and nodes have specific characteristics, suitably configured, which, in combination, allow the description of the entire network of hydraulic flow. In the schematization used by the block, the branches are essentially conduits of the drainage system (canals in the case of open sections) and allow you to spread the flow from one node to another. The nodes represent the wells that exist in the sewage system (or the points of intersection of the branches, for channels); the nodes are localized flow input (from the runoff and expressed as hydrographs generated from rainfall-runoff model) and the flow that exit from the network.

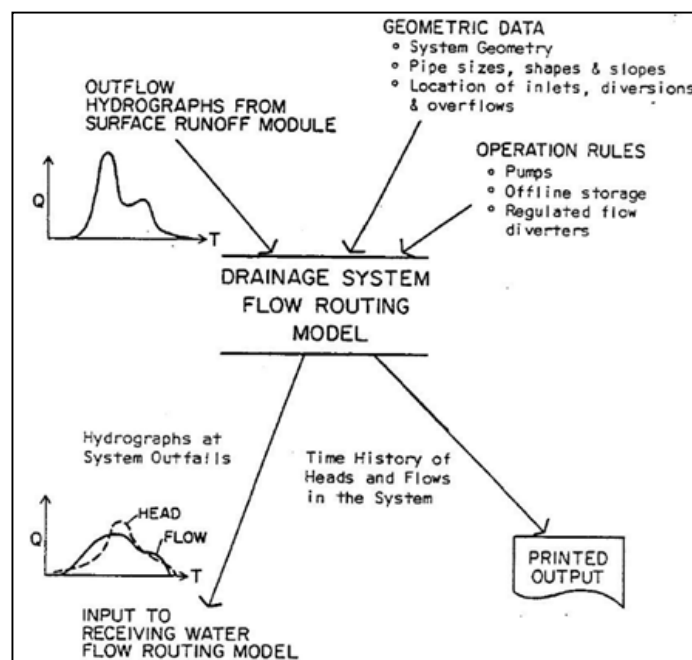


Figure 4.3 Flow routing model description.

The use of Extran block is recommended when it is necessary to represent regurgitation conditions and reverse flow, and when there are special regulating elements such spillways, pumps and reservoirs. The simulation for channels and small pipelines, where the hypothesis of non-linear cascade reservoirs and uniform motion are best suited to the characteristics of the Runoff-Transport modules, which allow a saving of resources being simpler (data, lower computing power, less simulation time) [U.S. EPA, 1992].

### **4.3 Structure and operation of hydraulic routine**

SWMM uses a description "branches-nodes" of the system for drainage of water, thereby facilitating the discrete representation of the physical model and the mathematical solution of the equations of motion gradually-varied (De Saint Venant) which constitute the basis of the mathematical model and Extran block.

The drainage network, as already previously explained, is idealized as a series of branches, each one associated to a geometric shape, connected together at the nodes.

The properties constants associated to the branches, are the section type, length, slope and roughness; the flow rate, the speed, the wet area of the flow, the hydraulic radius and the width of the free surface are determined at every step of the calculation; the last three properties are a function of the instantaneous water level.

The fundamental independent variable in the branches is the flow rate  $Q$ , and is assumed constant in each branch during a step of the calculation. Speed and wet area of the flow, or the level, are quantities that varies in the same branch.

The constant properties associated to the nodes are sliding or input level of the branch respect to the ground; the volume, the area of the free surface and the hydraulic load  $H$  are the properties that are determined at every step of the calculation and function of the water level in the node. The independent key variable in the nodes is the hydraulic load, time variable, but constant in single node during a computation step. Inflows and outflows occur at the nodes of the system. The volume change in the node during a given step of the calculation is the basis for the following calculations of flow rate and hydraulic load.

#### *4.3.1 Fundamental equations of SWMM code*

The equations that the program uses are classic differential partial derivatives equations of the first order of De Saint Venant:

$$\frac{\partial A}{\partial t} + \frac{\partial Q}{\partial x} = 0 \quad (4.2)$$

$$\frac{\partial Q}{\partial t} + \frac{\partial \left( \frac{Q^2}{A} \right)}{\partial t} + gAS \frac{\partial H}{\partial x} + gaS_f = 0$$

A wet area of the flow;

Q flow rate;

x distance along the axis of the conduit;

t time;

g gravity constant;

H total hydraulic load, given by  $z + h$ ;

z flux level;

h water level;

Sf falling water table.

The first equation is continuity equation of a various motion without lateral inflows and outflows. A, considering a constant section conduit, depends only on  $h(x,t)$  level and not from x distance. If B represents the width of the flow when there is the free water table level,  $dA/dt=B*dz/dt$ .

Equation 4.2 is the equation of the moment of momentum, and represents the single pressure drop for continuous resistances. This last equation can be written in many ways, depending on the independent variables chosen.

The De Saint Venant System is impossible to solve analytically, so many solutions are adopted in a numerical way, and for example they are transformed in algebrical equations that are valid for a limited number of sections.

By unifying the equation of the moment of momentum and continuity equation, a third equation is obtained and this is solved for each pipe and for each step of calculus:

$$\frac{\partial Q}{\partial t} + gaS_f - 2V \frac{\partial A}{\partial t} - V^2 \frac{\partial A}{\partial x} + gA \frac{\partial H}{\partial x} = 0 \quad (4.3)$$

With:

Q Flow rate along the conduit;

V average speed along the conduit;

A cross-sectional wet area of the conduit ;

H hydraulic load;

Sf water table falling.

Equation 4.3 is obtained from 4.2 by replacing the following identities:



$$\frac{Q^2}{A} = V^2 A \quad (4.4)$$

$$\frac{\partial V^2 A}{\partial x} = 2AV \frac{\partial V}{\partial x} + V^2 \frac{\partial A}{\partial x} \quad (4.5)$$

And from 4.2:

$$\frac{\partial Q}{\partial t} + gaS_f + 2AV \frac{\partial V}{\partial x} + V^2 \frac{\partial A}{\partial x} + gA \frac{\partial H}{\partial x} = 0 \quad (4.6)$$

The continuity equation (4.1) may be reformulated to substitute the second term in 4.6, known that  $Q=AV$ :

$$\frac{\partial A}{\partial t} + A \frac{\partial V}{\partial x} + V \frac{\partial A}{\partial x} = 0 \quad (4.7)$$

So multiplying to V:

$$AV \frac{\partial V}{\partial t} = -V \frac{\partial A}{\partial t} - V^2 \frac{\partial A}{\partial x} \quad (4.8)$$

The, 4.8 is substituted in 4.6 and equation 4.3 is obtained from motion equation, resolved along the branches in SWMM:

$$\frac{\partial Q}{\partial t} + gaS_f - 2V \frac{\partial A}{\partial t} - V^2 \frac{\partial A}{\partial x} + gA \frac{\partial H}{\partial x} = 0 \quad (4.3)$$

The formula utilized to describe the pressure drop (piezometric falling) is defined through Manning equation:

$$S_f = \frac{k}{gAR^{\frac{4}{3}}} Q|V| \quad (4.9)$$

-k parameter  $gn^2$ ;

-n Manning roughness coefficient;

-g gravitational constant;

-Q flowrate;

-V medium spees;

-R hydraulic radius.

The presente of V value as absolute value transform  $S_f$  in a directional size and assure thatfriction forces oppose to motion [U.S. EPA, 1992].

#### 4.3.2 Flow Routing

Flow routing within a conduit link in SWMM is governed by the conservation of mass and momentum equations for gradually varied, unsteady flow (i.e., the Saint Venant flow equations). The SWMM user has a choice on the level of sophistication used to solve these equations: Steady Flow Routing, Kinematic Wave Routing, Dynamic Wave Routing.

#### 4.3.2.1 *Steady Flow Routing*

Steady Flow routing represents the simplest type of routing possible (actually no routing) by assuming that within each computational time step flow is uniform and steady. Thus it simply translates inflow hydrographs at the upstream end of the conduit to the downstream end, with no delay or change in shape. The normal flow equation is used to relate flow rate to flow area (or depth).

This type of routing cannot account for channel storage, backwater effects, entrance/exit losses, flow reversal or pressurized flow. It can only be used with dendritic conveyance networks, where each node has only a single outflow link (unless the node is a divider in which case two outflow links are required). This form of routing is insensitive to the time step employed and is really only appropriate for preliminary analysis using long-term continuous simulations.

#### 4.3.2.2 *Kinematic Wave Routing*

This model is obtained when kinetic term and  $dh/dx$  term (insignificant respect to ground slope  $i$ ) are neglected, so the system becomes:

$$\frac{\partial Q}{\partial x} + B \frac{\partial h}{\partial t} = 0$$
$$j = L$$

This routing method solves the continuity equation along with a simplified form of the momentum equation in each conduit. The latter requires that the slope of the water surface equal the slope of the conduit.

The maximum flow that can be conveyed through a conduit is the full normal flow value. Any flow in excess of this entering the inlet node is either lost from the system or can pond atop the inlet node and be re-introduced into the conduit as capacity becomes available.

Kinematic wave routing allows flow and area to vary both spatially and temporally within a conduit. This can result in attenuated and delayed outflow hydrographs as inflow is routed through the channel. However this form of routing cannot account for backwater effects, entrance/exit losses, flow reversal, or pressurized flow, and is also restricted to dendritic network layouts. It can usually maintain numerical stability with moderately large time steps, on the order of 5 to 15 minutes. If the aforementioned effects are not expected to be

significant then this alternative can be an accurate and efficient routing method, especially for long-term simulations [Larry W. Mays, 2001]..

This method is useful for investigation propagation with a huge slope of the ground so with torrent characteristics

#### 4.3.2.3 *Dynamic Wave Routing*

Dynamic Wave routing solves the complete one-dimensional Saint Venant flow equations and therefore produces the most theoretically accurate results.

This routing method is obtained by neglecting only the kinetic terms of motion equation.

$$\frac{\partial Q}{\partial x} + B \frac{\partial h}{\partial t} = 0$$

$$\frac{\partial h}{\partial x} = i - J$$

These equations consist of the continuity and momentum equations for conduits and a volume continuity equation at nodes.

With this form of routing it is possible to represent pressurized flow when a closed conduit becomes full, such that flows can exceed the full normal flow value. Flooding occurs when the water depth at a node exceeds the maximum available depth, and the excess flow is either lost from the system or can pond atop the node and re-enter the drainage system [Larry W. Mays, 2001].

Dynamic wave routing can account for channel storage, backwater, entrance/exit losses, flow reversal, and pressurized flow. Because it couples together the solution for both water levels at nodes and flow in conduits it can be applied to any general network layout, even those containing multiple downstream diversions and loops. It is the method of choice for systems subjected to significant backwater effects due to downstream flow restrictions and with flow regulation via weirs and orifices. This generality comes at a price of having to use much smaller time steps, on the order of a minute or less (SWMM will automatically reduce the user-defined maximum time step as needed to maintain numerical stability). Each of these routing methods employs the Manning equation to relate flow rate to flow depth and bed (or friction) slope. The one exception is for circular Force Main shapes under pressurized flow, where either the Hazen-Williams or Darcy-Weisbach equation is used instead.

### **4.4 Schematization of the drainage area**

A network of channels in order to be implemented in SWMM, needs to be schematized with key elements well characterized (Figure 4.4).

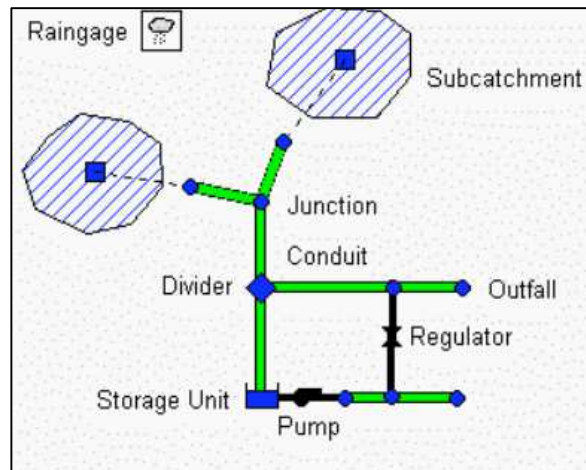


Figure 4.4 Schematization of SWMM physical elements

**Nodes:** Nodes are points of a conveyance system that connect conveyance links together. Junctions are drainage system nodes where links join together. Physically they can represent the confluence of natural surface channels, manholes in a sewer system, or pipe connection fittings.

External inflows can enter the system at junctions. Excess water at a junction can become partially pressurized while connecting conduits are surcharged and can either be lost from the system or be allowed to pond atop the junction and subsequently drain back into the junction.

Some nodes play an important role in the reproduction of the network represented in SWMM, because they represent the site of release of runoff. The whole flow of the sub catchment is schematically shown by the software in such a way as to converge in a single point, represented by the start node of the drainage channel.

**Links:** Links are the conveyance components of a drainage system and always lie between a pair of nodes. Conduits are pipes or channels that move water from one node to another in the conveyance system. Their cross-sectional shapes can be selected from a variety of standard open and closed geometries.

In the representation process of the hydraulic network, each channel should be divided into several branches, and in the corresponding nodes. Each branch is modeled as a pipe with constant characteristics of shape, slope, roughness, etc. so any branch represents each different variation of the channel, each confluence of more collectors, bottom opening, depth variations or section. In the same node more branches can converge together, each pipe at a different height compared with the bottom.

An interesting point is the maximum height that can be reached by the node; in the case of channels and nodes that are open, this represents the level of altitude beyond which there is

a leakage of water and this level is calculated taking into account the heights of the channels that are convergent in the node.

*Outfall Nodes:* Outfalls are terminal nodes of the drainage system used to define final downstream boundaries under Dynamic Wave flow routing.

The boundary conditions at an outfall can be described by any one of the following stage relationships:

- the critical or normal flow depth in the connecting conduit
- a fixed stage elevation
- a tidal stage described in a table of tide height versus hour of the day
- a user-defined time series of stage versus time.

*Pumps:* Pumps are links used to lift water to higher elevations. Il funzionamento di queste deve essere definito da una specifica relazione tra la portata sollevata ed una condizione dei nodi ai quali è collegata. A pump curve describes the relation between a pump's flow rate and conditions at its inlet and outlet nodes.

*Storage Units:* Storage Units are drainage system nodes that provide storage volume. Physically they could represent storage facilities as small as a catchbasin or as large as a lake. The volumetric properties of a storage unit are described by a function or table of surface area versus height. In addition to receiving inflows and discharging outflows to other nodes in the drainage network, storage nodes can also lose water from surface evaporation and from infiltration into native soil.

The principal input parameters for storage units include:

- invert (bottom) elevation
- maximum depth
- depth-surface area data
- evaporation potential
- seepage rate (optional)
- external inflow data (optional).

*Weir:* Weirs, like orifices, are used to model outlet and diversion structures in a drainage system. Weirs are typically located in a manhole, along the side of a channel, or within a storage unit. They are internally represented in SWMM as a link connecting two nodes, where the weir itself is placed at the upstream node. A flap gate can be included to prevent backflow. Four varieties of weirs are available, each incorporating a different formula for computing flow as a function of area, discharge coefficient and head difference across the weir:



- Transverse (rectangular shape)
- Side flow (rectangular shape)
- V-notch (triangular shape)
- Trapezoidal (trapezoidal shape).

Weirs can be used as storage unit outlets under all types of flow routing. If not attached to a storage unit, they can only be used in drainage networks that are analyzed with Dynamic Wave flow routing.

*Orifices:* Orifices are used to model outlet and diversion structures in drainage systems which are typically openings in the wall of a manhole, storage facility, or control gate. They are internally represented in SWMM as a link connecting two nodes. An orifice can have either a circular or rectangular shape, be located either at the bottom or along the side of the upstream node, and have a flap gate to prevent backflow. Orifices can be used as storage unit outlets under all types of flow routing. If not attached to a storage unit node, they can only be used in drainage networks that are analyzed with Dynamic Wave flow routing.

## **4.5 Hydrological elements**

### *4.5.1 Subcatchments description*

Subcatchments are hydrologic units of land whose topography and drainage system elements direct surface runoff to a single discharge point. The user is responsible for dividing a study area into an appropriate number of subcatchments, and for identifying the outlet point of each subcatchment. Discharge outlet points can be either nodes of the drainage system or other subcatchments.

Subcatchments are divided into pervious and impervious subareas. Surface runoff can infiltrate into the upper soil zone of the pervious subarea, but not through the impervious subarea. Impervious areas are divided into two subareas - one that contains depression storage and another that does not. Runoff flow from one subarea in a subcatchment can be routed to the other subarea, or both subareas can drain to the subcatchment outlet.

Concerning the different basins there are many parameters that must be defined to characterize the area. It is necessary to insert in the program SWMM the values of the different areas that have been identified, and then to define physical values as the mean slope of the basin, the width, the description of permeable and impermeable area through the Manning coefficient and the surface depressions height.

The parameters are defined by the program:

**Area and slope:** Area value (ha) and average percent slope of the basin

**Width:** Characteristic width of the overland flow path for sheet flow runoff (feet or meters). An initial estimate of the characteristic width is given by the subcatchment area divided by the average maximum overland flow length. The maximum overland flow length is the length of the flow path from the outlet to the furthest drainage point of the subcatchment. Maximum lengths from several different possible flow paths should be averaged. These paths should reflect slow flow, such as over pervious surfaces, more than rapid flow over pavement, for example. Adjustments should be made to the width parameter to produce good fits to measured runoff hydrographs.

**% impervious area:** percent of the land area which is impervious. This value is completed by the definition of the Manning's n for overland flow over the impervious and pervious portion of the subcatchments

**Surface depression storage:** depth of depression storage on the impervious portion of the subcatchment (inches or millimeters). The height of water in surface depressions is considered as a loss caused by several factors, among which we can mention the stagnation of water and interception by the roughness of the terrain and surfaces.

The water stored in the permeable surfaces' depressions infiltrates or evaporates, so it is continuously and quickly replaced, and in an impermeable surface this is depleted only by evaporation, and is renewed more slowly. A percentage of impervious surfaces' area in which there are no depressions and no storage of water is defined: a part of the impervious surfaces responds immediately, generating a surface flow in a short time.

For the surface runoff, S.W.M.M. uses a conceptual model in which each sub-basin is expressed as a non-linear reservoir with a single input in a node. The tank capacity is the maximum value of depression storage, and losses result from surface runoff, infiltration and evaporation.

The surface runoff can begin only if the height of the storage tank is higher than the depression value  $d_p$ , that is firstly established and it changes according to the nature of the soil, permeable or not [U.S. EPA, 1992]..

#### 4.5.2 *Rainfall representation*

To design a drainage work or to verify the proper operation an existing structure, it is necessary to simulate the effects of a strong rainfall event on the basin. This rainfall event is taken as a reference. The rain of the project can be obtained from an exceptional event that was actually observed or represented by a hypothetical event that has been defined artificially. The attribution of a strong rainfall to the catchment is used to calculate the flow and to size the elements of the hydraulic network, so that they are designed to resist to the maximum flow that is coming into the system.

Rainfalls events in SWMM are defined by defining Rain Gages that provide rainfall data on the subcatchments. These data can be entered manually in SWMM through appropriate editor, or

they can be loaded from an external text file. The main properties input of rain gages include information about the intensity or the amount of rain and the amount of data logging (hourly, 30 minutes, 15 minutes, etc).

Rain Gages supply precipitation data for one or more subcatchment areas in a study region. The rainfall data can be either a user-defined time series or come from an external file. Several different popular rainfall file formats currently in use are supported, as well as a standard user defined format.

The principal input properties of rain gages include:

- rainfall data type (e.g., intensity, volume, or cumulative volume)
- recording time interval (e.g., hourly, 15-minute, etc.)
- source of rainfall data (input time series or external file)
- name of rainfall data source

#### 4.5.3 Surface runoff

The surface runoff is created by a fraction of the rainfall that flows on the surface and is collected by the drainage network. The phenomena as infiltration, interception and accumulation in the surface storage depressions are the main losses in the simulations, so they are subtracted from the total meteoric supply giving the value of net rainfall that contributes to the surface runoff.

The surface runoff is below resumed:

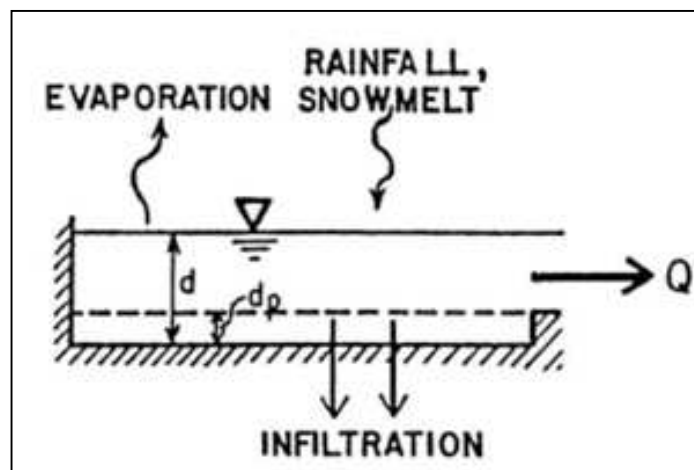


Figure 4.5 Hydrological cycle representation

Each basin surface is treated as a non linear reservoir. The input values are obtained from rainfall events or snow melting and the output are different and are represented by evaporation, infiltration and run-off. The volume of this tank is represented by the maximum storage capacity of the depressions; it is the volume of water intercepted by depressions, bumps and surface ponding.

The runoff per unit area,  $Q$ , triggers whenever the height of water in the tank exceeds the value of the depressions  $d_p$ , and in this case the flow that exits is given by the equation:

$$Q = W \frac{1,49}{n} (d - d_p)^{\frac{5}{3}} * S^{\frac{1}{2}}$$

$Q$  = surface runoff;

$W$  = width of the basin;

$n$  = Manning coefficient;

$d$  = water height;

$d_p$  = surface depressions height;

$S$  = slope of the subcatchments.

The height of water in the sub-basins is continuously updated during the calculation, numerically solving a balance of water.

#### 4.5.4 *Hydrological losses*

The physical phenomena occurring within the drainage basin in conjunction with an event of rain and causing major hydrological losses substantially are:

- Interception, evaporation and transpiration due to the presence of vegetation;
- Ponding in surface depressions; Infiltration in permeable surfaces.

For individual rainfall events, the only components to be assessed are: the accumulation of water in depressions and infiltration on permeable surfaces. The evaluation of the losses for interception or evapotranspiration become important only if we consider long periods in which the rain is interspersed with periods of dry weather.

The retention of water in surface depressions is more relevant in impervious areas than those permeable, also because in the latter it is difficult to distinguish it from the infiltration; the significant difference between the volumes of water accumulated depends on the irregularities of the real surfaces, on different slope, and on water retention that anyway participates to outflow. After the rainfall event volumes subtracted by retention are again included in the hydrological cycle, as a result of evaporation and infiltration.

#### 4.5.5 *Infiltration*

The more consistent hydrological loss in a subcatchment is infiltration. Infiltration rate is defined as the volume of water that infiltrates in a time unit through unit area of the ground. It has the size of a velocity and it is defined as mm/h. it depends on different factors:

- Scope of precipitation
- Soil structure (it depends on the possibility of infiltration, greater in the case of sandy soils compared to clays);

- Water content in the soil at the time of precipitation (a higher moisture content makes infiltration more difficult).

Table 4.1 Soil group definition

Group	Meaning	Saturated Hydraulic Conductivity (in/hr)
A	Low runoff potential. Soils having high infiltration rates even when thoroughly wetted and consisting chiefly of deep, well to excessively drained sands or gravels.	$\geq 0.45$
B	Soils having moderate infiltration rates when thoroughly wetted and consisting chiefly of moderately deep to deep, moderately well to well-drained soils with moderately fine to moderately coarse textures. E.g., shallow loess, sandy loam.	0.30 - 0.15
C	Soils having slow infiltration rates when thoroughly wetted and consisting chiefly of soils with a layer that impedes downward movement of water, or soils with moderately fine to fine textures. E.g., clay loams, shallow sandy loam.	0.15 - 0.05
D	High runoff potential. Soils having very slow infiltration rates when thoroughly wetted and consisting chiefly of clay soils with a high swelling potential, soils with a permanent high water table, soils with a clay-pan or clay layer at or near the surface, and shallow soils over nearly impervious material.	0.05 - 0.00

SWMM offers three different methods to calculate infiltration:

- Green-Ampt method
- Horton method
- Curve Number method

#### 4.5.5.1 Green-Ampt method

The conceptual scheme is represented in Figure 4.6.

The model tells that infiltration process starts when a layer of water has been accumulated on the soil surface. The soil is characterized with initial moisture that is supposed to be homogeneous and equal to  $\theta_i$ .

The humid front is represented by an horizontal surface  $S_u$  that in the initial moment of infiltration process corresponds to  $S_h$ . Subsequently, while it is raining,  $S_u$  advances in the subsoil by moving in vertical direction and keeping the same arrangement, it is assumed that infiltration takes place by liquid vertical trajectories and with the infiltration velocity vector that is invariant in space.



When the humid front passes, the moisture assumes the value of the water storage capacity of the soil  $C_s$ . With  $\theta_r$  the residual moisture of the soil is defined, it persists after a long gravity drainage process [Da Deppo L. et al., 2004].

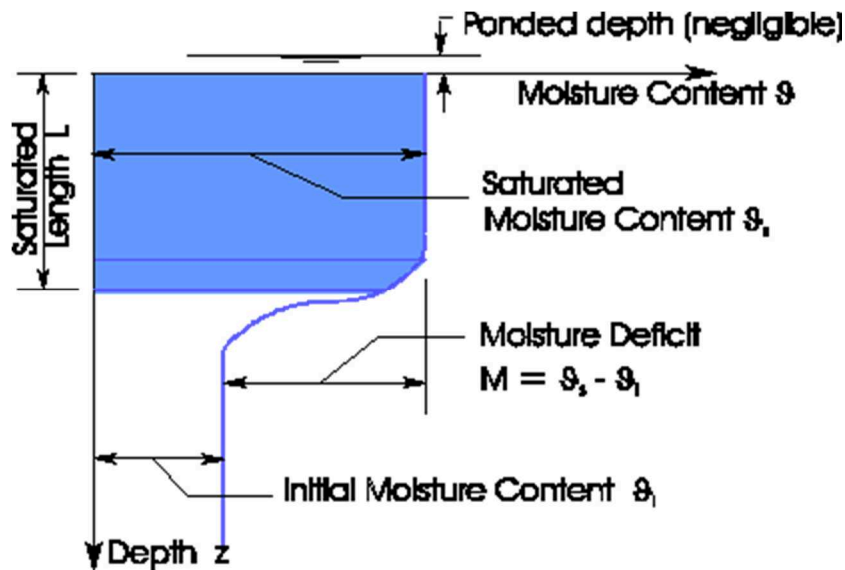


Figure 4.6 Green-Ampt process description

#### 4.5.5.2 SCS method

The method S.C.S. Curve Number, developed by the Soil Conservation Service, is a useful method to study the flow in the case of small rural basins. According to this method the total infiltration capacity of a soil is linked to the characteristics geopedological of the basin, to the intended use and to the initial conditions of the soil. At the start of the event volume  $V_0$  is required, and it is the volume needed for the saturation of the soil before the run-off. This parameter represents the initial loss that is dependent on the condition of the soil before the start of precipitation (usually the ground is taken as average wet). Since the absorption capacity of the soil is exhausted, a part of the precipitation infiltrates while the remainder contributes to the sliding surface [Da Deppo L. et al., 2004]. The volume that infiltrates from reached saturation until the time considered is:

$$\frac{V_i}{S} = \frac{P_e}{(P - V_0)}$$

Where  $S$  is the maximum infiltration capacity that is storable in the basin,  $P_e$  is the effective volume of rain (or the flow rate to be drained from the reservoir) and  $P$  the total volume flowed. You can have an immediate view looking at the graph in Figure 4.7:

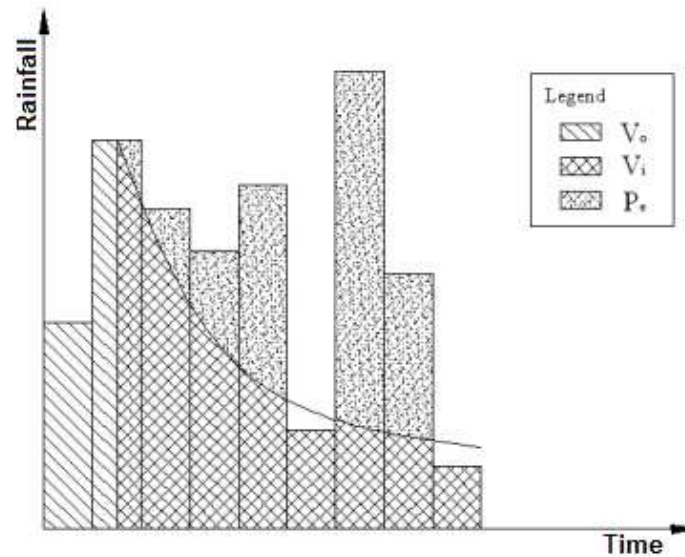


Figure 4.7 SCS method quantities

Utilizing the continuity equation:

$$P = Pe + Vo + Vi$$

The outflow relation that belongs to SCS method is:

$$P = \frac{(P - V_o)^2}{P - V_o + S}$$

Generally, for an average moisture soil, these values are assumed:

$$V_o = 0,2 S \text{ with } S = \frac{25400}{CN} - 254 \text{ [mm]}$$

Table 4.2 CN values proposed by SCS

Land Use Description	Hydrologic Soil Group			
	A	B	C	D
Cultivated land				
Without conservation treatment	72	81	88	91
With conservation treatment	62	71	78	81
Pasture or range land				
Poor condition	68	79	86	89
Good condition	39	61	74	80
Meadow				
Good condition	30	58	71	78
Wood or forest land				
Thin stand, poor cover, no mulch	45	66	77	83
Good cover <sup>2</sup>	25	55	70	77
Open spaces, lawns, parks, golf courses, cemeteries, etc.				
Good condition: grass cover on 75% or more of the area	39	61	74	80
Fair condition: grass cover on 50-75% of the area	49	69	79	84
Commercial and business areas (85% impervious)	89	92	94	95
Industrial districts (72% impervious)	81	88	91	93
Paved parking lots, roofs, driveways, etc. <sup>5</sup>	98	98	98	98

The CN parameter is a number whose value is between 0, completely permeable soil, and 100, totally impervious surfaces. The CN represents the attitude of the basin examined to produce runoff and is estimated in relation to the hydrological characteristics of the soil and vegetation cover located in the basin. The determination of this parameter requires knowledge of the hydrologic group of each soil analyzed.

#### 4.5.5.3 Horton method

This method is based on normalized curves of infiltration capacity compared to time and expressed a mathematic model. It demonstrates that infiltration in permeable areas exponentially decreases from a maximum value to a minimum one that is asymptotically reached, during a rainfall event. Soil infiltration capacity ( $t$ ) is defined as:

$$f(t) = f_c + (f_o - f_c)e^{-kt}$$

The factors are:  $f_o$  is infiltration at the beginning of the event,  $f_c$  is the limit infiltration value that is asymptotically reached and  $k$  is a depletion constant that specify the time step of  $f_o$  to become  $f_c$ .

The curves obtained for each couple of values  $f_c$  and  $k$ , with  $f_0$  varying, may be all included in a curve only through an horizontal. The depletion coefficient  $k$  describes the velocity of the function to decrease in time that is the time in which the dry soil gets saturated.

Horton model relates the infiltrated rainfall with the soil degree of saturation to evaluate the starting point of surface flow [Da Deppo L. et al., 2004].





## 5. Rainfall characterization

Since the meteorological events are very complex and variable, a statistical analysis of the precipitation measurements is used, then a prediction on frequency of more intense events, which significantly affect the size of a possible hydraulic work to be carried out, is extrapolated.

To define rain events amplitude and obtain a reliable analysis, historical data of precipitation are used to study the development of a uniform and sufficiently large sample of items.

Frequency is easily definable for data collected in the past, it is the number of times that a rainfall event has occurred in a wide series of events. To make an analysis looking to the future it is necessary to artificially extend the field of study to a large number of observations, identifying probability distribution to fit the known observations.

The processing of data, obtained from Annali Idrologici, aims to determine the intensity-duration equation of rainfall. To do this, a statistical approach based on the Gumbel distribution (or double exponential distribution) is adopted, because it studies the possible extreme events. The method of Gumbel bases his study on the probable frequency of non-exceedance of an event, which is the inverse of the return time, that is the average value of time (years) in which an event is on average equaled or exceeded.

In hydraulic works, when the risk associated with a certain event must be evaluate, firstly the probability that a formidable event (an event that meets or exceeds a given threshold design) occurs at least once during the expected life of the work is calculated.

Having a sufficiently long period of rain observations the pluviometric probability curve is easily obtained. Pluviometric curve describes the relationship between the maximum heights and durations of rain that can occur in a given area, for a given value of the return period.

This curve can be represented with good accuracy by the following exponential expression:

$h=at^n$  with  $a$  and  $n$  are two characteristic parameters of the pluviographic station under examination.

To analyze rainfall events in Padua there are two different sources:

1. Data from 1936 to 1994 can be found in Annali Idrologici.

2. Data from 1994 to 2014 have been registered in the Orta Botanico station, in Padua,

The data from the first source are maximum annual values for 1, 3, 9, 12, 24 hours of rainfall: data available are 5 for each year.

The second source is wider: these values are hourly registered so there are thousand of values. The more recent data have been analyzed and grouped to obtain the maximum yearly values in order to compare the two series and get them homogeneous [Da Deppo L. et al., 2004].

## 5.1 Comparison of historical rainfall data of Padua

The rainfall data that we have analyzed come from two different sources.

The data that we have been provided belong to a very wide period: from 1936 to 1994 we find data on Hydrological Annals and subsequent data were provided by the Regional Agency Veneto. The activities of observation and measurement were carried out in Italy by a dedicated service of the state defined and Servizio Idrografico e Mareografico Nazionale (SIMN), it was involved in obtaining and publishing measured variables in Hydrological Annals, activities now coordinated by the Regional Agencies (ARPAV in Veneto) and the Autonomous Provinces [Dal Maso, A., 2006].

The two categories of data, 1936-1994 and 1994-2014 have been analyzed from a statistical point of view to see if the content can be compared. The first section of data is longer than the second and within it, the acquired data are not very homogeneous and the variance will be greater than the variance of the latest data, which refer to a smaller period of time.

Table 5.1 Statistical characterization of rainfall data

		<u>1936-1994</u>			
		TIME OF RAINFALL (hours)			
		1	3	6	12
<b>AVERAGE</b>		29,63	39,87	47,47	55,94
<b>VARIANCE</b>		127,95	277,91	406,08	507,41

		<u>1994-2014</u>			
		TIME OF RAINFALL (hours)			
		1	3	6	12
<b>AVERAGE</b>		30,33	38,59	44,83	54,98
<b>VARIANCE</b>		103,81	207,61	309,01	626,50

If the averages are compared, it is evident that these are equal, and the two data samples appear homogeneous. The problem arises when we look at the variance, because it is very different from one sample to another, surely this problem is the width of the timeframe of the second sample, probably also by the change of the measuring instrument used data are heterogeneous with each other, many datas measured in this period time have been deleted because they were not so realistic.

In order to proceed and consider the data as a single sample, a statistical test will be done.

Given two random samples of measurements,  $(Y_1..Y_n)$  and  $(Z_1..Z_n)$  from two independent processes, there are three types of questions regarding the true standard deviations of the processes that can be addressed with the sample data. They are:

Are the standard deviations from the two processes the same?

Is the standard deviation of one process less than the standard deviation of the other process?

Is the standard deviation of one process greater than the standard deviation of the other process?

Formulation of the hypothesis:

$$H_0: \sigma_1^2 = \sigma_2^2$$

$$H_0: \sigma_1^2 \neq \sigma_2^2$$

The basic statistics for the test are the sample variances

$$s_1^2 = \frac{1}{N_1 - 1} \sum_{i=1}^{N_1} (Y_i - \bar{Y})^2$$

$$s_2^2 = \frac{1}{N_2 - 1} \sum_{i=1}^{N_2} (Z_i - \bar{Z})^2$$

and degrees of freedom  $v_1=N_1-1$  and  $v_2=N_2-1$ , respectively.

The test statistic is

$$F = \frac{s_1^2}{s_2^2}$$

The strategy for testing the hypotheses is to calculate the F statistic from the formula above, and then perform a test at significance level  $\alpha$ , where  $\alpha$  is chosen to be small, typically 0.01, 0.05 or 0.10.

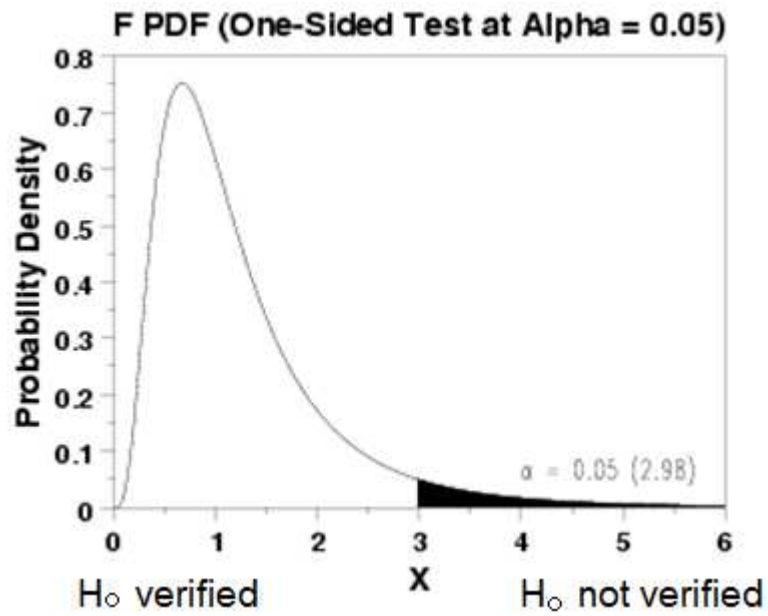
The two variances should be put in the report, placing the greatest variance in the numerator:

$$F = \left( \frac{127,95}{103,81} \right)^2 = 1,52$$

Once defined a significance level  $\alpha = 0.05$ , the table of critical values for that level, shows the value of which depends on the degrees of freedom of the numerator  $v_1$  and denominator  $v_2$ .

Table 5.2 Statistical characterization of the processes

	PROCESSES	
	1	2
<b>AVERAGE</b>	30,33	29,63
<b>VARIANCE</b>	103,81	127,95
<b>NUM</b>	22	43
<b>DEGREE OF FREEDOM</b>	21	42



Graph 5.1 Statistical representation of the analysis

Due to the fact that  $F_{\text{calc}} = 1,52$  is less than the critical value  $F_{\text{critical}} = 1,82$ , we can't reject  $H_0$  hypothesis, so the two variances are homogeneous and the two samples can be used joined. The complete rainfall data are listed in Annex I.



## 5.2 Analysis of data

For the determination of pluviometric curves the analysis of the cumulative frequency is used, these are built for the time series of the maximum annual rainy duration of 1, 3, 6, 12 hours, and through the Gumbel probabilistic model parameters to be used in the curves are identified.

Disposing of data, these are grouped for 3, 6, 12 hours.

Every year must be taken individually, and hourly data are grouped together to 3, 6, 12 hours getting 4 columns. Each of these columns is sorted in descending order and the first line that contains the annual maximum values recorded for various durations is extracted.

When this operation is performed for all the years of registration, a matrix is obtained (Annex II). The number of columns is equal to that of the durations analyzed and number of rows equal to the period of observation, 22 in this analysis.

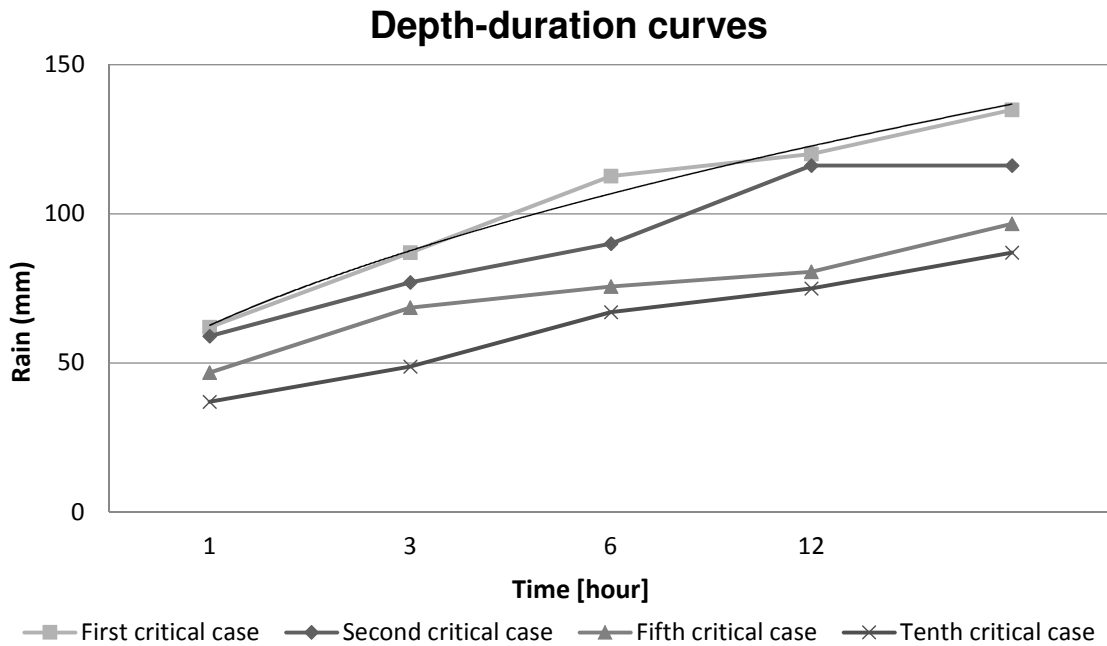
The columns of the matrix are re-arranged according to a descending order to study the events of major rain.

The first row of the matrix describes the first depth-duration curve that is a precipitation height representative of a very rare event.

Table 5.3 Rainfall data matrix. The entire table is listed in Annex II

YEAR	HOURLY RAIN				
	1 HOUR	3 HOURS	6 HOURS	12 HOURS	24 HOURS
1	62	87	112,6	134,6	158,20
2	59	77	92,4	120	134,8
3	56	73,4	90	116,2	116,2
4	54	71,8	82	103,2	104
5	52,8	70,8	80,6	101	98,60
6	51,6	68,6	75,6	86	97,40
7	46,8	68	75	82,2	97
8	45,2	66,4	73,8	80,6	96,6

...



Graph 5.2 Graphical representation of depth-duration curves

Data are analyzed for each duration of rainfall every time.

Heights of precipitation are organized in a descending order and the cumulative distribution function is defined for each row of the matrix.

The probable frequency of non-exceedance of an event is also known as the log-Weibull distribution

$$F_H (h_i) \approx F_H (y_i) = \frac{i}{N+1}$$

Con  $i \rightarrow$  position occupied by the  $i$ -th value recorded

$N \rightarrow$  total number of observations

The term  $N + 1$  is inserted in the denominator in order to prevent that the last value of the data series has unitary probability not to be exceeded, so that it represents certain event, and this is obviously not true, since a greater precipitation may be registered.

The analysis proceeds with the Gumbel distribution elaboration, which well fits the sample of studied data.

The cumulative distribution function of the Gumbel distribution is  $f(h) = \alpha e^{-\alpha(x-u)} - e^{-\alpha(x-u)}$

Its distribution function or probability density function is  $F(h) = e^{-e^{-\alpha(h-u)}}$

$$h = u - \alpha \ln[-\ln F(h)]$$

$F_H(h)$  is closely related to the return period  $T_R$ :  $T_R = \frac{1}{P[H \geq h]} = \frac{1}{1 - P[H \leq h]} = \frac{1}{1 - F_H(h)}$

Making  $h$  height of precipitation more clear, probability  $P[H \geq h]$  of exceedance is obtained and directly also  $P[H \leq h]$  probability of non-exceedance (cumulative distribution function).

The aim of the model is to detect the unknown parameters  $\alpha$  and  $u$ , by the creation of  $y$ :  $y = \alpha(h - u)$  reduced variable.

Gumbel distribution can be easily rewritten:

$$F_H(h_i) = e^{-e^{-y_i}}$$

For each  $i$ -th rainfall value and each  $F_H(h_i)$ , a  $y_i$  corresponds:  $F_H(h_i) \leftrightarrow y_i$

The definition of  $y_i$  reduced variable is derived:

$$F_H(y_i) = \frac{i}{N+1} = e^{-e^{-y}}$$

$$\ln\left(\frac{i}{N+1}\right) = -e^{-y}$$

$$-\ln\left(\ln\left(\frac{i}{N+1}\right)\right) = -y_i$$

$$y_i = -\ln\left(-\ln\left(\frac{i}{N+1}\right)\right)$$

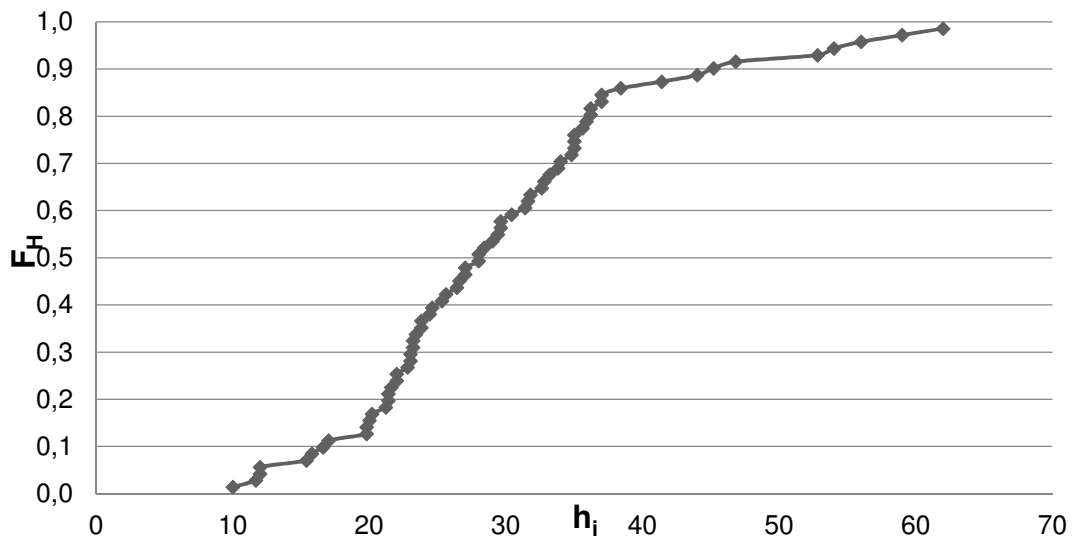
Once fixed the return time and duration of rain, by using the using double exponential method, the calculation of the pluviometric possibility curve proceeds. For each return period corresponds a different probability curve of rainfall, but if  $T_R$  is varying the exponent  $n$  should remain constant, as it depends on the characteristics of the place where precipitation are measured, while the coefficient  $a$  changes.

The curve is obtained, one for each duration of rainfall.

### 5.2.1 Analysis of 1 hour precipitations

$H_i$  and  $F_H(y_i)$  provide the following graph which describes the cumulative frequency distribution:

### Density–duration–frequency curve



Graph 5.3 Cumulative frequency distribution for 1 hour rainfall

Gumbel distribution (which depends on the parameters  $(\alpha, u)$ ) is adapted to the sample data, so values of  $\alpha, u$  that make minimum the sum of the distances of the points  $(h_i; y_i)$  from the line  $y = \alpha (h - u)$  are searched through the method of least squares.

Through average values  $m_h, m_y$ , and standard deviations  $S_h, S_y$ ,  $\alpha, u$  are immediately calculated for  $\tau = 1$  hour:

$m_h = \frac{\sum h_i}{N}$	$m_y = \frac{\sum y_i}{N}$
$S_y = \sqrt{\frac{\sum (y_i - m_y)^2}{N - 1}}$	$S_h = \sqrt{\frac{\sum (h_i - m_h)^2}{N - 1}}$
$\alpha = \frac{S_y}{S_h}$	$u = m_h - \frac{m_y}{\alpha}$

<b>m<sub>h</sub></b>	29,48
<b>m<sub>y</sub></b>	0,55
<b>S<sub>h</sub></b>	13,25
<b>S<sub>y</sub></b>	1,43
<b>α</b>	0,11
<b>u</b>	24,35



The possibility climatic curve pluviometrica should now be determined.

Once fixed  $Tr$  the definition shows

$$Tr = \frac{1}{P[H \geq h]} = \frac{1}{1 - P[H < h]} = \frac{1}{1 - F(h)} = \frac{1}{1 - e^{-e^{-\alpha(h-u)}}$$

The equation for the maximum height of rain  $f$  (duration,  $Tr$ ) is extrapolated

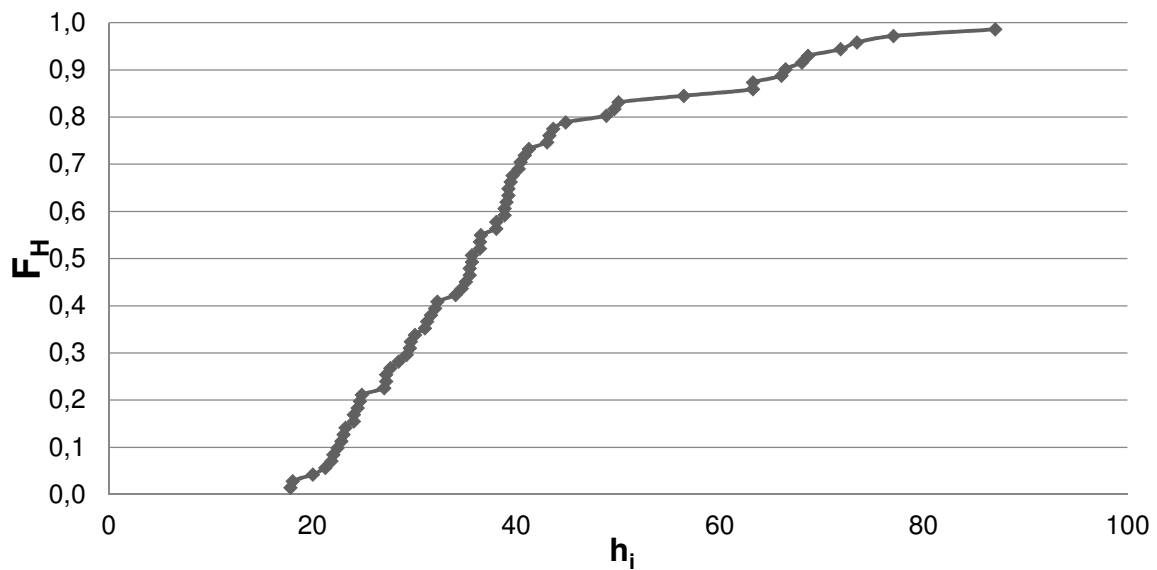
$$h_{1\ hour} = u - \frac{1}{\alpha} \ln\left(-\ln\left(\frac{1}{1 - Tr}\right)\right)$$

Table 5.4 Calculated values of 1 hour precipitation height  $f(Tr)$

Rainfall Time 1 hour	
Tr [years]	h [mm]
5	38,65
10	45,79
20	52,76
50	61,77
100	68,52

5.2.2 Analysis of 3 hours precipitations

**Density–duration–frequency curve**



Graph 5.4 Cumulative frequency distribution for 3 hours rainfall

<b>m<sub>h</sub></b>	38,56
<b>m<sub>y</sub></b>	0,55477
<b>S<sub>h</sub></b>	18,7027
<b>S<sub>y</sub></b>	1,43145
<b>α</b>	0,07654
<b>u</b>	31,3116

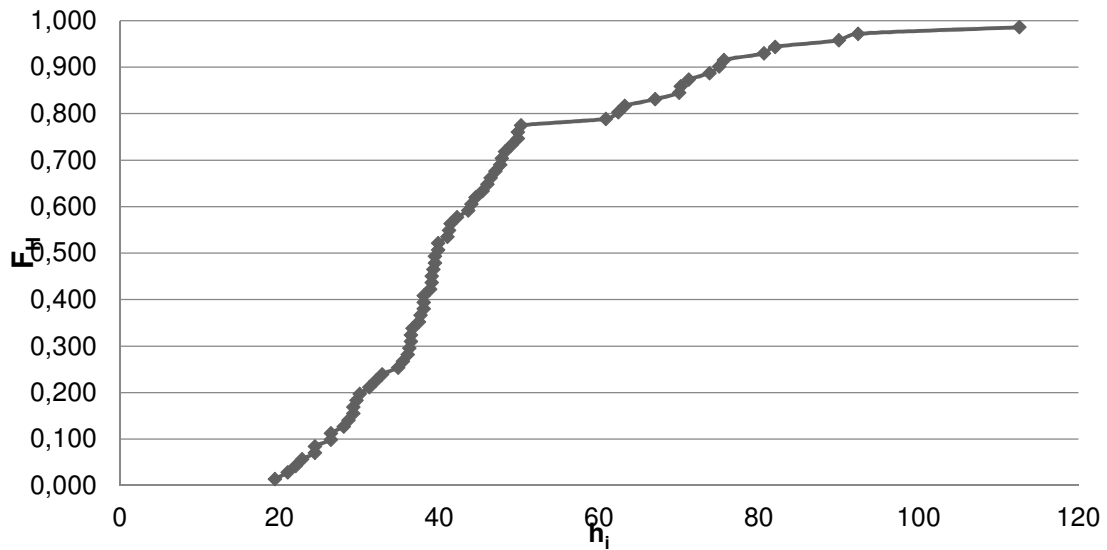
$$h_{3\text{ hours}} = u - \frac{1}{\alpha} \ln\left(-\ln\left(\frac{1}{1 - T_R}\right)\right)$$

Table 5.5 Calculated values of 3 hours precipitation height  $f(T_r)$

<b>Rainfall Time 3 hours</b>	
<b>Tr [years]</b>	<b>h [mm]</b>
5	52,42
10	60,17
20	69,35
50	81,22
100	90,11

### 5.2.3 Analysis of 6 hours precipitations

#### Density–duration–frequency curve



Graph 5.5 Cumulative frequency distribution for 6 hours rainfall

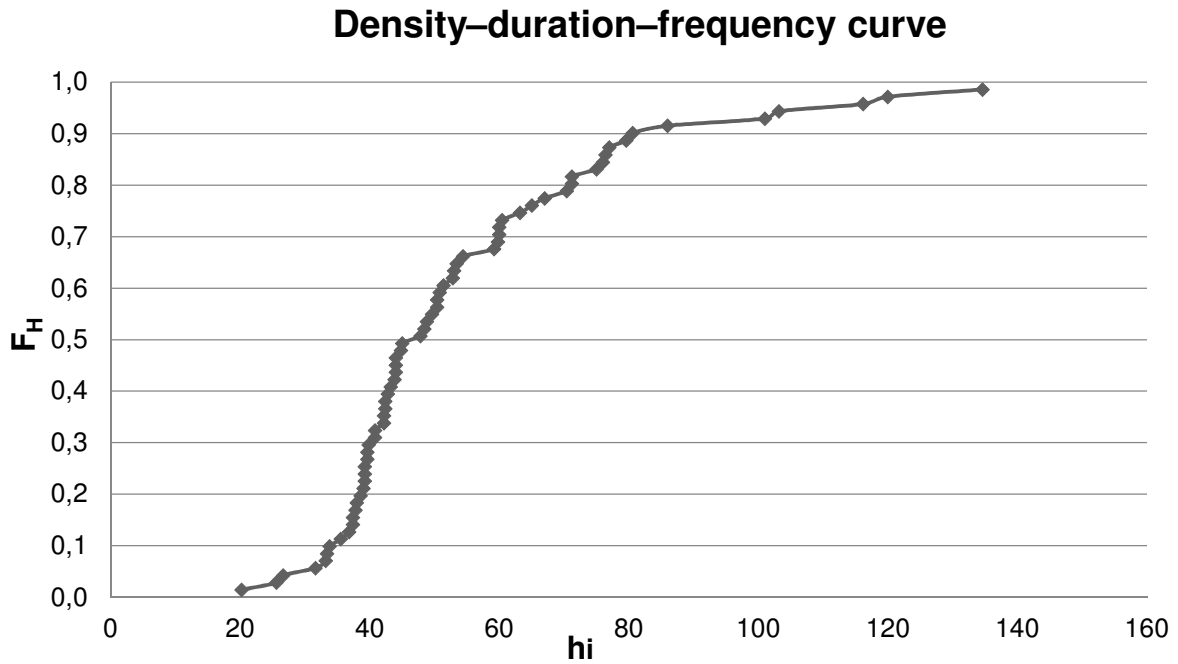
<b><math>m_h</math></b>	45,4929
<b><math>m_y</math></b>	0,55477
<b><math>S_h</math></b>	22,6069
<b><math>S_y</math></b>	1,43145
<b><math>\alpha</math></b>	0,06332
<b><math>u</math></b>	36,7314

$$h_{6 \text{ ORE}} = u - \frac{1}{\alpha} \ln\left(-\ln\left(\frac{1}{1 - T_R}\right)\right)$$

Table 5.6 Calculated values of 6 hours precipitation height  $f(T_R)$

<b>Rainfall Time 6 hours</b>	
<b>Tr [years]</b>	<b>h [mm]</b>
5	63,54
10	71,49
20	82,41
50	96,54
100	107,10

5.2.4 Analysis of 12 hours precipitations



Graph 5.6 Cumulative frequency distribution for 12 hours rainfall

<b>m<sub>h</sub></b>	54,1157
<b>m<sub>y</sub></b>	0,55477
<b>S<sub>h</sub></b>	26,9572
<b>S<sub>y</sub></b>	1,43145
<b>α</b>	0,0531
<b>u</b>	43,6682

$$h_{12\text{ORE}} = u - \frac{1}{\alpha} \ln\left(-\ln\left(\frac{1}{1 - T_R}\right)\right)$$

Table 5.7 Calculated values of 12 hours precipitation height  $f(T_R)$

Rainfall Time 12 hours	
Tr [years]	h [mm]
5	77,02
10	84,93
20	97,92
50	114,74
100	127,31

### 5.3 Validation of results

In order to assess whether the Gumbel hypothesis is correct, it is necessary to perform a statistical analysis, a test hypothesis. The Pearson test (or  $\chi^2$ ) defines the level of significance of 5%. This Percentage fixes limit that allows us to say if the hypothesis is correct or is initially placed wrong. If the curve is 95 times out of 100 well suited written, the model is correct.

Only the analytical steps for one hour precipitation will be shown, the proceed is similar for all other durations of precipitation.

The measured heights of precipitation are reported in ascending order. The sample is divided into k classes to which is associated the same probability,  $p = 1 / k$ , according to the probability distribution considered (in this case the double-exponential Gumbel).

The  $y_i$  value that corresponds to  $P_i = (k-i) \cdot p$  ( $1 \leq i \leq k-1$ ) probability is calculated with:

$$y_i = -\ln(-\ln(P_i))$$

$h_i$  and corresponding  $y_i$  values are obtained with the equation:

$$h_i = u + \frac{y_i}{\alpha}$$

With  $\alpha$  e  $u$  calculated using Gumbel.  $h_i$  values define the upper bounds of the first k-1 classes that must be used in the test.

Once calculated the number of  $h_i$  values for each class ( $N_i$ ), this is compared with the expected number that follows the probability distribution ( $N_p$ ), by the application of Pearson equation:

$$\chi^2 = \sum_{i=1}^k \frac{(N_i - N_p)^2}{N_p}$$

Number of degree,  $v$ , is defined as  $v = k - m - 1$

With k number of classes and m the number of parameters for the chosen distribution ( $m = 2$  in Gumbel method).

Depending on the number of degree, this must be compared with the value  $\chi^2$  in the given table, which must be greater because the Pearson test has occurred.

The table of  $\chi^2$  can be found in scientific literature. Some values are reported below, for a significance level of 0,05:



Table 5.8  $\chi^2$  tabulated as function of  $v$

<b>v</b>	<b>1</b>	<b>2</b>	<b>3</b>	<b>4</b>	<b>5</b>	<b>6</b>
$\chi^2$	3,84	5,99	7,81	9,49	11,1	12,6

Choosing  $k = 4$ , so  $p = \frac{1}{4} = 0,25$ , the following data are obtained, and  $h_i$  is the maximum value for each class.

In the case in which the test was not occurred, it would mean that the distribution of the initial data is not uniform enough, or there would be clusters of values in some intervals that would make the tests not verified.

Pearson analysis reveals that the hypothesis of Gumbel is proper and the statistical description of the data is well represented by reality. The Pearson test has occurred for all the durations of precipitation: the method of Gumbel used to calculate the maximum height of precipitation is verified for 1, 3, 6, 12, 24 hours events.

Pearson test tables are listed in Annex IV.

#### **5.4 Extraction of pluviometric possibility curve**

Holding  $T_R$  fast and replacing  $(\alpha; u)$  depending of each duration, four couples of values are obtained  $(\tau_p; h_p)$ , one for each duration.

Es.

Table 5.9 Resume of calculated values

<b><math>\tau_p</math> (hours)</b>	<b><math>h_p</math> (mm)</b>
1	37,63
3	48,08
6	57,72
12	74,48

To find the curve that best fits the five points  $(\tau_p; h_p)$ , the least square method is used.

Once known the  $(\tau_p; h_p)$  values a logarithmic graph is constructed: the abscissa shows the logarithm of the time and ordinate the logarithm of heights. As there is certainty in time values, because it is assumed that the data are accurate, a least-squares of the only ordered is done. This equation written in logarithmic form permits to represent in logarithmic plane the functional link according to a straight line having an angular coefficient  $n$ , and an intercept at the origin ( $\tau = 1$ ) equal to the value of  $a$ .

The equation of the curve  $h = a \tau^n$  becomes the definition of a straight line

$$\ln(h) = \ln(a) + n \ln(\tau)$$

Where the five point, suitably processed, are included  $((\tau_p) ; \ln(h_p))$ .

For convenience, a substitution of variables is done:

$$x_p = (\tau_p) \quad y_p = \ln(h_p) \quad b = \ln(a)$$

Average values are  $m_x = \frac{\sum x_i}{M}$   $m_y = \frac{\sum y_i}{M}$

Variance is  $var_x = \frac{\sum (m_x - x_p)^2}{M}$

Co-variance is  $covar_{xy} = \frac{\sum (m_x - x_p)(m_y - y_p)}{M}$

Finally the parameters are  $n = covar_{xy} / var_x$   $b = m_y - n m_x$

The final conversion is  $a = e^b$ .

Once found  $a$ , the pluviometric possibility curve is defined for each Tr:  $h = a \cdot \tau^n$ .

#### 5.4.1 Pluviometric curve for TR = 5 years

Table 5.10 Pluviometric curve trasposed in logaritmic plane

$\tau$ (hours)	$\ln \tau$	$h$ (mm)	$\ln h$
1	0,00	38,2316	3,64
3	1,10	50,9092	3,93
6	1,79	60,4199	4,10
12	2,48	71,9153	4,28
24	3,18	83,8592	4,43

The parameters  $a$  and  $n$  are obtained by least squares linear regression or graphically through the equation that describes the trend line, and these values are inserted in  $h = a \cdot \tau^n$ : numerical and graphical results are reported in chapter 5.5.

#### 5.4.2 Pluviometric curve for TR = 10 years

Table 5.11 Pluviometric curve trasposed in logaritmic plane

$\tau$ (hours)	$\ln \tau$	$h$ (mm)	$\ln h$
1	0,00	45,18	3,811
3	1,10	60,71	4,106
6	1,79	72,27	4,28
12	2,49	86,05	4,455
24	3,18	98,94	4,594

The parameters  $a$  and  $n$  are obtained by least squares linear regression or graphically through the equation that describes the trend line, and these values are inserted in  $h = a \cdot \tau^n$ : numerical and graphical results are reported in chapter 5.5 and Annex III.

#### 5.4.3 Pluviometric curve for $TR = 20$ years

Table 5.12 Pluviometric curve trasposed in logarithmic plane

$\tau$ (hours)	$\ln \tau$	$h$ (mm)	$\ln h$
1	0	51,84	3,948
3	1,099	70,12	4,25
6	1,792	83,64	4,427
12	2,485	99,60	4,601
24	3,178	113,40	4,731

The parameters  $a$  and  $n$  are obtained by least squares linear regression or graphically through the equation that describes the trend line, and these values are inserted in  $h = a \cdot \tau^n$ : numerical and graphical results are reported in chapter 5.5 and Annex III.

#### 5.4.4 Pluviometric curve for $TR = 50$ years

Table 5.13 Pluviometric curve trasposed in logarithmic plane

$\tau$ (hours)	$\ln \tau$	$h$ (mm)	$\ln h$
1	0	60,462	4,102
3	1,099	82,293	4,410
6	1,792	98,355	4,589
12	2,485	117,150	4,763
24	3,178	132,117	4,884

The parameters  $a$  and  $n$  are obtained by least squares linear regression or graphically through the equation that describes the trend line, and these values are inserted in  $h = a \cdot \tau^n$ : numerical and graphical results are reported in chapter 5.5 and Annex III.

#### 5.4.5 Pluviometric curve for TR = 100 years

Table 5.14 Pluviometric curve trasposed in logarithmic plane

$\tau$ (hours)	$\ln \tau$	$h$ (mm)	$\ln h$
1	0	66,923	4,204
3	1,099	91,415	4,515
6	1,792	109,381	4,695
12	2,485	130,299	4,870
24	3,178	146,145	4,985

The parameters  $a$  and  $n$  are obtained by least squares linear regression or graphically through the equation that describes the trend line, and these values are inserted in  $h = a \cdot \tau^n$ : numerical and graphical results are reported in chapter 5.5 and Annex III.

### 5.5 Rainfall analysis results

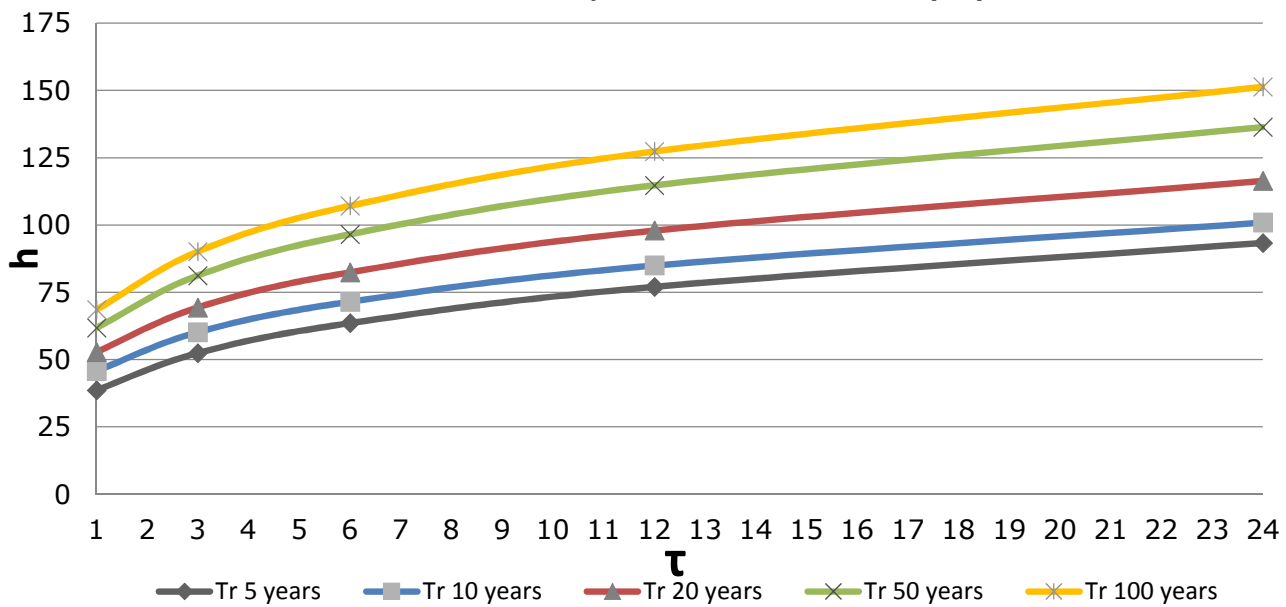
Table 5.15 "a" and "n" values depending on Tr

Tr (years)	a (mm/ore <sup>n</sup> )	n
5	38,53	0,25
10	45,79	0,25
20	52,76	0,25
50	61,77	0,25
100	68,52	0,25

Table 5.16 Height of precipitation for each duration of rainfall, depending on Tr

Tr (years)	5	10	20	50	100
$\tau$ (ore)	h (mm)				
1	38,532	45,792	52,757	61,769	68,518
3	50,606	60,172	69,349	81,221	90,106
6	60,102	71,488	82,407	96,535	107,102
12	71,379	84,932	97,924	114,737	127,305
24	84,773	100,903	116,363	136,370	151,319

### Rainfall intensity-duration curve $f(Tr)$



Graph 5.7 Rainfall intensity-duration curve for each return time





# 6. Preliminary design of the network with rational method

## 6.1 Description of method

The dimensioning of the logs of the drainage system is sized with the rational method.

The rational method or of corrivation delay method, is known in the international literature as rational method, and is one of two mathematical global and conceptual models, used to calculate the flow rate from a drainage basin, when it is assigned a specific precipitation; it is used for the draining surfaces of relatively limited extension.

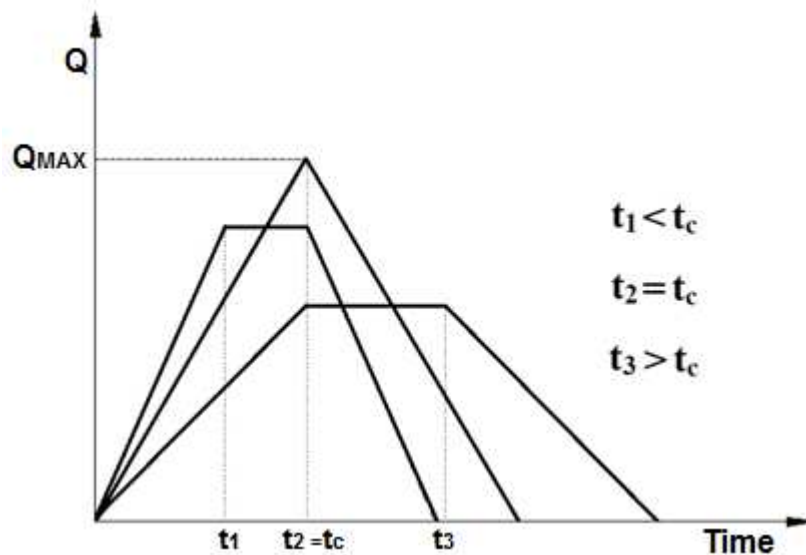
The basin is represented as a single rectangular surface drainage that feeds a collector, with the fundamental assumption that the velocity of flow in the channel is greater than a few orders of magnitude as compared to the speed of sliding along the slope. The measurement of the flow in the channel is performed in the terminal section, so as to be able to consider all incoming water from the various areas of the sub-basin.

Studying the area, a precipitation of height  $h$  in the time  $t$  is supposed; only a fraction of the total volume precipitated comes within the collecting channel, this fraction is estimated by the flow coefficient ( $\varphi$ , while the remaining portion  $1-\varphi$  is dispersed by evaporation and infiltration).

The fraction  $\varphi$  of the whole volume meteor  $S * h$  contributes to the formation of the average flow rate  $\bar{Q}$ , that is

$$\bar{Q} = \frac{\varphi * S * h}{t + t_c}$$

with  $t_c$  is the corrivation time . This average value is not a significative datum since the purpose of the design of the drainage system is necessary to calculate the maximum capacity for the basin outflow for that particular time of rain. This maximum value is obtained through the study of the diagram flow rates that fall off in the basin, as a function of precipitation time  $t$ , and of the delay of corrivation  $t_c$ ; analyzing the variation of the flow rate vs. time of precipitation. Three different cases exist:



Graph 6.1 Flow trend the three cases of rainfall event.

As can be seen from the diagram of the flow, the case in which it has the maximum value of the drainage flow is that in which the water have contributions from all surfaces of the basin or when the precipitation time  $t$  is the time of corrivation  $t_c$ .

If  $t < t_c$  the maximum value isn't reached, because the rainfall event finishes before that the water droplet, that has fell in the furthest hydraulic points, could reach the terminal section of the basin.

From the graph a very rapidly increasing of flowrate can be noticed, it is caused by the bigger intensity  $j = h/t$ , because if the same heigh value  $h$  is considered, the time value is lower.

In the same case, by choosing  $t > t_c$ , the intensity  $j$  decreases respect to  $t = t_c$ , so the maximum value of flowrate is reached at  $t_c$  and the flowrate can not increase anymore.

The  $Q_{max}$  value that corresponds to  $t = t_c$  is:

$$Q_{MAX} = \frac{\varphi * S * h}{t_c}$$

With  $h$  given in mm and  $\tau_c$  in seconds, the udometric coefficient represents the specific contribution to a flood and its unit of measurement is l/s, ha:

$$u = \bar{\varphi} \frac{h}{\tau_c}$$

The order of magnitude of the udometric coefficient depends on the extent of the basin and the type of work considered: for urban sewage systems the value is about 10 to 100 l/(s\*ha). The runoff coefficient  $\bar{\varphi}$  is to be calculated as the average weighed on areas that form the entire basin analyzed. The precipitation height  $h$  is obtained from the equation pluviometric

possibility multiplying by the factor 4/3 the exponent  $n$  in order to consider the variation of  $\phi$  with the duration of precipitation.

Table 6.1 Common Design Frequencies for Hydraulic

Type of structure	Return period (years)
Highway culverts:	
Low traffic	5–10
Intermediate traffic	10–25
High traffic	50–100
Highway bridges	
Secondary system	10–50
Primary system	50–100
Urban drainage	
Storm sewers in small cities	2–25
Storm sewers in large cities	25–50
Airfields	
Low traffic	5–10
Intermediate traffic	10–25
High traffic	50–100

In the calculation of the drainage network a return period of 10 years is considered, using:

$$n=0,249$$

$$a=45,792$$

With  $n$  that is a dimensionless coefficient and in  $\text{mm}/\text{hours}^n$ . The time of concentration is estimated according to the speed  $v_i$ , calculated for the different sections of pipeline, and the residence time  $\tau'$  out of net that can be hypothesized between 10 and 20 minutes, in this case we used a residence time of out of network equal to 15 minutes.

Corrivation time is thus obtained:

$$\tau_c = \tau' + \sum_i L_i/v_i$$

The path chosen for determining the corrivation time is the path that maximizes the result. The calculation starts from the of the mountain, progressing gradually to the sizing of those further downstream, each time making reference to the river basin uniquely identified by the end section of the trunk that you have to size: thus assuming the runoff average coefficient, weighed on the area is being considered.

The project of the network assumes speed in pipelines equal to 1 m/s.

The new network has been delineated starting from the area of Arena where manholes are missing and collects many manholes in the souther part of the garden to discharge all the contributions into Piovego river. The Figure below explains how the network has been designed: red points are the hypotized manholes and the yellow points represent the drains that already exist.

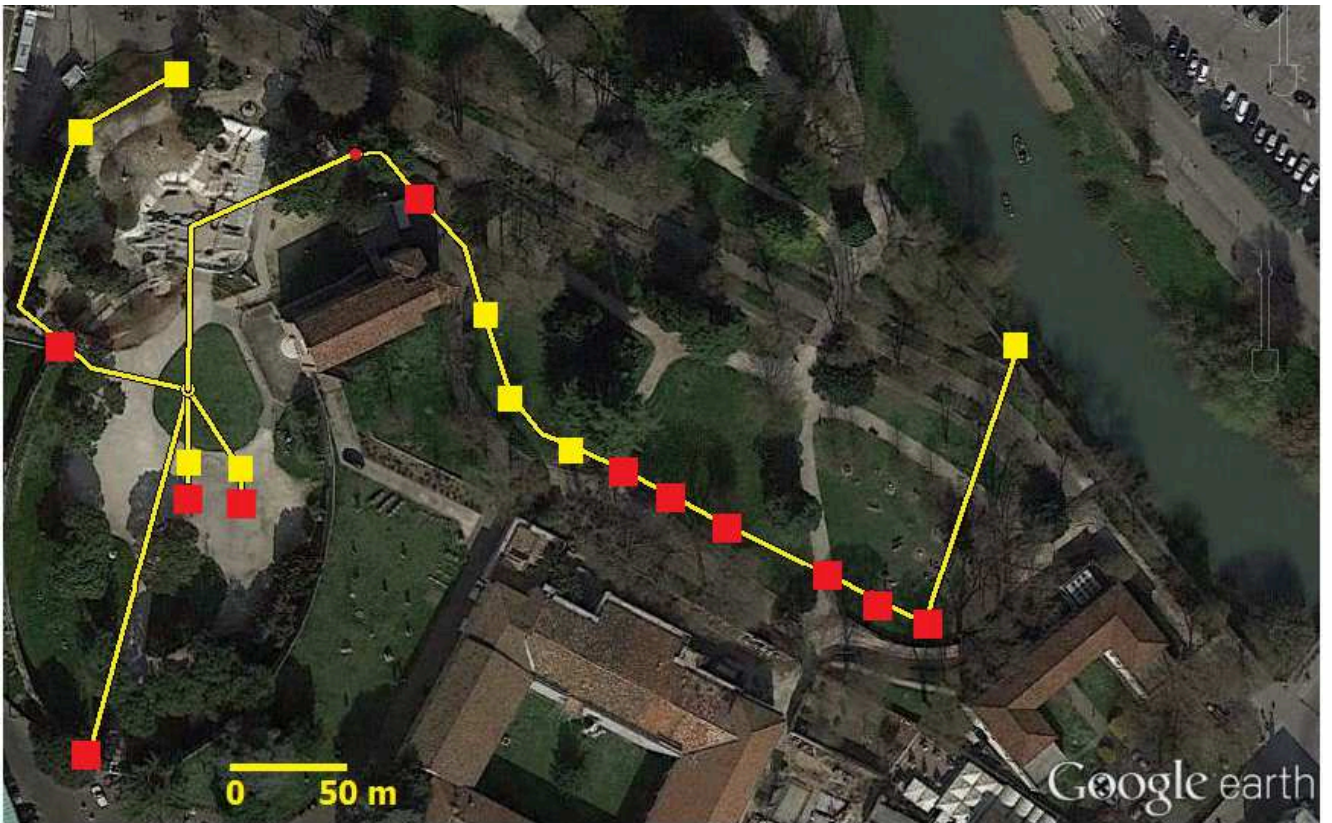


Figure 6.1 Surposition of network and area

## 6.2 Design of the network

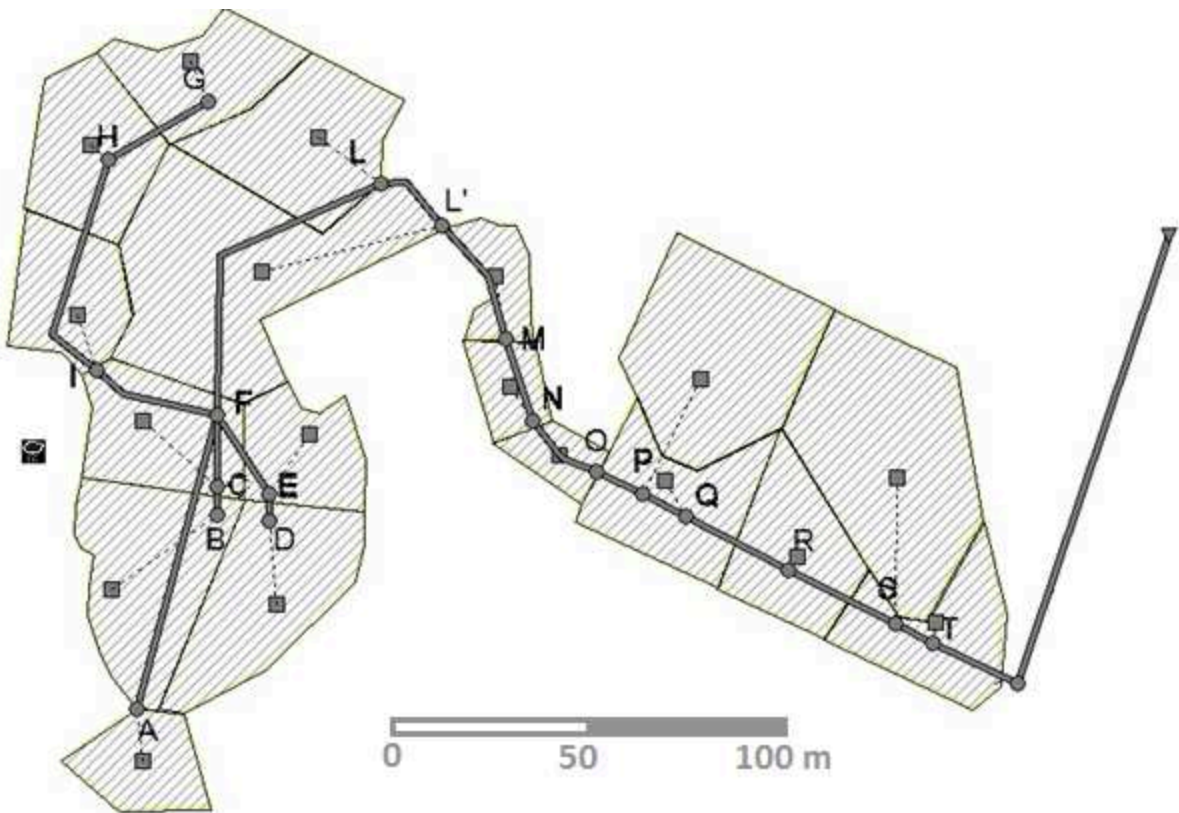


Figure 6.2 Network design



Table 6.2 Data of the network

PIPE	L (m)	Saff (m <sup>2</sup> )	Saff (ha)	Stot (m <sup>2</sup> )	Stot (ha)	Φ	vel (m/s)	t vers (min)
AF	56	398	0,040	398	0,040	0,3	1	10
BC	3,6	750	0,075	750	0,075	0,3	1	10
CF	12	569	0,057	1319	0,132	0,3	1	10
DE	3,6	750	0,075	750	0,075	0,3	1	10
EF	16,3	407,6	0,041	1157,6	0,116	0,3	1	10
GH	20,5	353,13	0,035	353,13	0,035	0,3	1	10
HI	42,3	340,65	0,034	693,78	0,069	0,3	1	10
IF	23	399	0,040	1092,78	0,109	0,3	1	10
FL	60,3	582	0,058	4549,38	0,455	0,3	1	10
LM	38	170	0,017	4719,38	0,472	0,3	1	10
MN	16	140	0,014	4859,38	0,486	0,3	1	10
NO	17	130	0,013	4989,38	0,499	0,3	1	10
OP	10,72	100	0,010	5089,38	0,509	0,3	1	10
PQ	7,97	400	0,040	5489,38	0,549	0,3	1	10
QR	19,33	400	0,040	5889,38	0,589	0,3	1	10
RS	22,45	1000	0,100	6889,38	0,689	0,3	1	10
ST	6,2	400	0,040	7289,38	0,729	0,3	1	10

Table 6.3 Cinematic method results

	L [m]	T <sub>c</sub> (s)	h(mm)	u (l/s,ha)	Q(l/s)	A'(m <sup>2</sup> )	D(m)	A'/D <sup>2</sup>	y/D	R <sub>H</sub> /D	R <sub>H</sub>	i	T (Pa)
AF	54,44	954,44	32,90	137,89	4,26	0,004	0,12	0,303	0,41	0,2182	0,026	0,013	3,32
BC	5	905	32,47	143,51	11,14	0,011	0,15	0,472	0,58	0,2728	0,042	0,007	2,82
CF	12	917	32,57	142,09	18,86	0,019	0,19	0,511	0,62	0,2821	0,054	0,005	2,59
DE	5	905	32,47	143,51	10,23	0,010	0,15	0,433	0,54	0,2621	0,040	0,007	2,86
EF	15,88	920,88	32,61	141,64	15,63	0,016	0,19	0,423	0,53	0,2592	0,050	0,005	2,67
GH	20,72	920,72	32,61	141,66	6,46	0,006	0,12	0,459	0,57	0,2703	0,032	0,010	3,09
HI	41,68	962,4	32,97	137,03	13,80	0,014	0,15	0,585	0,7	0,2962	0,045	0,006	2,75
IF	23,93	986,33	33,17	134,52	19,48	0,019	0,19	0,528	0,53	0,2592	0,050	0,005	2,67
FL	59,96	1046,29	33,66	128,69	62,69	0,063	0,38	0,425	0,53	0,2592	0,100	0,002	2,12
LL'	14,51	1060,8	33,78	127,37	79,06	0,079	0,38	0,536	0,64	0,2862	0,110	0,002	2,05
L'M	23,16	1083,96	33,96	128,17	82,05	0,082	0,38	0,556	0,67	0,2917	0,112	0,002	2,03
MN	15,68	1099,64	34,08	129,27	85,09	0,085	0,38	0,576	0,69	0,2948	0,113	0,002	2,03
MO	14,46	1114,1	34,19	129,87	87,35	0,087	0,38	0,592	0,71	0,2975	0,114	0,002	2,02
OP	8,51	1122,61	34,26	122,06	91,88	0,092	0,38	0,622	0,74	0,3	0,115	0,002	2,02
PQ	8,83	1131,44	34,32	121,35	98,52	0,099	0,38	0,667	0,79	0,3039	0,117	0,002	2,01
QR	23,08	1154,52	34,50	119,52	102,79	0,103	0,48	0,446	0,55	0,2649	0,127	0,002	1,95
RS	24,64	1179,16	34,68	117,64	112,60	0,113	0,48	0,489	0,59	0,2753	0,132	0,001	1,93
ST	7,32	1186,48	34,73	117,10	117,36	0,117	0,48	0,509	0,62	0,2821	0,135	0,001	1,91

Table 6.4 Commercial values of pipes diameter

PVC PIPES DIAMETER [mm]	
EXTERNAL	INTERNAL
125	118,6
160	153,6
200	192,2
250	240,2
315	302,6
400	384,2
500	480,4

To define altimetrical disposal of pipelines and determine the longitudinal profile, is necessary to line up the free surface of water in the conduits. The alignment of the bottom of two pipelines must be strictly avoided, because the hydraulic jump originate pressure on the conduct upstream.

To define the altitude of the conduit the calculation starts from the initial point of the network: A, B, D and G points. The depth of the pipeline is determined by studying the loads that exist above it, but his area is not subjected to strong loads as coming from the street and caused by car passing, so the conduits have been determined starting from 60 cm of depth from the ground level.

The slope of coduits must be more than 0,05‰ to to avoid the formation of solid material deposits in the bottom of the pipeline. The results of the calculation of longitudinal profile are reported in the table below.

Table 6.5 Elevation of conduits

	Elevation z [m.s.m.m.]		
	crown	free surface	invert
<b>A</b>	12,581	12,532	12,462
<b>B</b>	12,000	11,911	11,846
<b>C</b>	11,966	11,877	11,812
<b>D</b>	11,600	11,517	11,446
<b>E</b>	11,564	11,481	11,410
<b>G</b>	13,300	13,232	13,181
<b>H</b>	13,097	13,029	12,978
<b>I</b>	12,840	12,772	12,721
<b>F</b>	11,477	11,394	11,324
<b>L</b>	11,347	11,264	11,194
<b>L'</b>	11,320	11,237	11,166
<b>M</b>	11,277	11,194	11,123
<b>N</b>	11,248	11,165	11,095
<b>O</b>	11,222	11,139	11,069
<b>P</b>	11,207	11,124	11,053
<b>Q</b>	11,192	11,109	11,038
<b>R</b>	11,155	11,072	11,002
<b>S</b>	11,119	11,036	10,965
<b>T</b>	11,108	11,025	10,955



## 7. S.W.M.M. analysis

SWMM can display a backdrop image behind the Study Area Map. The backdrop image might be a street map, utility map, topographic map, site development plan, or any other relevant picture or drawing. The backdrop Image must be a Windows metafile, bitmap, or JPEG image created outside of SWMM. Once imported, its features cannot be edited, although its scale and viewing area will change as the map window is zoomed and panned.

The backdrop has been taken by AutoCAD drawing of the area. The area has been traced by topograph to exactly define the plan of Arena Gardens: both altitude than geographical coordinates have been defined with GPS technology, with a centimetrical precision. All the points measured are represented as red points in the Figure below.

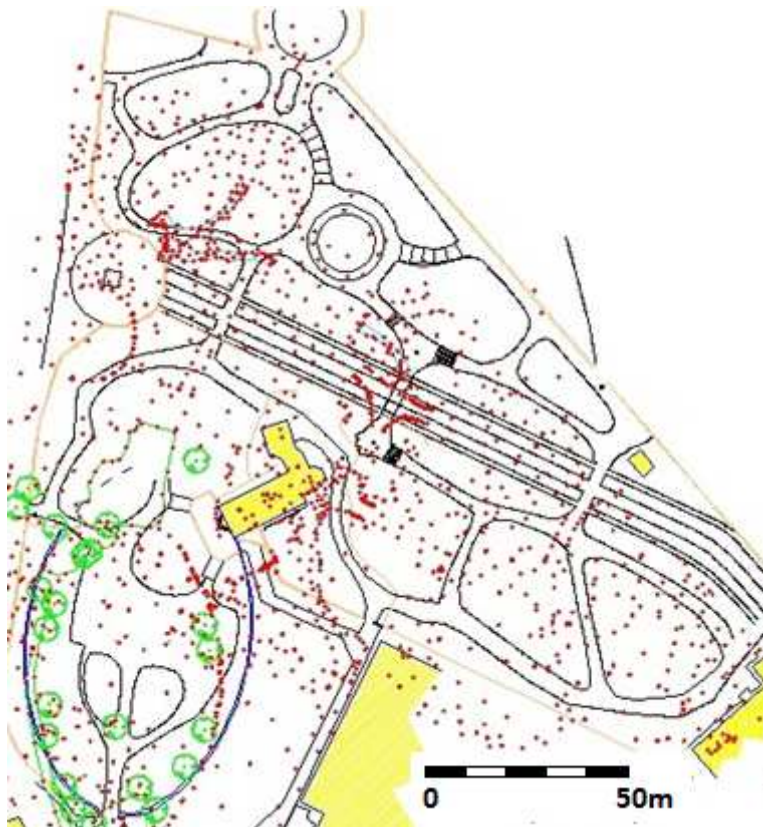


*Figure 7.1 Point whose coordinates have been detected*

The geographical reference of each point of the map has permit to define the X and Y coordinates of map's lower left and upper right corners, so the JPG image has been scaled and the dimensions of the backdrop image coincide with the real dimensions.

Switching on Autosize function, the definition of subcatchments and pipes become easier because their dimensions are automatically defined.

Starting from the knowledge of the Z coordinate of the area, the main slopes have been founded and permit to know the sliding surfaces of rain.

X, Y and Z coordinates were imported in the program Surfer by which a uniform grid is obtained. With the process of gridding the trend of a certain variable is rebuilt following a regular grid of nodes, equally spaced, starting from a series of discrete values and irregularly distributed in space.

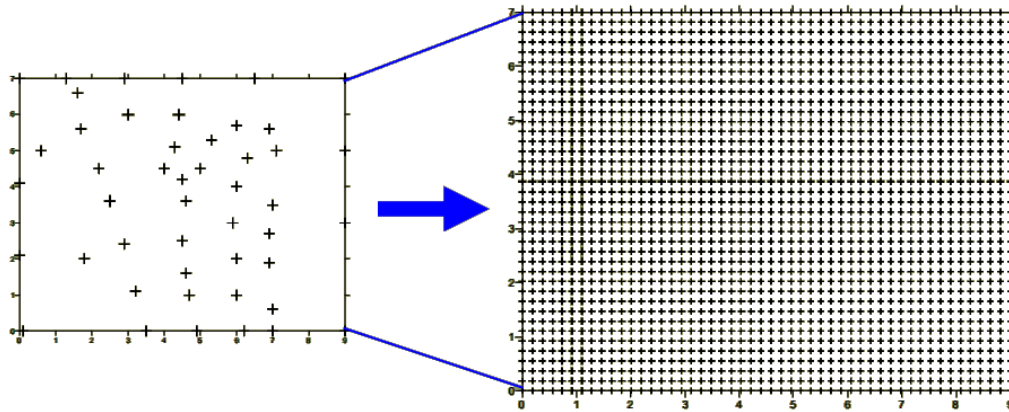


Figure 7.2 Grid creation method

Grid files are created using the *Grid | Data* command. The *Grid | Data* command requires data in three columns: one column containing X data, one column containing Y data, and one column containing Z data.

The *Grid Data* dialog allows to control the gridding parameters.

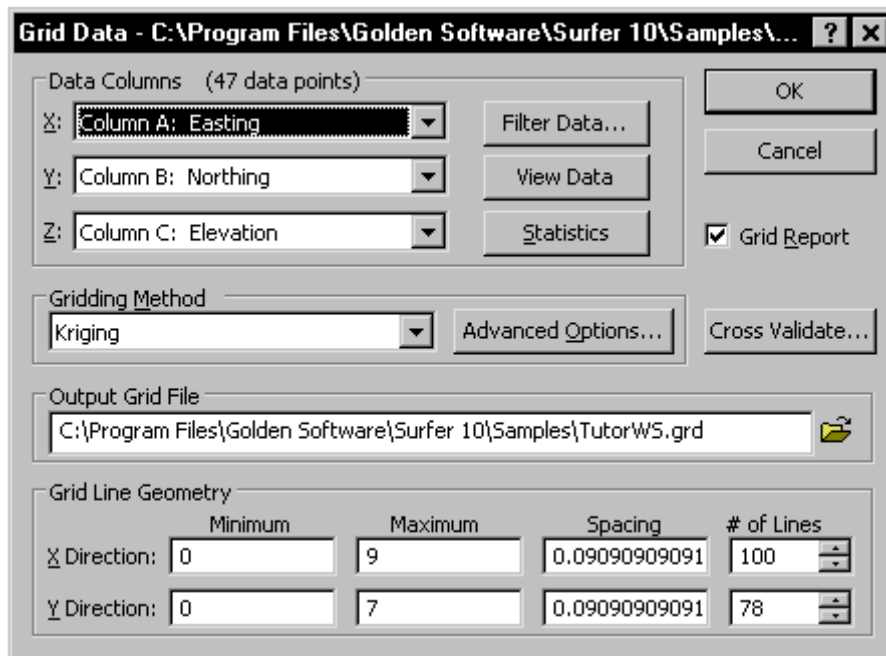


Figure 7.3 Gridding window in Surfer

Kriging is a geostatistical gridding method that has proven useful and popular in many fields.

This method produces visually appealing maps from irregularly spaced data.

Kriging is a very flexible gridding method. Kriging defaults are accepted to produce an accurate grid of your data, or Kriging can be custom-fit to a data set by specifying the appropriate variogram model. Within Surfer, Kriging can be either an exact or a smoothing interpolator depending on the user-specified parameters. It incorporates anisotropy and underlying trends in an efficient and natural manner.

An important component of the kriging gridding method is the variogram. The default linear variogram provides a reasonable grid in most circumstances, as long as a nugget effect is not used.

The variogram is a measure of how quickly things change on the average. The underlying principle is that, on the average, two observations closer together are more similar than two observations farther apart. Because the underlying processes of the data often have preferred orientations, values may change more quickly in one direction than another. As such, the variogram is a function of direction.

Grid method parameters control the interpolation procedures. The differences between gridding methods are in the mathematical algorithms used to compute the weights during grid node interpolation. Each method results in a different representation of your data.

Because Surfer maps are created from gridded data, the original data are not necessarily honored in the grid file. When the original data points are posted on a contour map, some of the contour lines might be positioned "wrong" relative to the original data. This happens because the locations of the contour lines are determined solely by the interpolated grid node values and not directly by the original data.

Through cross validation the method has been assessed. Generally, cross validation can be considered an objective method of assessing the quality of a gridding method, or to compare the relative quality of two or more candidate gridding methods. In Surfer, cross validation can be used with all gridding methods.

Once defined the gridding method, the *Map | New | Contour Map* command creates a contour map from the grid file. A contour map is a two-dimensional representation of three-dimensional data. The first two dimensions are the X and Y coordinates. The third dimension (Z) is represented by lines of equal value. The relative spacing of the contour lines indicates the relative slope of the surface. The area between two contour lines contains only grid nodes having Z values within the limits defined by the two enclosing contours. The difference between two contour lines is defined as the contour interval.

The command property is used to determine the characteristics of the layer with the contour lines. These can be spaced as necessary, in our case, each 20 cm, 50 cm to 1 m, and the various visual clues make the map more illustrative.

Through the command *Grid vector map*, vector map information, direction and magnitude, can be derived from one grid. The arrow symbol points in the "downhill" direction and the



length of the arrow depends on the magnitude, or steepness, of the slope. A vector is drawn at each grid node unless some nodes are skipped by changing the *Frequency* setting.

For example, consider a grid containing elevation information. If water were poured over the surface, the direction arrows would point in the direction water flows - from high elevation to low elevation. Magnitude is indicated by arrow length. In the water flow example, the steeper slopes would have longer arrows. The area represented is the Arena garden map.

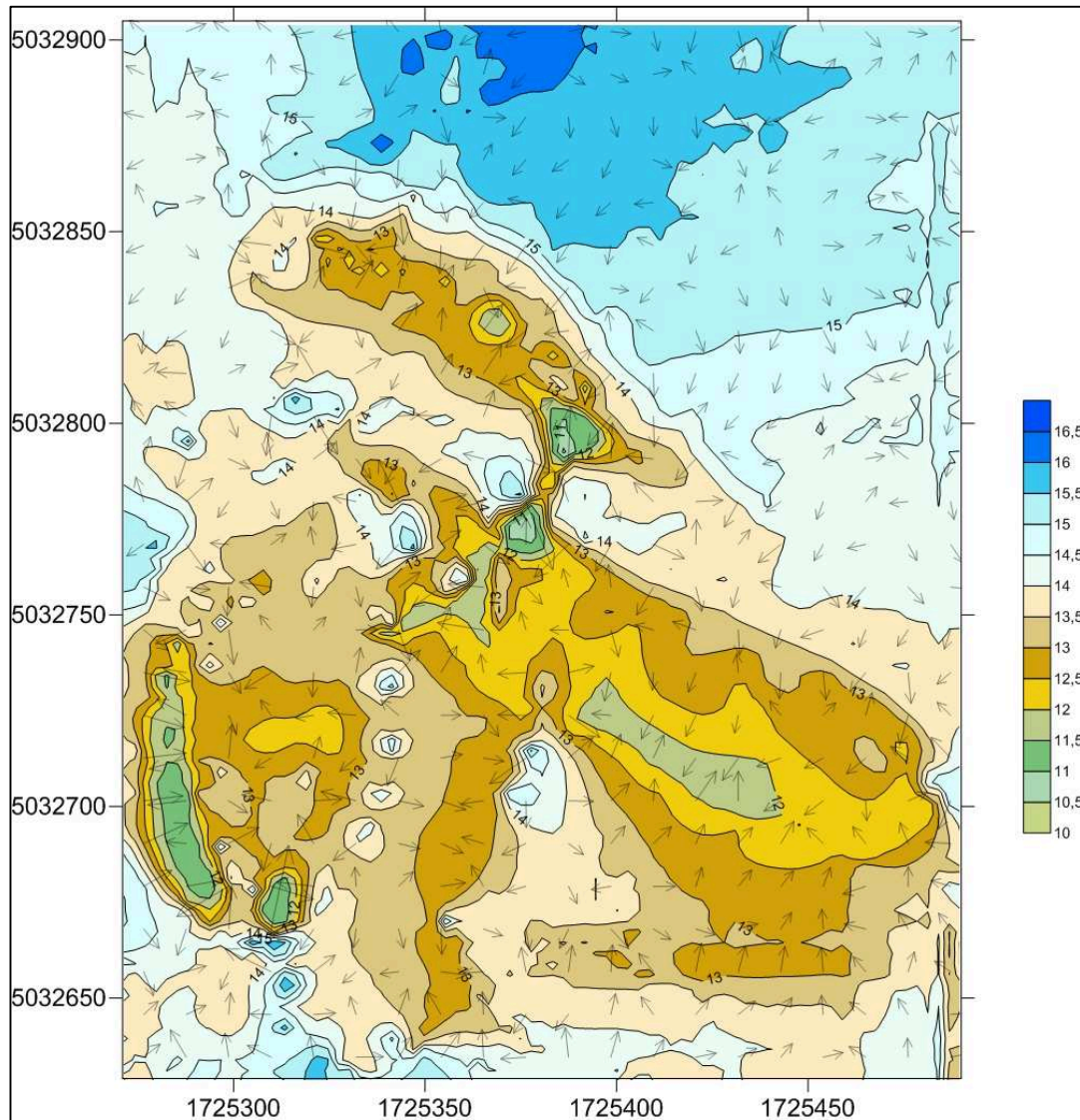


Figure 7.4 Grid vector map of the area

The level curves, characterized by precise coordinates, are overlaid on the georeferenced map in AutoCAD to obtain a precise description of the examined area.

Proceeding in this way it is possible to study the slope of the ground from which the water deposits depend, given that flow along the natural slopes and then infiltrate and accumulate in the soil.

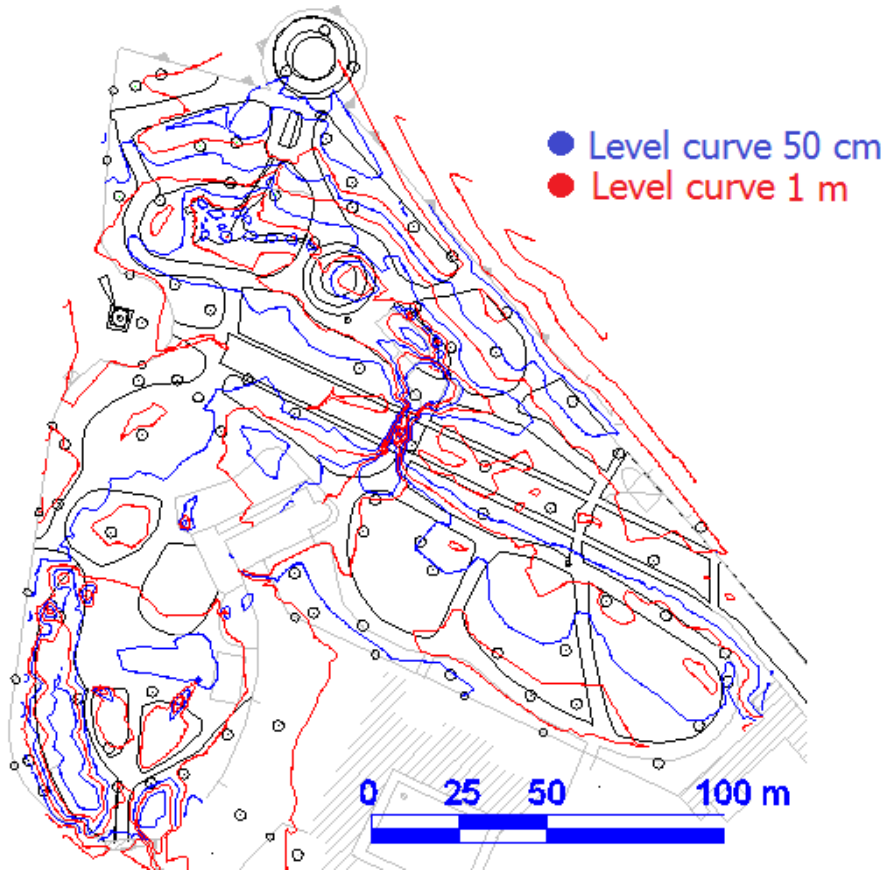


Figure 7.5 Representation of level curves

The definition of level curves permits to divide the unique basin into many drainage sub basins that are created by natural slope of the soil. Rain water accumulates as soil lead it in natural sliding, so each sub basin should drain the water to a manhole or to another sub basin, in order to avoid any backlog. The sub basins have been determined starting from the drainage network:

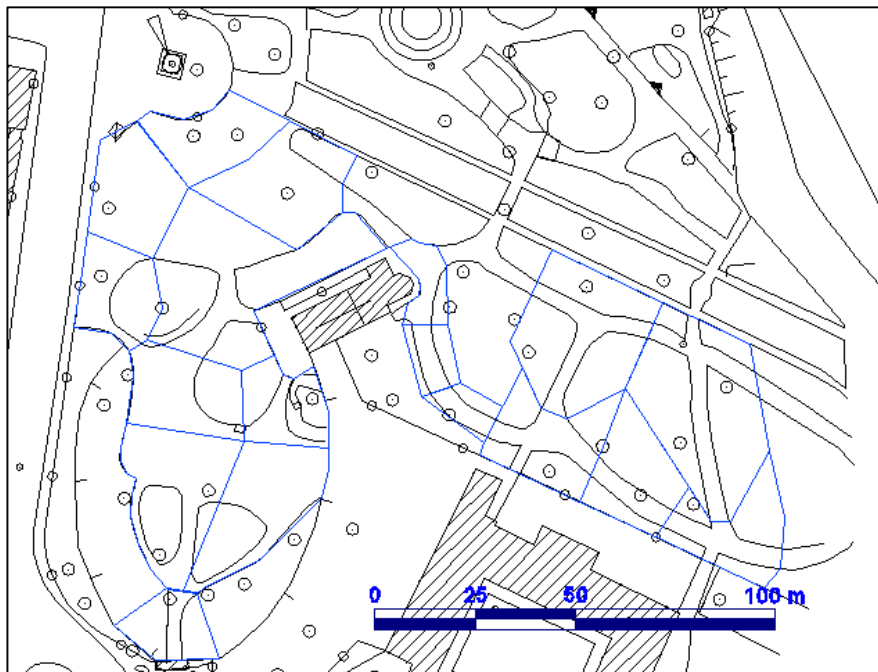


Figure 7.6 Sub-basins division.

From this map correlated to the actual sewage system plan, the analysis of drainage network have begun.

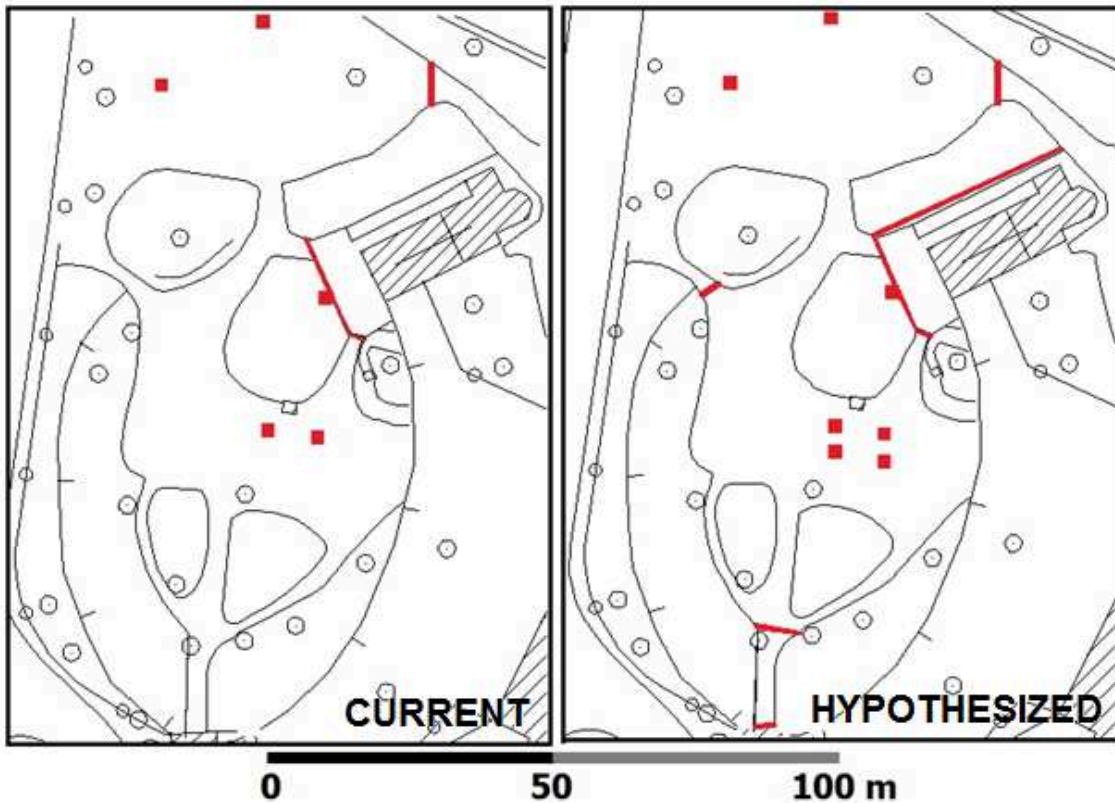


Figure 7.7 Details: current and hypothesized manholes in Arena zone.

The number of manholes in the Arena is too low to permit water to be drained without creating stagnation, so the project impose to add other manholes to increase the network.

This elements are added in the new pipeline network design (points A, B, D, I, P, Q, R, S, T, L') and are already considered in the definition of sub basins.

In B and D two manholes have been added in parallel to the other two already existent, A and I are two access ramps that need to be protected with a grid, and the other points are manholes and grids that have been inserted in the lower zone of the gardens, there altitude is 12 m.a.s.l. and water accumulates. In this part a pipeline, P-Q-R-S-T, arriving from the museum, must be built to drain museum contribute and to take water from the lowest area.

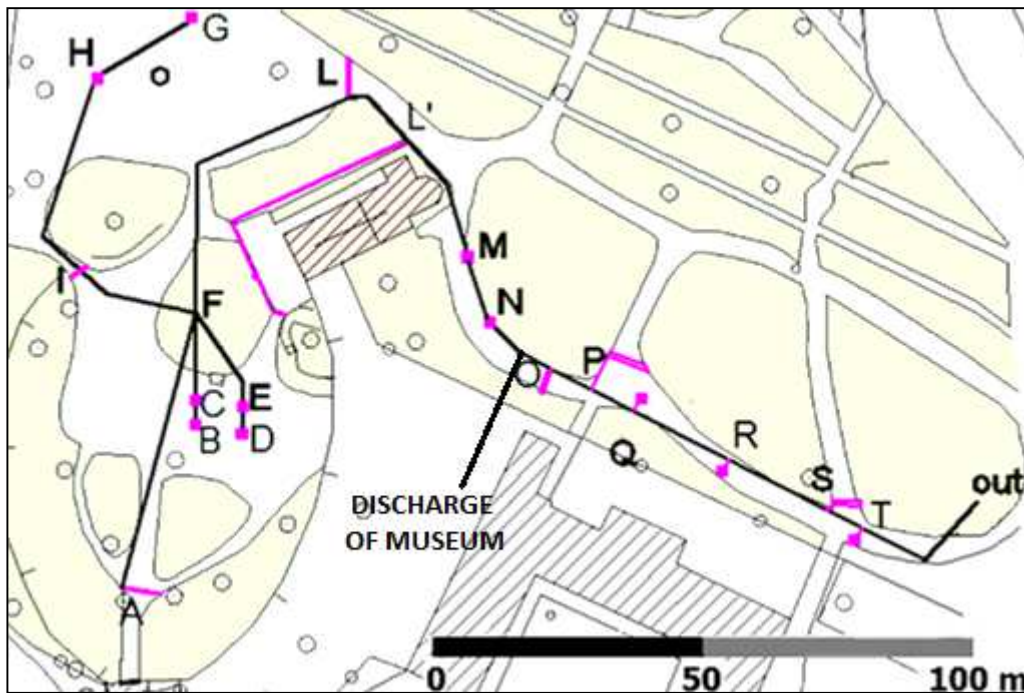


Figure 7.8 Drainage network created for the whole area.

The entire drainage basin is divided into fourteen sub-basins (discretization), each of which is imagined as a flat rectangular layer inclined towards the collector, which is related to the upstream junction, considering the direction of the outflow. The parameters required by the interface of the program, analyzed later, allow describing the behavior of the hydrological sub-basin, and together, determining the response that is estimated by the model. For the surface runoff, SWMM uses a conceptual model in which each sub-basin is expressed as a non-linear reservoir with a single output on a node. The tank capacity corresponds to the value of maximum depression storage, and losses resulting from surface runoff, infiltration and evaporation.

Sub basins and pipeline are inserted in the software SWMM and each basin is set to be drained in a node that is equivalent to a manhole. The network starts is G, A, B, D and ends in T point, where a pump station will be built to bring out water to outfall.

The surface flow starts only when the water level is greater than what can be contained in depression  $d$ , initially defined, and different according to the nature of the soil, permeable or impermeable. SWMM automatically defines the subcatchments' area and the conduits' length. Basins are pervious and infiltration is calculated with Green-Ampt model and the parameters utilized are defined following the soil categories and defined in Paragraph 8.3.

**Suction Head** Height of capillary rise

**Conductivity** Permeability or hydraulic conductivity of the soil in saturation conditions

**Initial Deficit** Deficiency of initial relative humidity of the soil compared to the saturation defined as the difference  $\Phi - \theta_i$



The variation of the parameter *Initial Deficit* creates significant differences in the total quantity of infiltrated water: in a saturated soil the value is  $\Phi \cong \theta_i$ , so the value of *Initial Deficit* is quite zero and consequently the flow will start before; on the contrary, in a completely dry soil the value is  $\theta_i = 0$ , that is, a large infiltration capacity which postpones the start of the outflow.

Property	Value
Description	
Tag	
Rain Gage	R1
Outlet	E
Area	0.04
Width	500
% Slope	0.1
% Imperv	1
N-Imperv	0.1
N-Perv	0.08
Dstore-Imperv	5
Dstore-Perv	5
%Zero-Imperv	5
Subarea Routing	OUTLET
Percent Routed	100
Infiltration	GREEN_AMPT
Optional comment or description	

Figure 7.9 Subcatchment description box

## 7.1 Rainfall event design

The process of computing a hydrograph begins with selection of a design storm, the first step of which is to select a design frequency. In an event-based design using methods of synthetic hydrology, the frequency of the storm event is assumed to equal the frequency of the resulting computed peak flow rate on the hydrograph. This is probably not true for individual events, but it is hoped that it approaches reality over the long term.

To design a drainage work, the effects on the basin of an event of particularly heavy rain are simulated, with an event that is taken as a reference and is denoted as project rain. The rain event may coincide with an exceptional event actually observed or represent a hypothetical event, defined artificially. The attribution of a reference precipitation is used to calculate the more onerous flowrate to the basin, according to which the elements of the hydraulic network are dimensioned so that they are able to dispose of the maximum affluent flow rate.

Spatial and temporal distributions of rainfall are assigned by means of hyetographs defined from rainfall data registered for the event in the different stations of the concerned area.

The runoff discharge hydrograph is a graph of discharge rate versus time, where the discharge is in units of volume/time (i.e., ft<sup>3</sup>/sec, acre-ft/day). The runoff hydrograph can also be expressed as might be defined for a stage-discharge relationship for a stream channel of floodway (i.e., the discharge rating curve for a channel cross section). The shape of the storm hydrograph is related to the rainfall hyetograph (intensity vs. time) and the combined effects of the storage in the watershed or channel.

The watershed and channel storage effects smooth out much of the variation evident in the storm hyetograph. The runoff hydrograph increases in magnitude shortly after the start of the rainfall event and reaches a peak after the maximum rainfall intensity has occurred.

A unit hydrograph (UH) is the hypothetical unit response of a watershed (in terms of runoff volume and timing) to a unit input of rainfall. It can be defined as the direct runoff hydrograph (DRH) resulting from one unit (e.g., one cm or one inch) of effective rainfall occurring uniformly over that watershed at a uniform rate over a unit period of time. An instantaneous unit hydrograph is a further refinement of the concept; for an IUH, the input rainfall is assumed to all take place at a discrete point in time (obviously, this isn't the case for actual rainstorms).

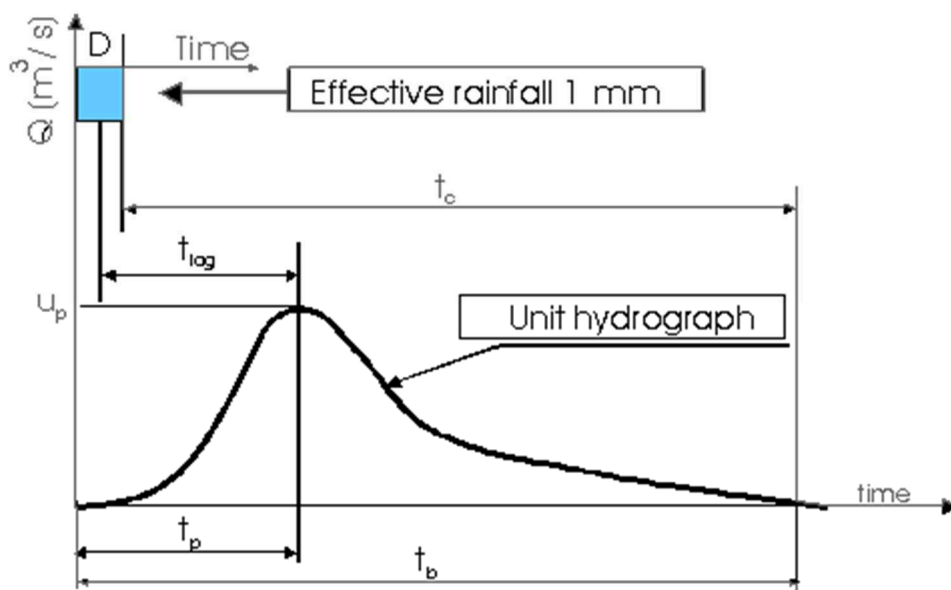


Figure 7.10 Relationship of storm, unit, and direct runoff hydrographs

The construction of the hyetograph is carried out starting from the curve pluviometric possibility (which can refer to punctual rain or to the average height of rain on the general surface).

The total duration and the length of temporal discretization as the method to follow in the construction of hyetograph are chosen arbitrarily.



The design and control of water infrastructures and systems require the use of design rainfall models to evaluate the effects of intense precipitation events over a certain basin or urban area under study. Despite the reproduction of observed events in natural or urban contexts being carried out within different simulation approaches, the prevailing practice is to generate synthetic hyetographs consistent with the intensity–duration–frequency (IDF) curve that corresponds to the desired return period.

Assuming uniformly distributed precipitation in space, as is common over relatively small basins, the duration and the form of the hyetograph are thus to be defined.

Parameters governing the form of the resulting precipitation pattern are to be determined so as to optimize flood discharge estimates.

Once defined the hyetograph the program calculates the number of elementary intervals of which it is composed hyetograph and readjusts the total duration, if necessary, so as to make it equal to an integer number of elementary intervals, calculates the corresponding height of rain, deriving it from the curve of climatic possibility, and distributes it in the different elementary intervals, according to the method chosen by the user.

For a channel of city sewer, it is important that the rain correctly reproduce the peaks of the intensity of rain, from which largely depends the peak flow. The choice of the duration of rainfall, obviously affects both the maximum intensity the rain hyetograph that the total volume of the influx.

In this particular case, the equation pluviometric possibility to be referred to is  $h=45,792*t^{0,249}$ .

The hyetographs examined, chosen from those available in the literature, are three: a constant intensity, Sifalda and Chicago.

To verify the acceptability of Hyetograph, the area under the curve of Hyetograph must be equal to the value of the height of precipitation. In the model S.W.M.M. to enter data, related to precipitation, blocking Rain Gages is used. The determination of the amount of precipitation that flows into the basin can be done using three formats:

**Intensity:** The relationship between rainfall and chosen time interval, [mm / h];

**Volume:** Volume of rain dropped during the time interval, [mm];

**Cumulative:** Cumulative Volume of rain since the beginning of the precipitation [mm];

The algorithm that acts in "Intensity" function, permits to calculate the volume through an integration process: once set a time step  $\Delta t$ , the whole duration of the meteoric event is divided into  $n$  intervals, with  $n = t_p / \Delta t$ .

For each interval the average value of the intensity is determined by multiplying that value by the time step  $\Delta t$ , you get the same amount of of rainfall on the interval; the sum of all  $n$  contributions corresponds to the value of the total precipitation.

The format chosen for this basin is, with a time interval  $dt$  equal to a second.

In the function *Time Series Editor*, the data relating to the intensity of rain are entered, obtained as a function of time.

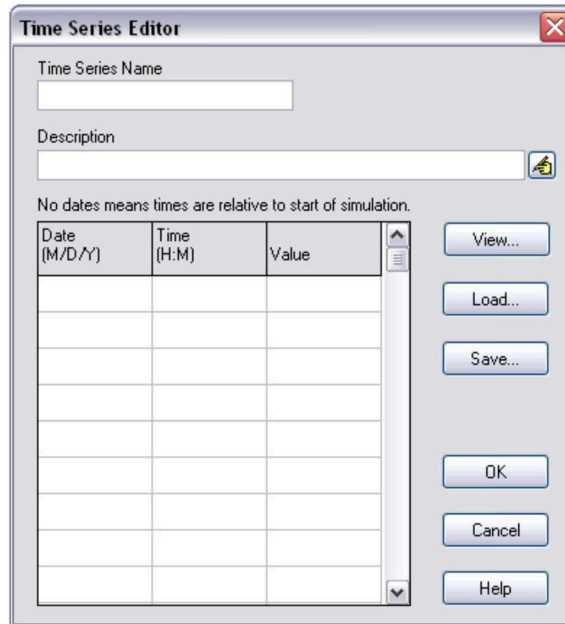


Figure 7.11 SWMM time series editor

For rainfall time series, it is only necessary to enter periods with non-zero rainfall amounts. SWMM interprets the rainfall value as a constant value lasting over the recording interval specified for the rain gage that utilizes the time series. For all other types of time series, SWMM uses interpolation to estimate values at times that fall in between the recorded values.

Also time step options must be set in Simulation Options dialog, it establishes the length of the time steps used for runoff computation, routing computation and results reporting. Time steps are specified in days and *hours: minutes: seconds* except for flow routing which is entered as decimal seconds. Reporting *Time Step* define the time interval for reporting of computed results, wet weather time step enter the time step length used to compute runoff from subcatchments during periods of rainfall or when ponded water still remains on the surface and dry weather time step enter the time step length used for runoff computations during periods when there is no rainfall and no ponded water.

This must be greater or equal to the wet weather time step.

It is important to point out that there is no best method to calculate hyetograph. It depends on the characteristics of the basin – size, urban or rural, on the data, on the soil type and utilization, and on the purpose of the study. The user must be well aware of the strengths and weaknesses of the method he chooses, and of its limitation. Moreover, particular attention must be taken in the choice of the parameters of the model, which could impact a lot on the result. Finally, before any simulation, the model should be tested with a rainfall event for which both rain and runoff measurements are available, to validate the choice of

parameters. The method that best fits our conditions in considering constant intensity rain of project.

Table 7.1 Comparison of the different methods to get a design hyetograph

<b>Method</b>	<b>Strengths</b>	<b>Weaknesses</b>	<b>Recommendation of use</b>
<b>Constant</b>	Simple	Not representative of a true rainfall event	Determination of peak discharge value
<b>Chicago</b>	Widely used Well defined Fit large basins	Parameters to adjust locally Need full IDF curves Overestimate the peak	Sewer design Large basins when IDF curves available
<b>Sifalda</b>	Same global pattern as Chicago Less parameters, easier to estimate	Less precise than Chicago	Large basins, when no IDF curves are available

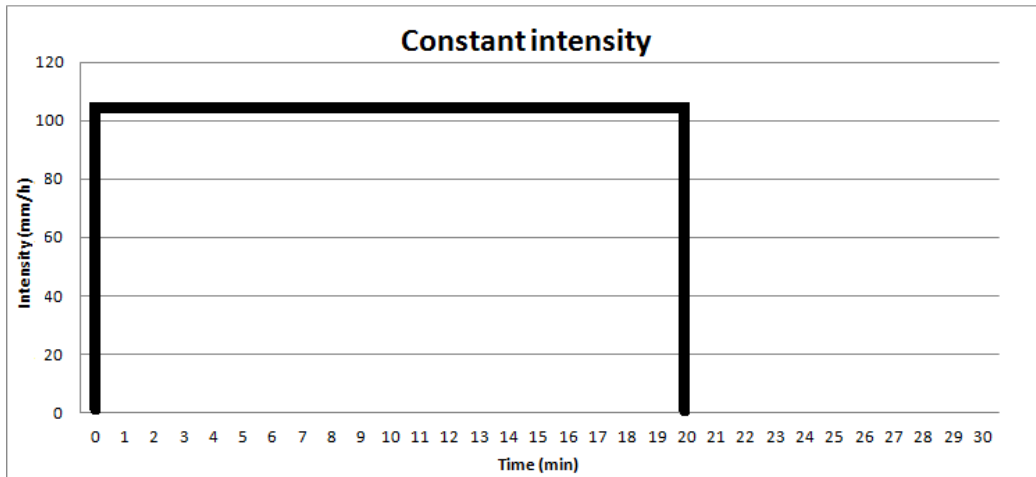
### 7.1.1 Constant intensity rain of project

This kind of rain utilized is the easiest one to use in the model.

There are several assumptions inherent to this method: the rainfall intensity is constant over a period that equals the time of concentration of the basin and is constant throughout the basin.

The frequency distribution of the event rainfall and the peak runoff rate are identical and the time of concentration of a basin is constant and is easily determined. The return period  $T_R$  and the total duration  $t_p$  of the event are defined before of all. The total rainfall height value is obtained by the pluviometric possibility curve. By calculating  $h/t_p$ , the intensity of rainfall  $I$  is defined, and it is assumed constant for the whole duration of the event.

It is very common to take into consideration rains of different durations, to identify the most onerous for the work. Although starting from a hypothesis that is not realistic, it is a method widely used in practice, especially for very small basins as the basin that we are considering in this project.



Graph 7.1 Hyetograph for constant intensity

### 7.1.2 Sifalda rain of project

The rain of project of Sifalda reproduces the average characteristics of a series of significant rainfall events recorded in 1973 in three different rainfall stations in Czechoslovakia, with duration comprised between 5 and 20 minutes. The Sifalda hyetograph is a kind of simplified Chicago hyetograph, where the parameters are the storm duration and the total rainfall depth. It is characterized by a variable intensity of rainfall and by a maximum that is in a central position.

The Hyetograph consists of three parts, relating to three contiguous time intervals: in the first interval the intensity grows linearly, is constant in the second and in the third decreases, still linearly. The first and the second interval each have a length equal to a quarter of the total duration  $t_p$ , while the third has duration equal to half  $t_p$ .

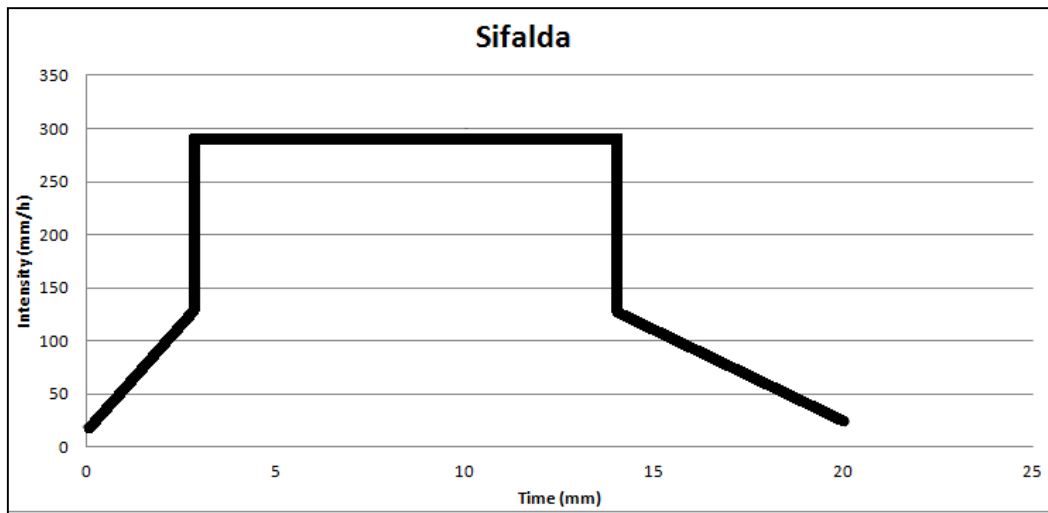
The Hyetograph is considered divided into three parts. In the central part, which comprises an interval of time between  $0.14t_p$  and  $0.70t_p$ , with  $t_p$  equal to the total duration of the rainfall event, the assigned rainfall intensity is given by:

$$i_c = \frac{h_c}{0,25 * t_p}$$

where  $h_c$  is the height of precipitation that is derived from the rain curve by entering  $t = 0.25 t_p$ .

In the first section of the graph that goes from  $t = 0$  to  $t = 0.14 t_p$ , it is assumed that the intensity grows linearly from a minimum value of  $0.065 i_c$  to a maximum value of  $0.435i_c$ .

In the last part of the Hyetograph, from  $t= 0.70t_p$  at  $t= t_p$ , it is assumed that the intensity decreases, always in a linear manner, from a maximum value to a minimum value of  $0.435i_c$  of  $0.087 i_c$ .



Graph 7.2 Hyetograph for Sifalda rain

### 7.1.3 Chicago rain of project

The method provides equations for calculating peak intensity, and then redistributes the rainfall before and after the peak with appropriate equations.

It is assumed in this case that the intensity of rainfall may grow in a continuous manner until it reaches a maximum peak beyond which tends to decrease gradually. The growing part of the curve is given by the equation:

$$i(t) = a * n * t_1^{n-1}$$

with:

$t_1 = (rt_p - t) / r$  with  $t_p$  = duration of the event ;

$r$  = the position of the peak variable to 0 to 1 and often place= 0.4.

The descending part of the graph is instead provided by the relationship:

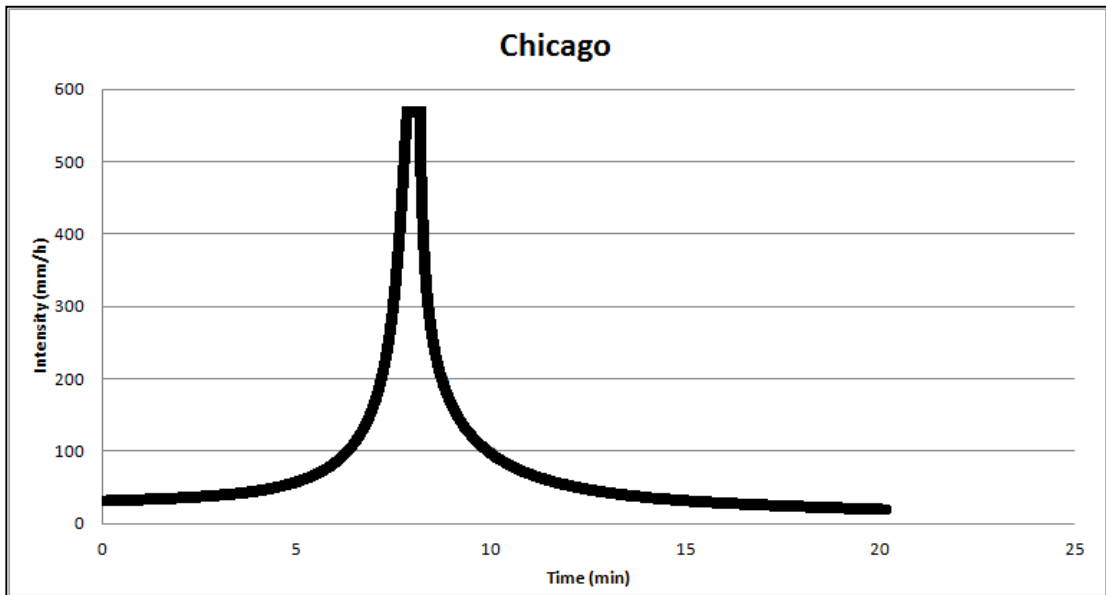
$$i(t) = a * n * t_2^{n-1}$$

With  $t$  ranging from 0 to  $rt_p$   $t$  che varia da  $t_p$  a  $rt_p$ .

In practice, a step of calculating time and peak position is secure, and apply the two reports, by varying  $t$  in a discreet manner in the range  $0-t_p$ , with step calculation that is chosen. This method, which provides a more realistic representation of the trend of the intensity of precipitation, compared to the previous method, can be used effectively for basins with areal extension of at least some hundreds of square kilometers and for durations of precipitation of at least a few hours. The use of calculation steps that are too small ( $<0.5$  h) may lead to excessive accentuation of the central peak.

The uncertainty of the position of the peak of precipitation, depending on the chosen value of  $r$ , makes this method very applicable for rapid thunders, while it is more useful for long rains in which there is a minor variation of the intensity.

Compared to our model, this type of hyetograph does not fit well to the conditions, since our basin is very small and we consider a time of rain less than an hour, then the central peak is in fact much overestimated.



Graph 7.3 Hyetograph for Chicago rain





# 8. S.W.M.M. results

## 8.1 Nodes analysis

SWMM results confirm the results obtained with rational method calculations.

Table 8.1 shows the report obtained from simulation concerning Node Inflow, where lateral inflow and total inflow are described as l/s: total inflow consists of lateral inflow plus inflow from connecting links.

Table 8.1 Node inflow - SWMM results

Node Inflow			
Node	Type	Maximum Lateral Inflow Node	Maximum Total Inflow Type
A	JUNCTION	3,7	3,7
B	JUNCTION	9,81	9,81
C	JUNCTION	6,15	15,95
D	JUNCTION	8,47	8,47
E	JUNCTION	4,93	13,38
F	JUNCTION	0	51,33
G	JUNCTION	6,15	6,15
H	JUNCTION	7,37	13,5
I	JUNCTION	4,93	18,33
L	JUNCTION	8,59	59,55
L'	JUNCTION	15,41	74,62
M	JUNCTION	2,47	76,96
N	JUNCTION	2,47	79,3
O	JUNCTION	0	79,26
P	JUNCTION	12,72	91,29
Q	JUNCTION	8,61	99,75
R	JUNCTION	6,15	105,75
S	JUNCTION	14,46	119,73
T	JUNCTION	6,15	125,72
out	OUTFALL	0	125,72

Table 8.2 Flowrate data (rational method)

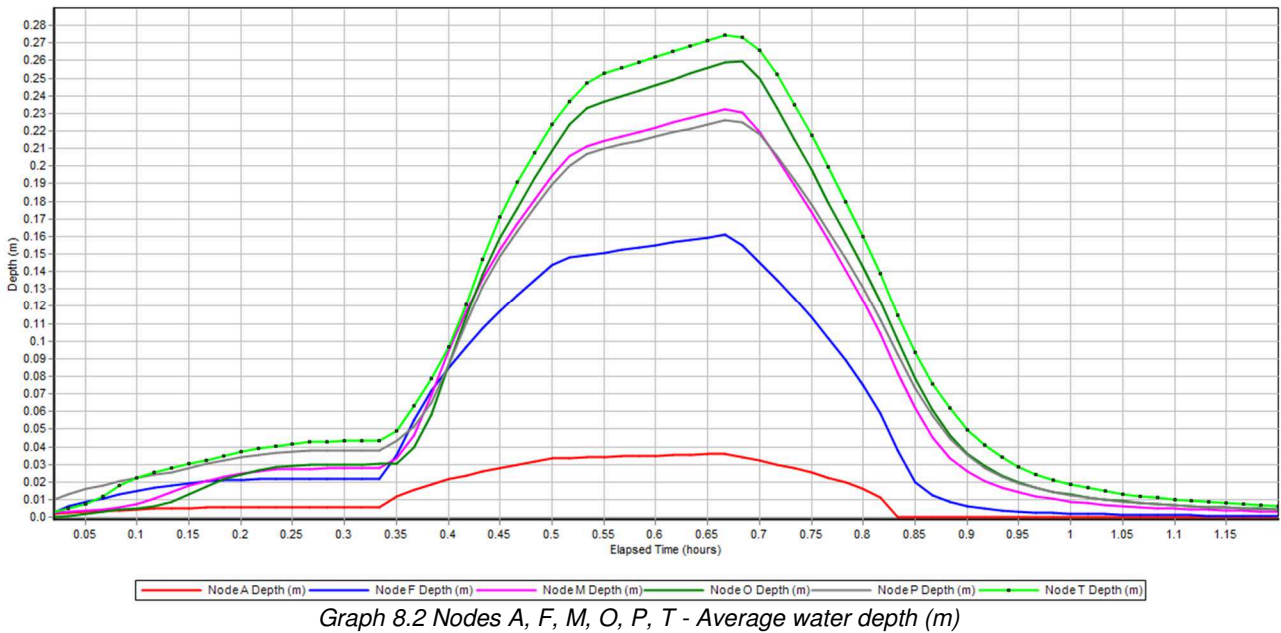
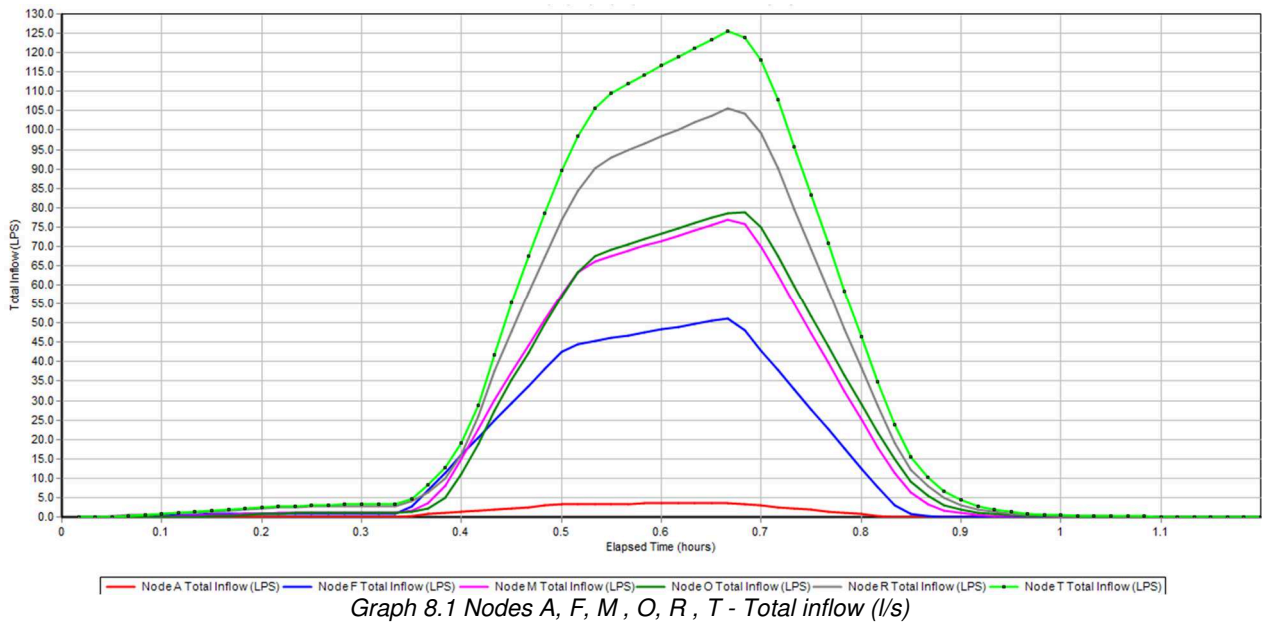
Pipe	Q(l/s)	Pipe	Q(l/s)
<b>AF</b>	4,26	<b>LL'</b>	79,06
<b>BC</b>	11,14	<b>L'M</b>	82,05
<b>CF</b>	18,86	<b>MN</b>	85,09
<b>DE</b>	10,23	<b>MO</b>	87,35
<b>EF</b>	15,63	<b>OP</b>	91,88
<b>GH</b>	6,46	<b>PQ</b>	98,52
<b>HI</b>	13,8	<b>QR</b>	102,79
<b>IF</b>	19,48	<b>RS</b>	112,6
<b>FL</b>	62,69	<b>ST</b>	117,36

Node T is the final junction of the system, before outlet, and maximum total inflow that arrives is equal to 117 l/s if using rational method. Data obtained with SWMM are nearly identical to those calculated. The difference, in this case of a few l/s is due to the fact that a complex software as SWMM considers many variables in the calculation of the network as the

slope of the area, infiltration, ponded areas, variation in the time of rain so the result is certainly different than that obtained with the manual calculations, which are effective but more simplified.

With certainty the method used and the model may be overlapped and the calculations were carried out in the correct manner, since the flow rate in output is the same obtained by SWMM.

Graph 8.3 represents water level above invert value in the conduit, so the values are the average water depth and its variation along time, for a 20 minutes rainfall event with constant intensity.



## 8.2 Links analysis

Table 8.1 Link flow SWMM summary

***** Link Flow Summary *****				
Link	Type	Maximum  Flow  LPS	Max Velocity m/sec	Max/ Full Depth
AF	CONDUIT	3,7	0,76	0,47
BC	CONDUIT	9,81	0,76	0,59
CF	CONDUIT	15,95	0,67	0,64
DE	CONDUIT	8,47	0,81	0,59
EF	CONDUIT	13,38	0,74	0,56
GH	CONDUIT	6,15	0,75	0,57
HI	CONDUIT	13,51	0,88	0,72
IF	CONDUIT	18,33	0,85	0,60
FL	CONDUIT	51,3	0,86	0,61
LL'	CONDUIT	59,54	0,87	0,66
L'M	CONDUIT	74,54	0,68	0,70
MN	CONDUIT	76,92	0,85	0,68
NO	CONDUIT	79,26	0,85	0,67
OP	CONDUIT	79,25	0,85	0,71
PQ	CONDUIT	91,29	0,88	0,68
QR	CONDUIT	99,72	0,78	0,67
RS	CONDUIT	105,7	0,91	0,69
ST	CONDUIT	119,72	0,89	0,71
Tout	CONDUIT	125,72	0,88	0,70

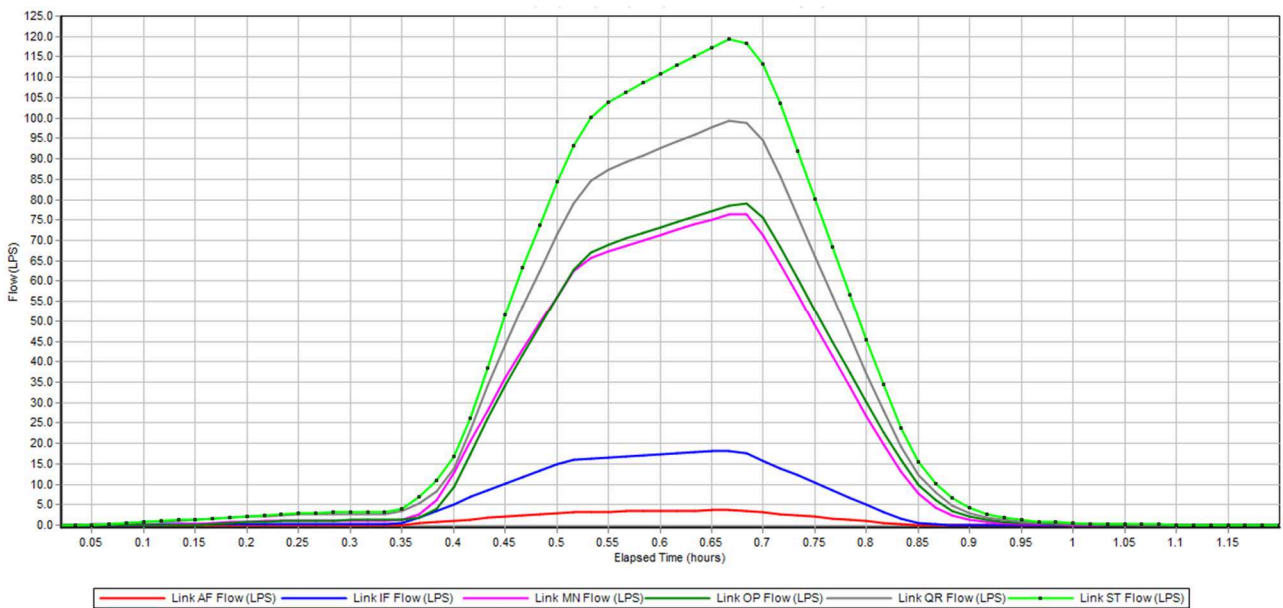
Table 8.2 Results obtained with rational method

	L [m]	Tc(s)	h(mm)	u(l/s,ha)	Q(l/s)	A'(m2)	D(m)	A'/D2	y/D	RH/D	RH	i	T (Pa)
AF	54,44	954,44	32,90	137,89	4,26	0,004	0,12	0,303	0,41	0,2182	0,026	0,013	3,32
BC	5	905	32,47	143,51	11,14	0,011	0,15	0,472	0,58	0,2728	0,042	0,007	2,82
CF	12	917	32,57	142,09	18,86	0,019	0,19	0,511	0,62	0,2821	0,054	0,005	2,59
DE	5	905	32,47	143,51	10,23	0,010	0,15	0,433	0,54	0,2621	0,040	0,007	2,86
EF	15,88	920,88	32,61	141,64	15,63	0,016	0,19	0,423	0,53	0,2592	0,050	0,005	2,67
GH	20,72	920,72	32,61	141,66	6,46	0,006	0,12	0,459	0,57	0,2703	0,032	0,010	3,09
HI	41,68	962,4	32,97	137,03	13,80	0,014	0,15	0,585	0,7	0,2962	0,045	0,006	2,75
IF	23,93	986,33	33,17	134,52	19,48	0,019	0,19	0,528	0,53	0,2592	0,050	0,005	2,67
FL	59,96	1046,29	33,66	128,69	62,69	0,063	0,38	0,425	0,53	0,2592	0,100	0,002	2,12
LL'	14,51	1060,8	33,78	127,37	79,06	0,079	0,38	0,536	0,64	0,2862	0,110	0,002	2,05
L'M	23,16	1083,96	33,96	128,17	82,05	0,082	0,38	0,556	0,67	0,2917	0,112	0,002	2,03
MN	15,68	1099,64	34,08	129,27	85,09	0,085	0,38	0,576	0,69	0,2948	0,113	0,002	2,03
MO	14,46	1114,1	34,19	129,87	87,35	0,087	0,38	0,592	0,71	0,2975	0,114	0,002	2,02
OP	8,51	1122,61	34,26	122,06	91,88	0,092	0,38	0,622	0,74	0,3	0,115	0,002	2,02
PQ	8,83	1131,44	34,32	121,35	98,52	0,099	0,38	0,667	0,79	0,3039	0,117	0,002	2,01
QR	23,08	1154,52	34,50	119,52	102,79	0,103	0,48	0,446	0,55	0,2649	0,127	0,002	1,95
RS	24,64	1179,16	34,68	117,64	112,60	0,113	0,48	0,489	0,59	0,2753	0,132	0,001	1,93
ST	7,32	1186,48	34,73	117,10	117,36	0,117	0,48	0,509	0,62	0,2821	0,135	0,001	1,91

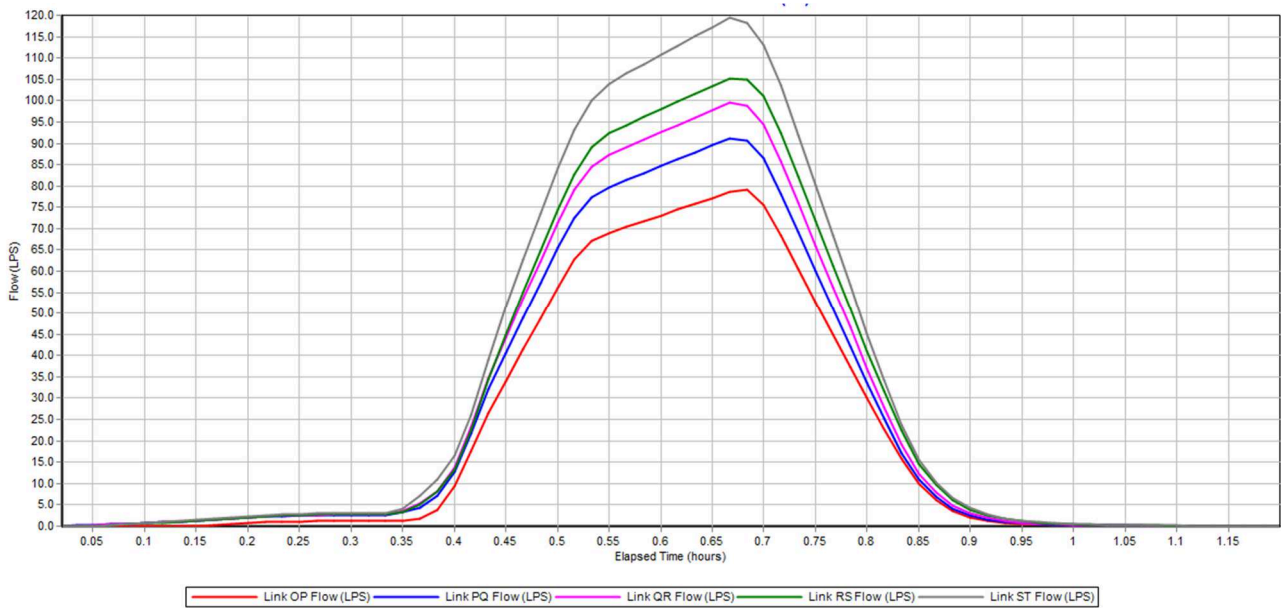
In SWMM, flooding will occur whenever the water surface at a node exceeds the maximum defined depth or if more flow volume enters a node than can be stored or released during a given time step. Normally such water will be lost from the system. The option also exists to have this water pond atop the node and be re-introduced into the drainage system when capacity exists to do so.

Flooding refers to all water that overflows a node, whether it ponds or not, and only those nodes that flood are listed. Our simulation demonstrates that no links are overflowed, the

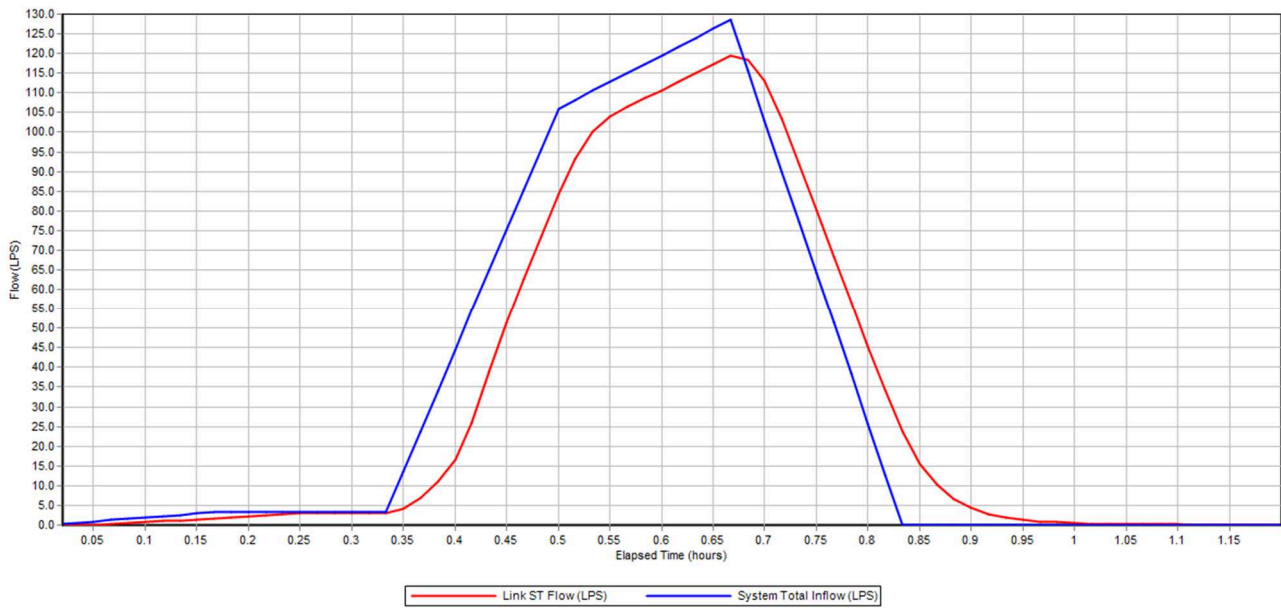
Max/ Full Flow column in table 8.3 shows the ratio of maximum height of flow in the conduit compared to the diameter of it. The type of motion that occurs in a pipeline, with a ratio  $y/D$  gradually more and more 'high (from 0.5), becomes less approximated with the formulas of uniform flow or motion gradually varied, since the instability the free surface (triggered also as a result of small "irregularities" on the wetted perimeter) initiate dissipative processes that "globally" increase the average roughness which regulates the same flow. For values greater than  $y/D = 0.8$  instabilities involved, due to changes in local pressure in the volume of air trapped between the free surface and the crown of the conduct. In the network this value is always under limit value.



Graph 8.3 Links AF, IF, MN, OP, QR, ST - Links Flow Rate (l/s)



Graph 8.4 Flow Rate (l/s) in the final pipelines of the system



Graph 8.5 Link flow rate vs system Total Inflow (l/s)

### 8.3 Subcatchments analysis

Infiltration of rainfall into the upper soil zone of subcatchments is modeled by using proper methods and parameters, depending on the properties of the soil, reported in Table 8.4.

Table 8.3 Soil Characteristics - Green Ampt parameters f(soil characteristics)

Soil Texture Class	K	$\Psi$	$\phi$	FC	WP
Sand	4.74	1.93	0.437	0.062	0.024
Loamy Sand	1.18	2.40	0.437	0.105	0.047
Sandy Loam	0.43	4.33	0.453	0.190	0.085
Loam	0.13	3.50	0.463	0.232	0.116
Silt Loam	0.26	6.69	0.501	0.284	0.135
Sandy Clay Loam	0.06	8.66	0.398	0.244	0.136
Clay Loam	0.04	8.27	0.464	0.310	0.187
Silty Clay Loam	0.04	10.63	0.471	0.342	0.210
Sandy Clay	0.02	9.45	0.430	0.321	0.221
Silty Clay	0.02	11.42	0.479	0.371	0.251
Clay	0.01	12.60	0.475	0.378	0.265

**K** = saturated hydraulic conductivity, in/hr

**$\Psi$**  = suction head, in.

**$\phi$**  = porosity, fraction

**FC** = field capacity, fraction

**WP** = wilting point, fraction

Source: Rawls, W.J. et al., (1983). *J. Hyd. Engr.*, 109:1316.



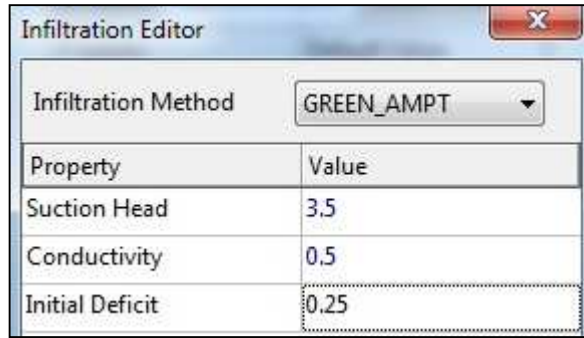


Figure 8.2 Infiltration dialog box [inch, inch/hour].

Once defined the characteristic values for Green-Ampt model for a sandy silty soil, SWMM model elaborates physical data of the network and parameters calibrated, the results is easily compared with data obtained by rational method calculations and they correspond.

The results from SWMM confirm the initial hypothesis of assuming runoff coefficient equal to 0.3, because of the predominance of green areas when water easily infiltrates

Table 8.4 Subcatchment runoff summary - Runoff data, SWMM.

```

*****
Subcatchment Runoff Summary
*****

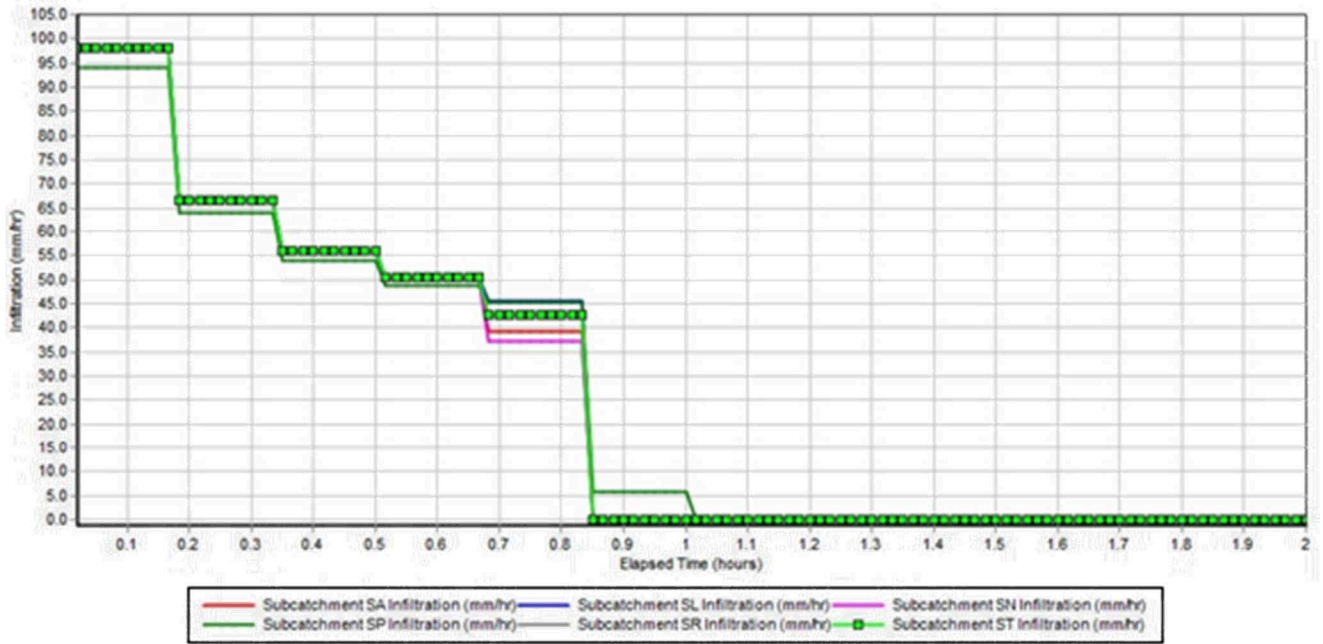
-----

Subcatchment      Runoff
                   Coeff

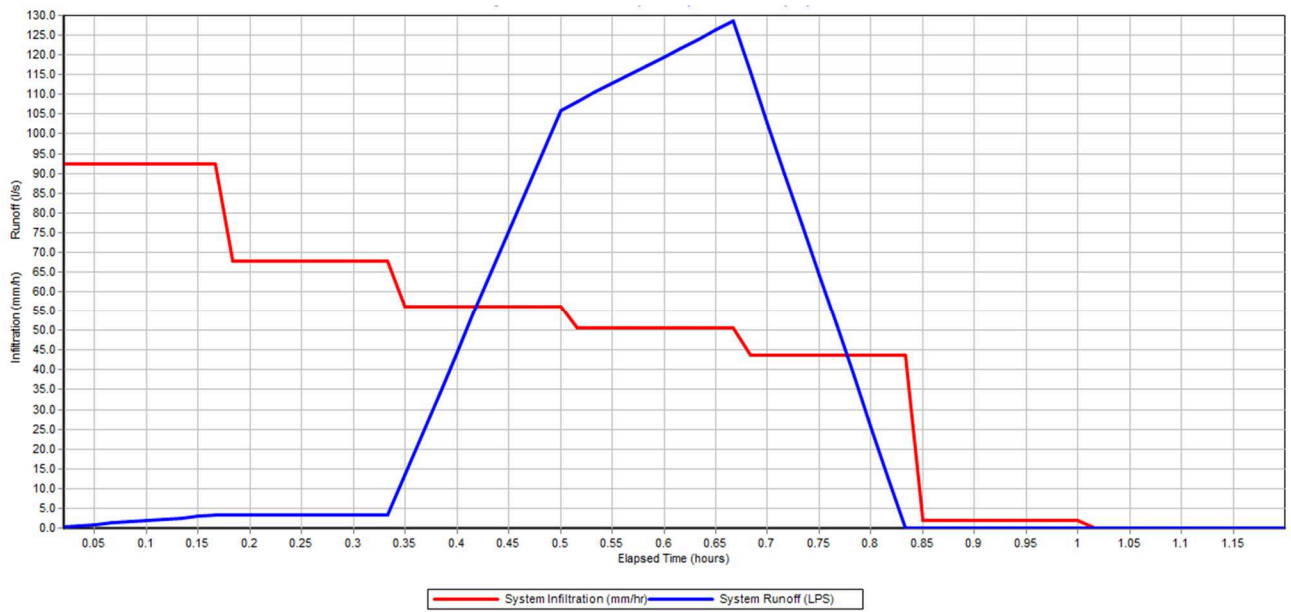
-----

SA                0,304
SB                0,299
SC                0,303
SD                0,289
SE                0,303
SG                0,303
SH                0,302
SI                0,303
SL                0,301
SL'              0,274
SM                0,304
SN                0,304
SO                0,304
SP                0,322
SQ                0,302
SR                0,303
SS                0,285
ST                0,303

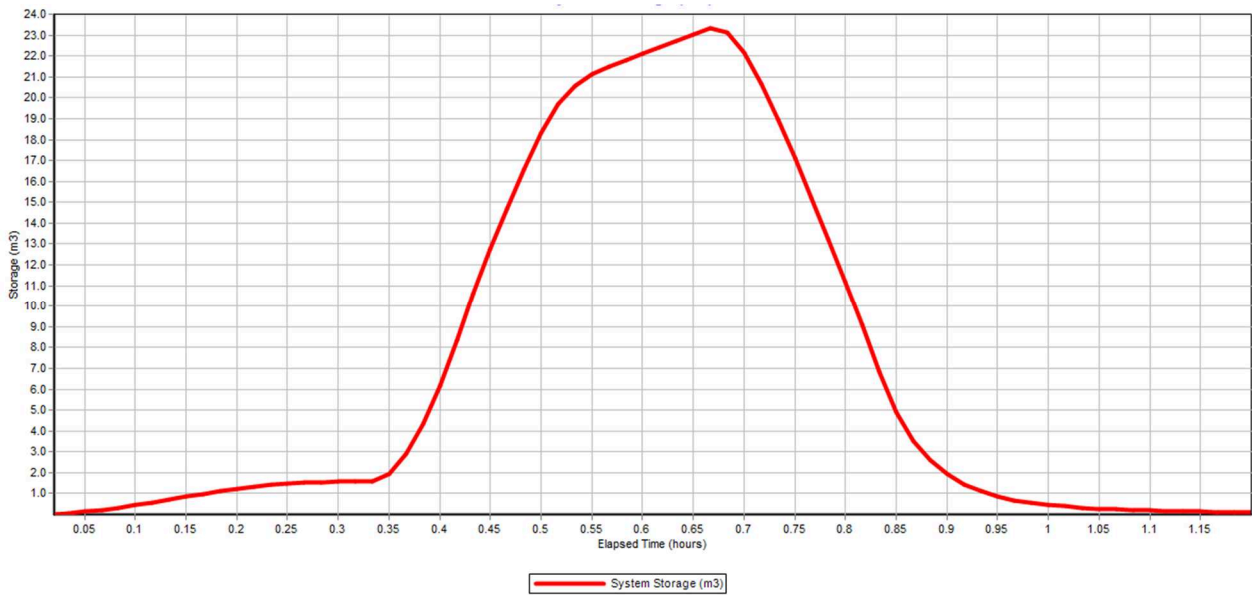
```



Graph 8.6 Subcatchments SA, SL, SN, SP, SR, ST - Infiltration (mm/h) in testing subcatchments



Graph 8.7 System Infiltration (mm/h) vs Runoff (l/s)



Graph 8.8 Normal curve of system storage value (m3)

### 8.4 Graphical elaboration

The Animator panel of the Map Browser contains controls for animating the Study Area Map and all Profile Plots through time, updating map color-coding and hydraulic grade line profile depths as the simulation time clock is automatically moved forward or back.

The Legend Editor is used to set numerical ranges to which different colors are assigned for viewing a particular parameter on the network map.

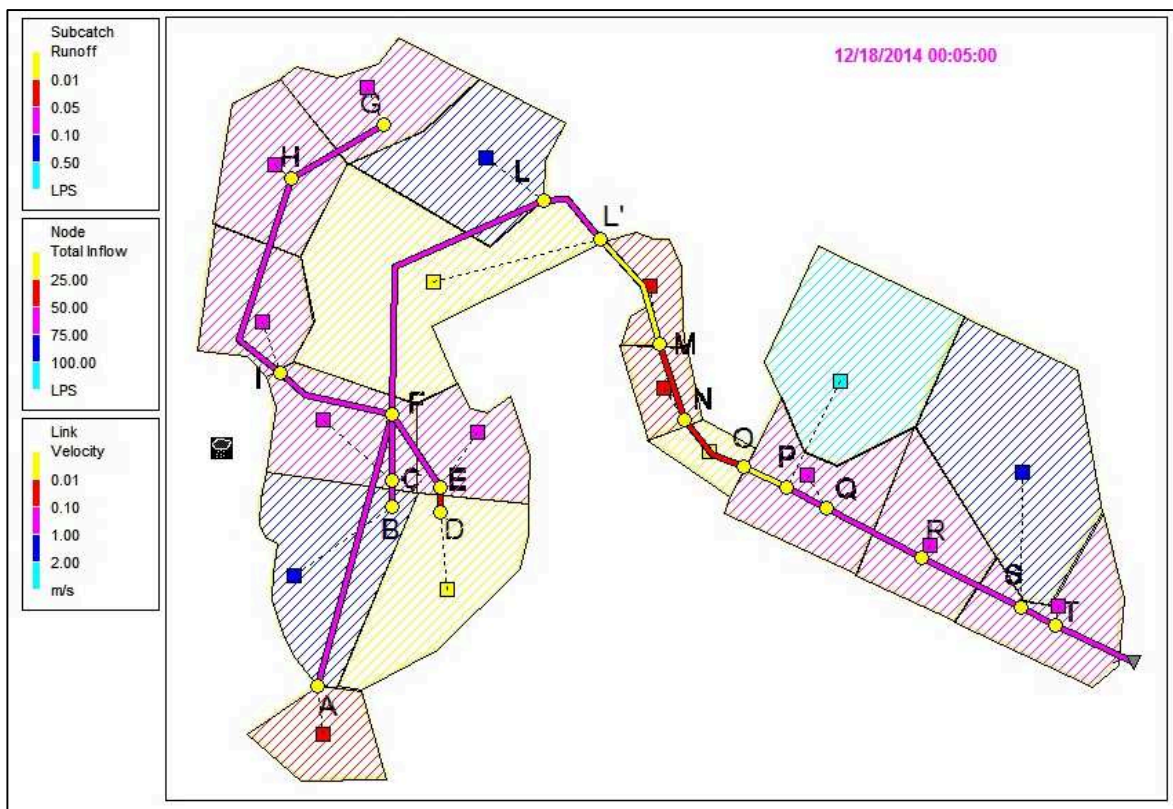


Figure 8.3 Network after 5 min of simulation

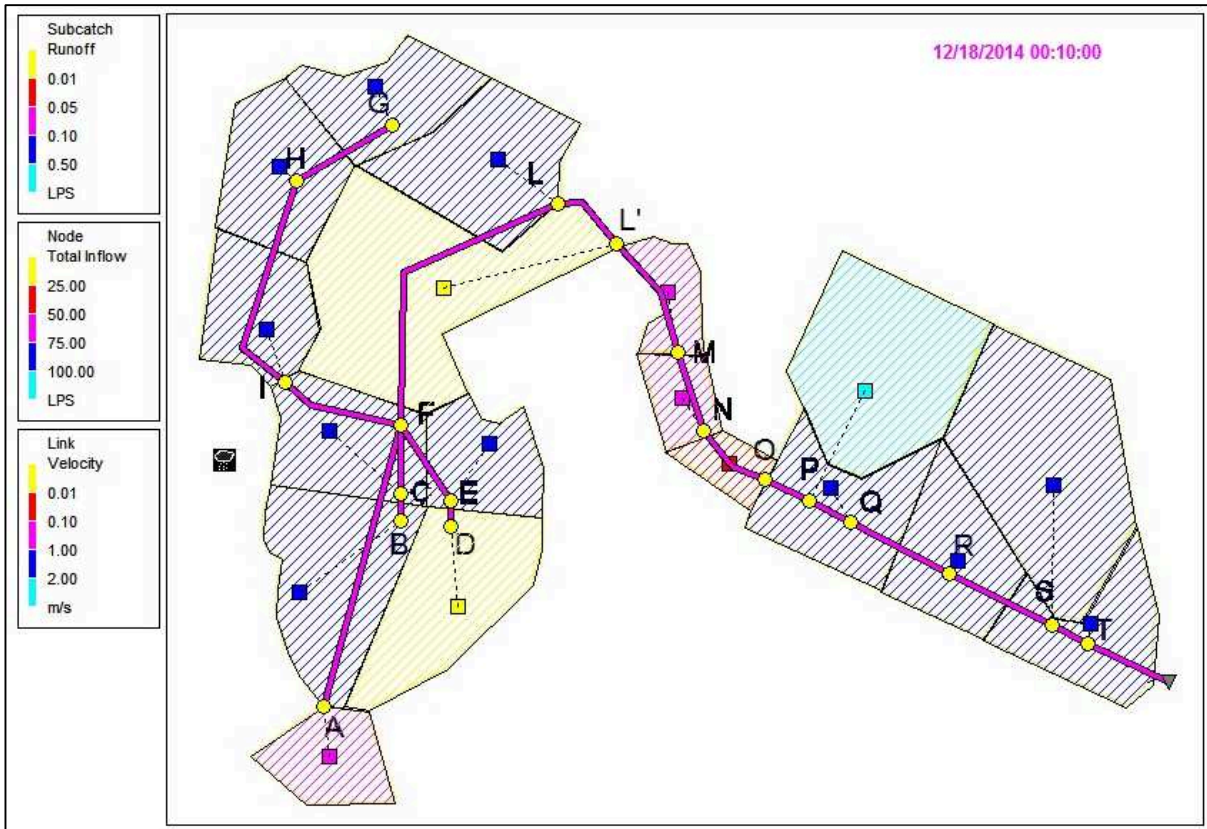


Figure 8.4 Network after 10 minutes of simulation

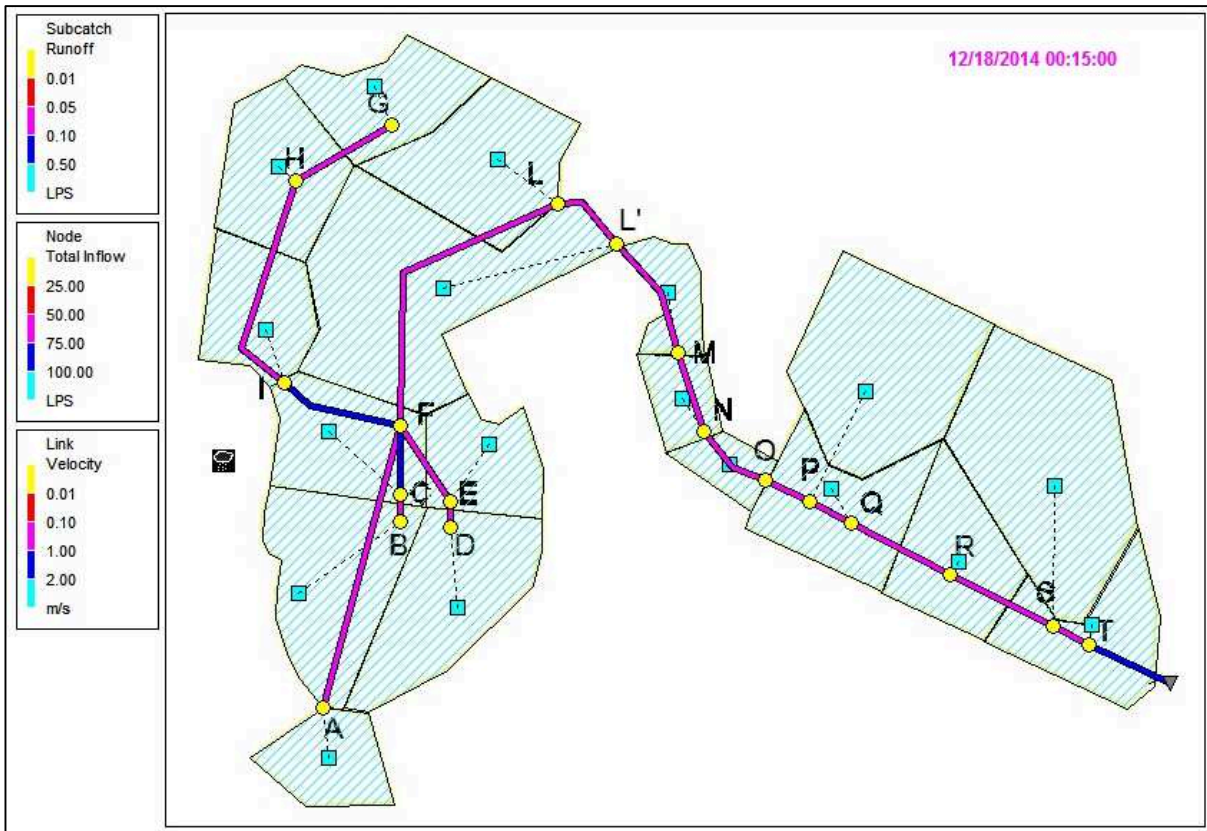


Figure 8.5 Network after 15 minutes of simulation



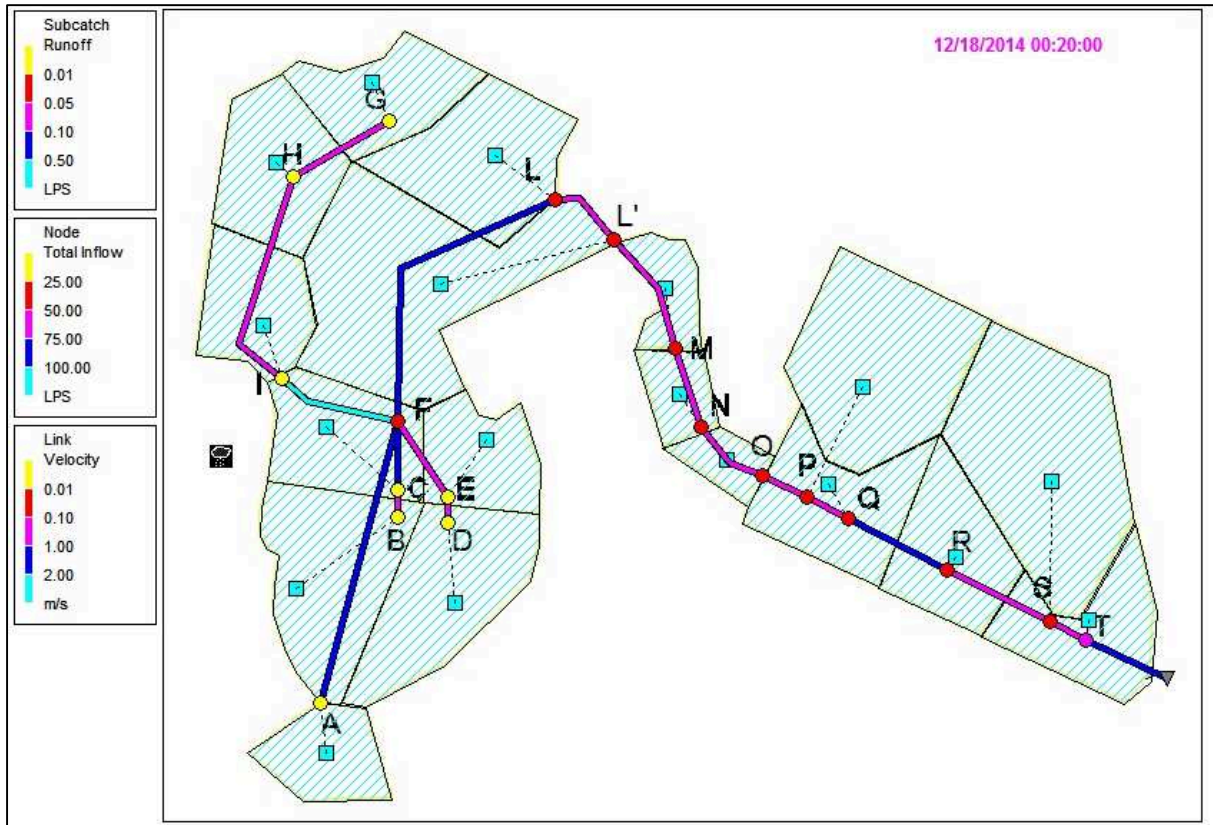


Figure 8.6 Network after 20 minutes of simulation

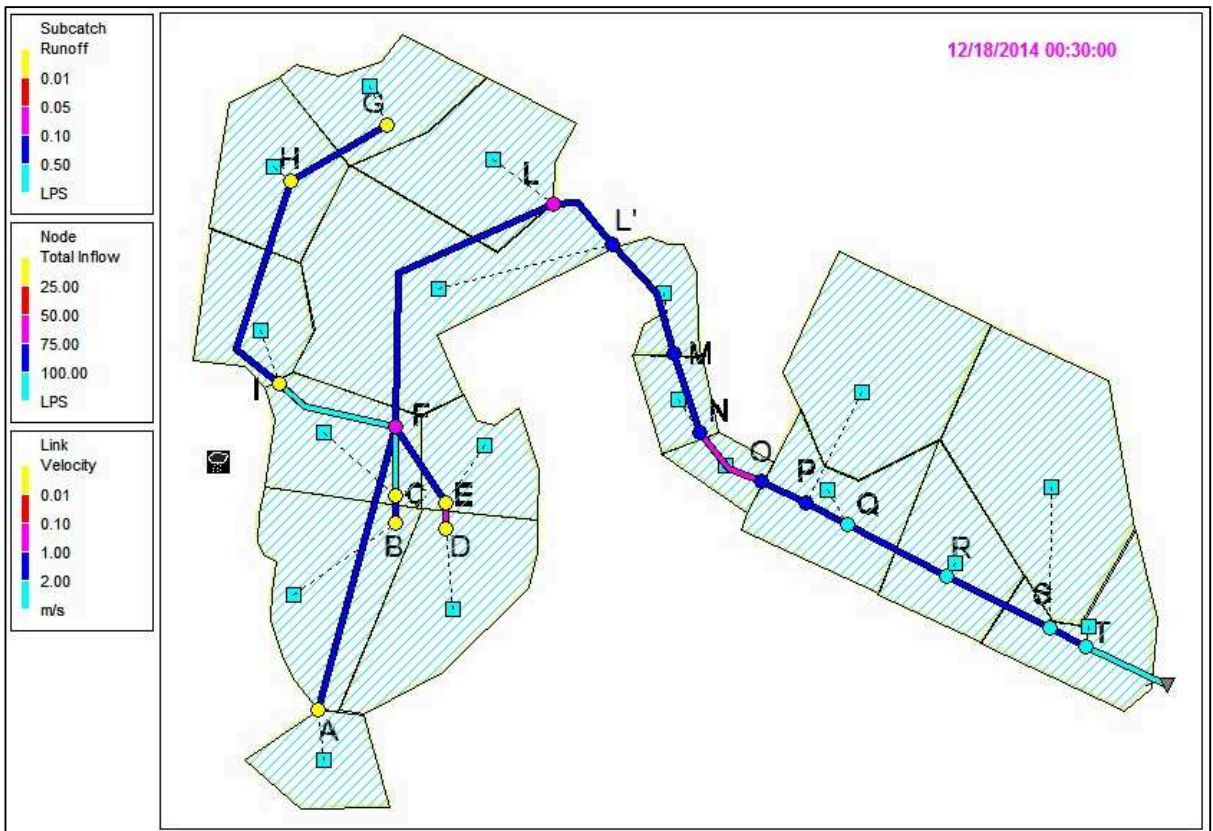


Figure 8.7 Network after 30 minutes of simulation

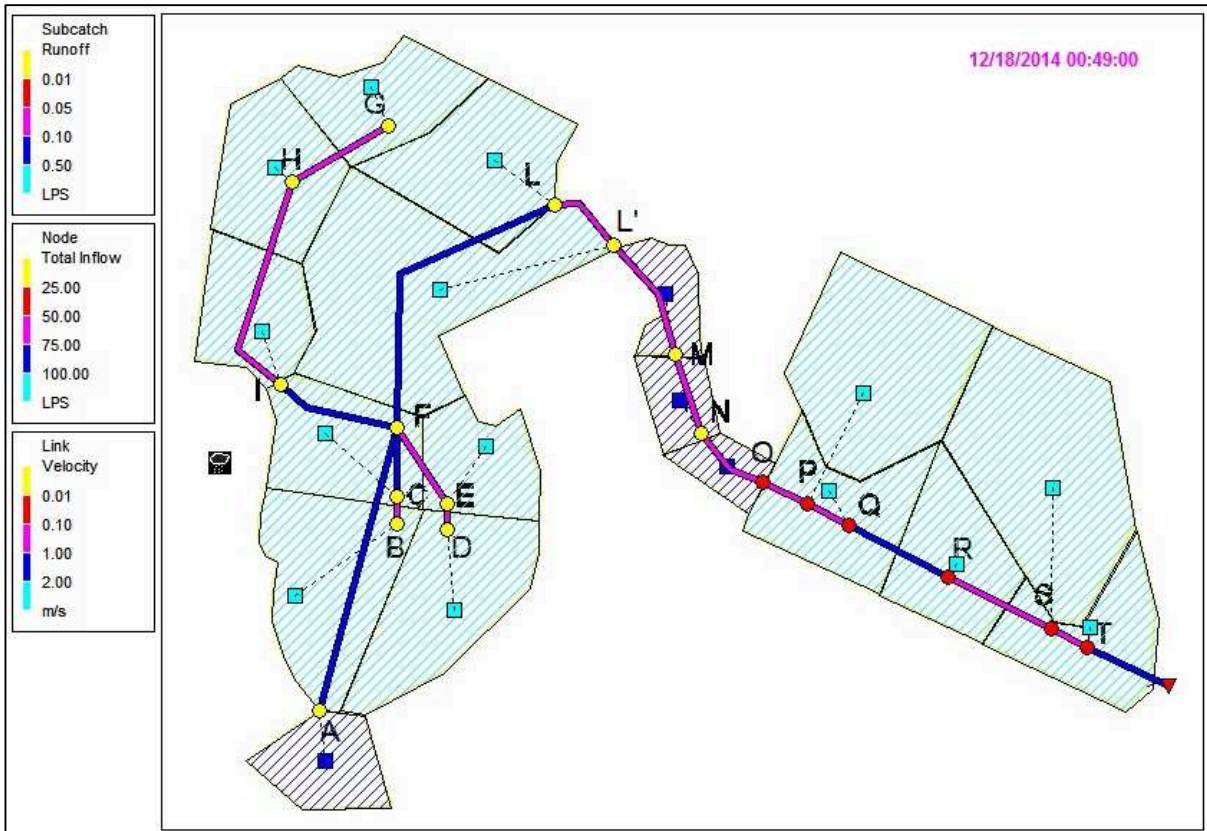


Figure 8.8 Network after 49 minutes of simulation

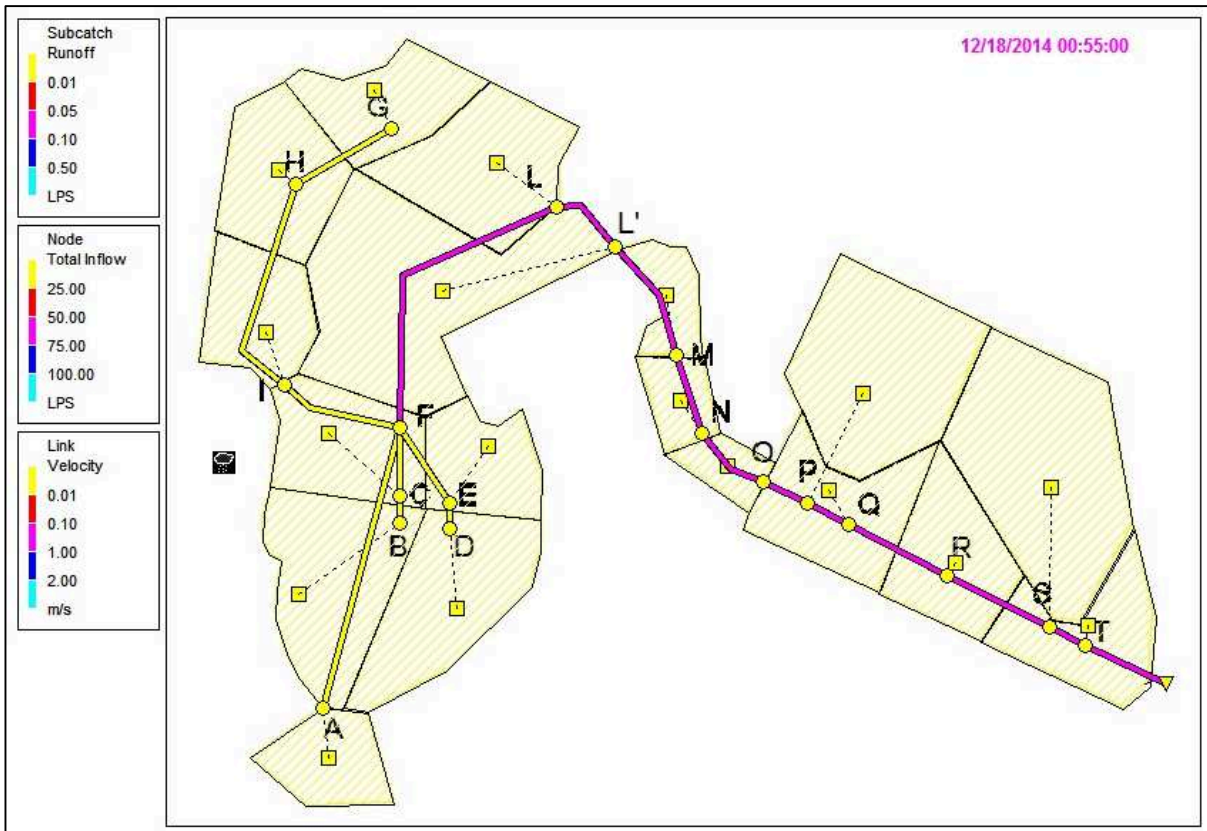


Figure 8.9 Network after 55 minutes of simulation



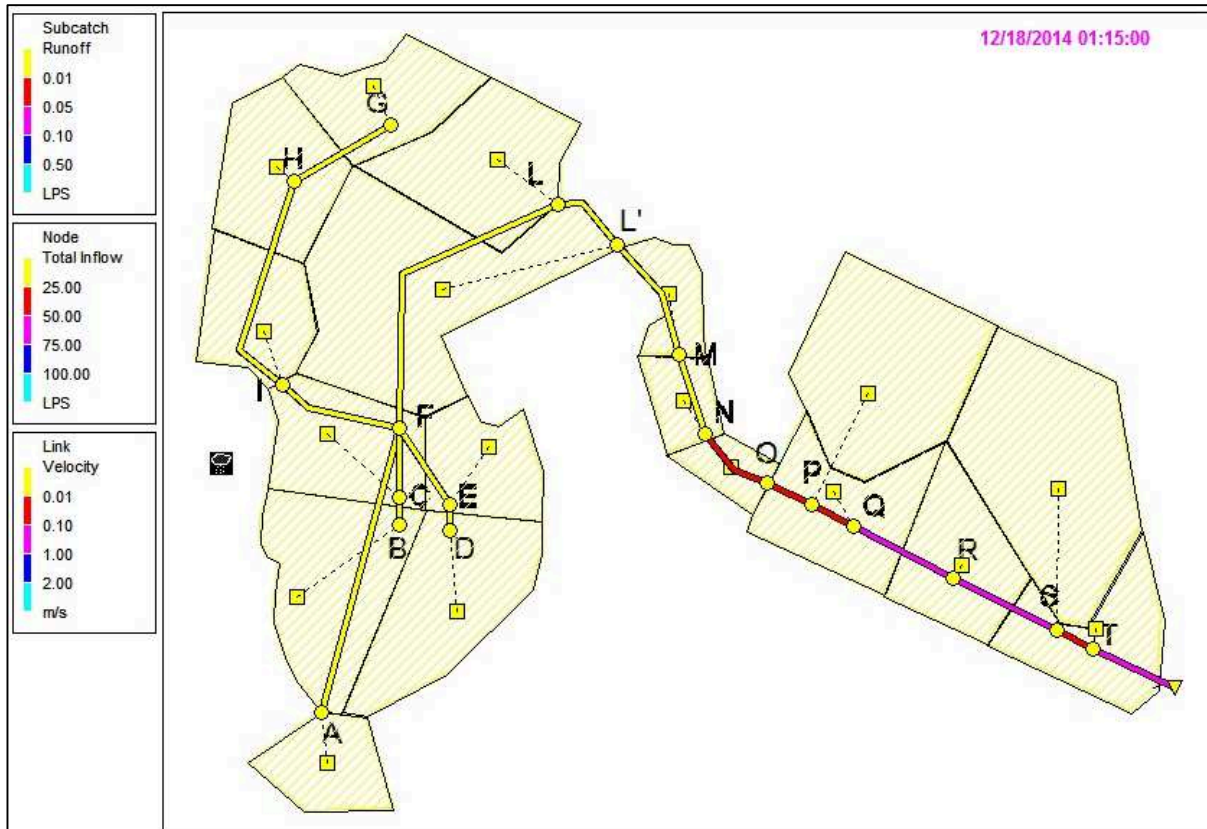


Figure 8.10 Network after 1 hour and 15 minutes of simulation

## 8.5 Museum confluence analysis

The simulation analyzed so far, does not consider an important new contribution that according to the project assumed would come in this drainage network. This contribution is represented by the 300 l/s coming from the area around the museum, currently drained near the Scrovegni Chapel. The project intends to discharge this onerous flow in the network that crosses the lower part of the gardens.

Considering this new contribution, the calculations were done again with the rational method, and with SWMM was added a new node to expand the network.

This node, named X, is the output node in which afferent download a surface of one hectare almost totally waterproof, with runoff coefficient assumed equal to 0.8. The new results obtained are shown in table 8.6.

Table 8.5 Rational method

Pipe	L [m]	T <sub>c</sub> (s)	H (mm)	u (l/s,ha)	Q (l/s)	A' (mq)	D (m)	A'/D <sup>2</sup>	y/D	R <sub>H</sub> /D	R <sub>H</sub>	i	τ
AF	54,44	954,44	32,90	137,89	4,26	0,004	0,1186	0,303	0,41	0,2182	0,026	0,013	3,3
BC	5,00\	905,00	32,47	143,51	11,14	0,011	0,1536	0,472	0,58	0,2728	0,042	0,007	2,8
CF	12,00	917,00	32,57	142,09	18,86	0,019	0,1922	0,511	0,62	0,2821	0,054	0,005	2,6
DE	5,00	905,00	32,47	143,51	10,23	0,010	0,1536	0,433	0,54	0,2621	0,040	0,007	2,9
EF	15,88	920,88	32,61	141,64	15,63	0,016	0,1922	0,423	0,53	0,2592	0,050	0,005	2,7
GH	20,72	920,72	32,61	141,66	6,46	0,006	0,1186	0,459	0,57	0,2703	0,032	0,010	3,1
HI	41,68	962,40	32,97	137,03	13,80	0,014	0,1536	0,585	0,7	0,2962	0,045	0,006	2,7
IF	23,93	986,33	33,17	134,52	19,48	0,019	0,192	0,528	0,53	0,2592	0,050	0,005	2,7
FL	59,96	1046,29	33,66	128,69	62,69	0,063	0,3842	0,425	0,53	0,2592	0,100	0,002	2,1
LL'	14,51	1060,80	33,78	127,37	79,06	0,079	0,3842	0,536	0,64	0,2862	0,110	0,002	2,0
L'M	23,16	1083,96	33,96	128,17	82,05	0,082	0,3842	0,556	0,67	0,2917	0,112	0,002	2,0
MN	15,68	1099,64	34,08	129,27	85,09	0,085	0,3842	0,576	0,69	0,2948	0,113	0,002	2,0
MO	14,46	1114,10	34,19	129,87	87,35	0,087	0,3842	0,592	0,71	0,2975	0,114	0,002	2,0
OX	100,00	1000,00	33,29	266,28	266,28	0,266	0,605	0,630	0,75	0,3017	0,196	0,001	1,7
OP	8,51	1122,61	34,26	122,06	213,95	0,214	0,605	0,594	0,71	0,2795	0,168	0,001	1,8
PQ	8,83	1131,44	34,32	121,35	219,87	0,220	0,605	0,611	0,72	0,2987	0,179	0,001	1,7
QR	23,08	1154,52	34,50	119,52	222,31	0,222	0,605	0,618	0,73	0,2998	0,180	0,001	1,7
RS	24,64	1179,16	34,68	117,64	230,24	0,230	0,605	0,640	0,76	0,3024	0,181	0,001	1,7
ST	7,32	1186,48	34,73	117,10	234,45	0,234	0,605	0,651	0,77	0,3031	0,182	0,001	1,7

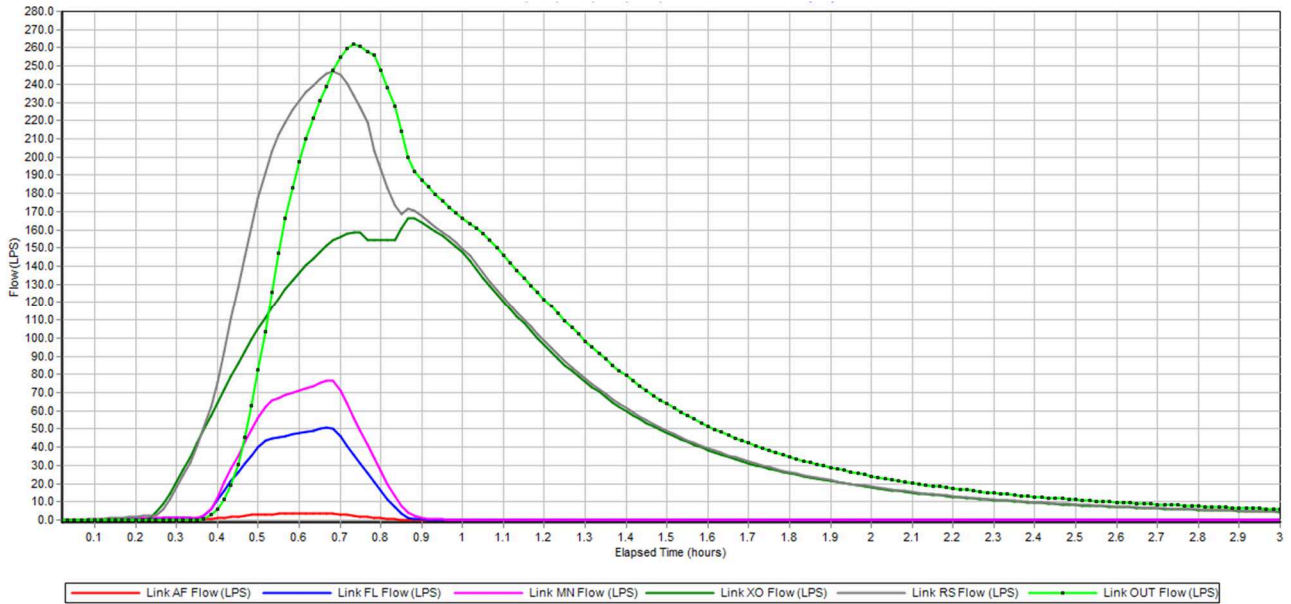
Table 8.6 Link flow summary - SWMM results

```

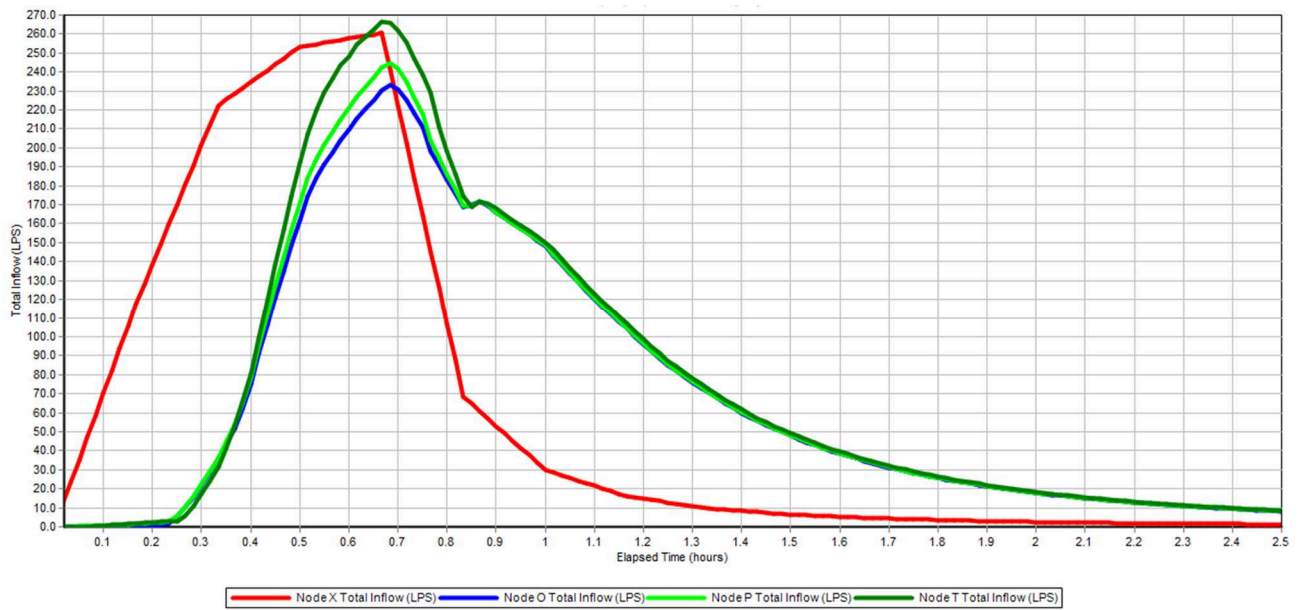
*****
Link Flow Summary
*****
-----
Link              Type              Maximum          Maximum          Max/          Max/
                  |Flow|            |Flow|            |Flow|          |Flow|
                  LPS              m/sec            LPS              m/sec            LPS              m/sec
-----
AF                CONDUIT            3.96             1.94             0.76           0.47
BC                CONDUIT           10.09            1.05             0.76           0.59
CF                CONDUIT           16.43            2.16             0.67           0.64
DE                CONDUIT            8.72             0.67             0.81           0.59
EF                CONDUIT           13.85            1.18             0.74           0.56
GH                CONDUIT            6.43             1.48             0.75           0.57
HI                CONDUIT           14.25            1.26             0.88           0.72
IF                CONDUIT           18.94            2.49             0.85           0.6
FL                CONDUIT           53.98            1.53             0.86           0.61
LL'              CONDUIT           61.44            1.03             0.87           0.66
L'M              CONDUIT           77.06            1.12             0.68           0.7
MN                CONDUIT           79.38            1.06             0.85           0.72
NO                CONDUIT           81.63            0.96             0.85           0.67
XO                CONDUIT          166.75            0.45             0.85           0.69
OP                CONDUIT          235.72            1.32             0.88           0.77
PQ                CONDUIT          235.35            1.31             0.71           0.75
QR                CONDUIT          248.83            2.18             0.76           0.71
RS                CONDUIT          253.56            1.43             0.82           0.71
ST                CONDUIT          267.61            1.32             0.81           0.73
OUT              CONDUIT          277.88            1.19             0.78           0.72

```

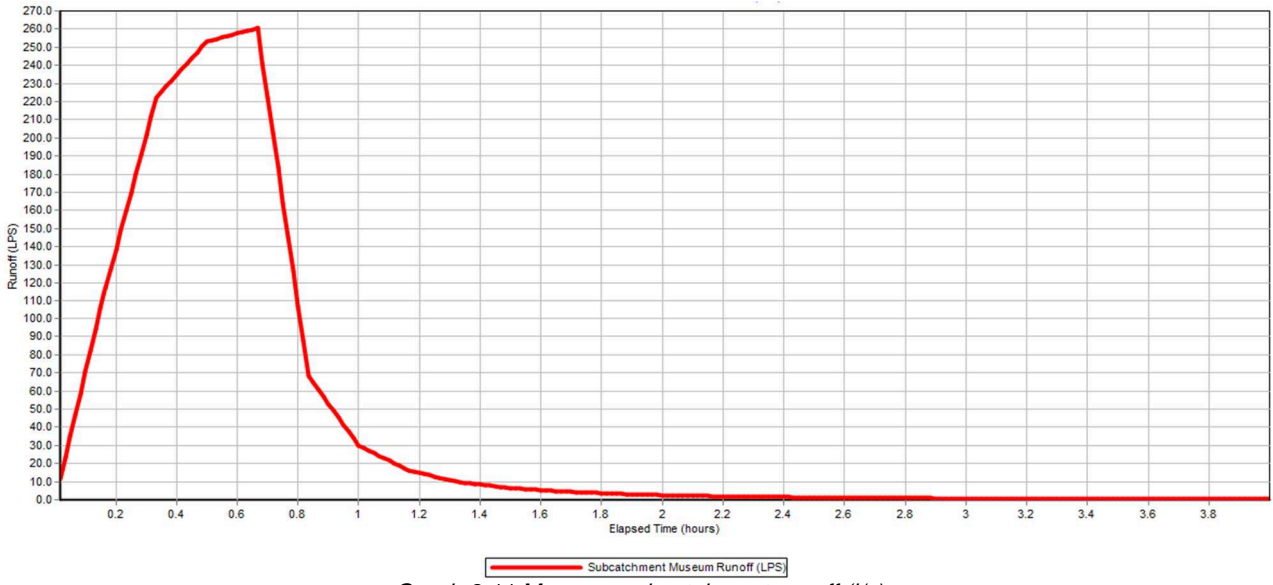
According to the calculation software SWMM the terminal section of the network is crossed, as the maximum value, by a flow rate of 277 l/s, according to the calculations instead the flow rate is lower of 30 l/s. The difference in flow rate is surely due to the complexity of the software and of all the parameters that it uses in a running simulation.



Graph 8.9 Links AF, FL, MN, XO, RS, OUT - Flow Rate (l/s)



Graph 8.10 Nodes X, O, P, T - Inflow (l/s)



Graph 8.11 Museum subcatchment runoff (l/s)

### 8.6 Graphical elaboration

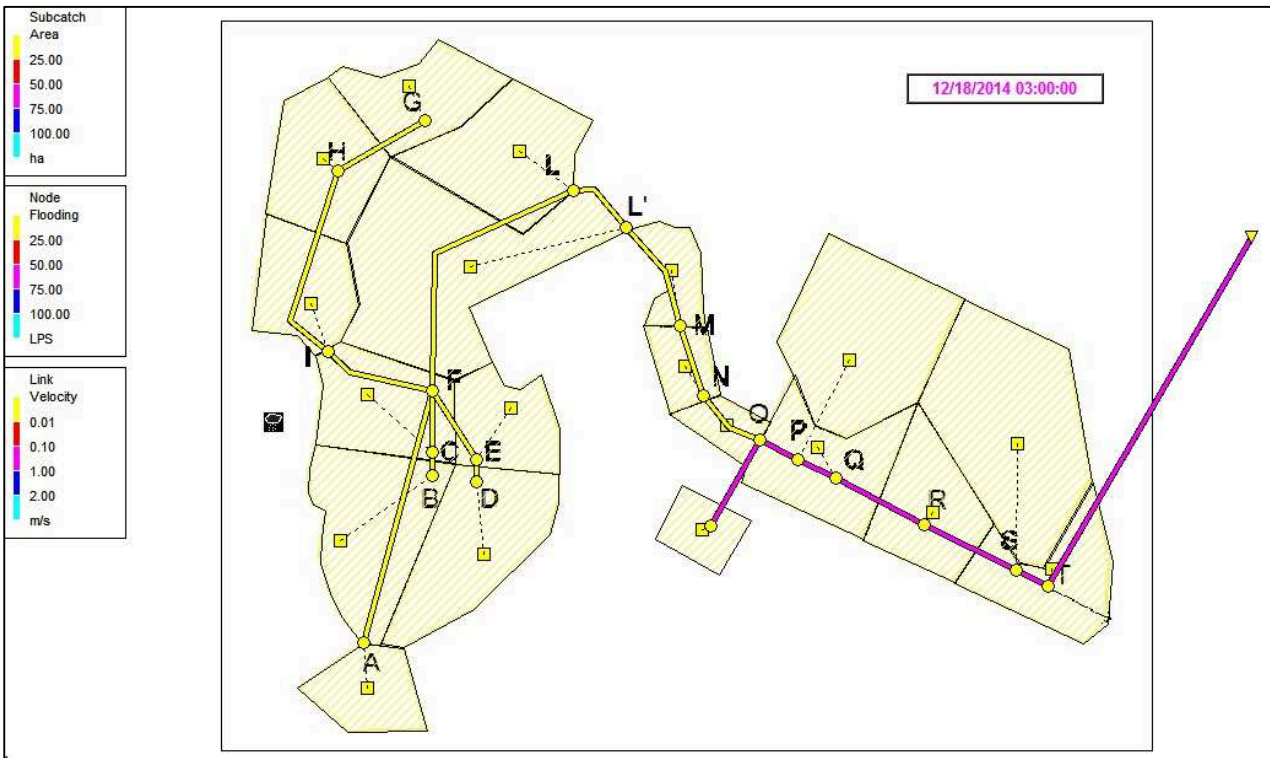


Figure 8.11 Network after 3 minutes of simulation



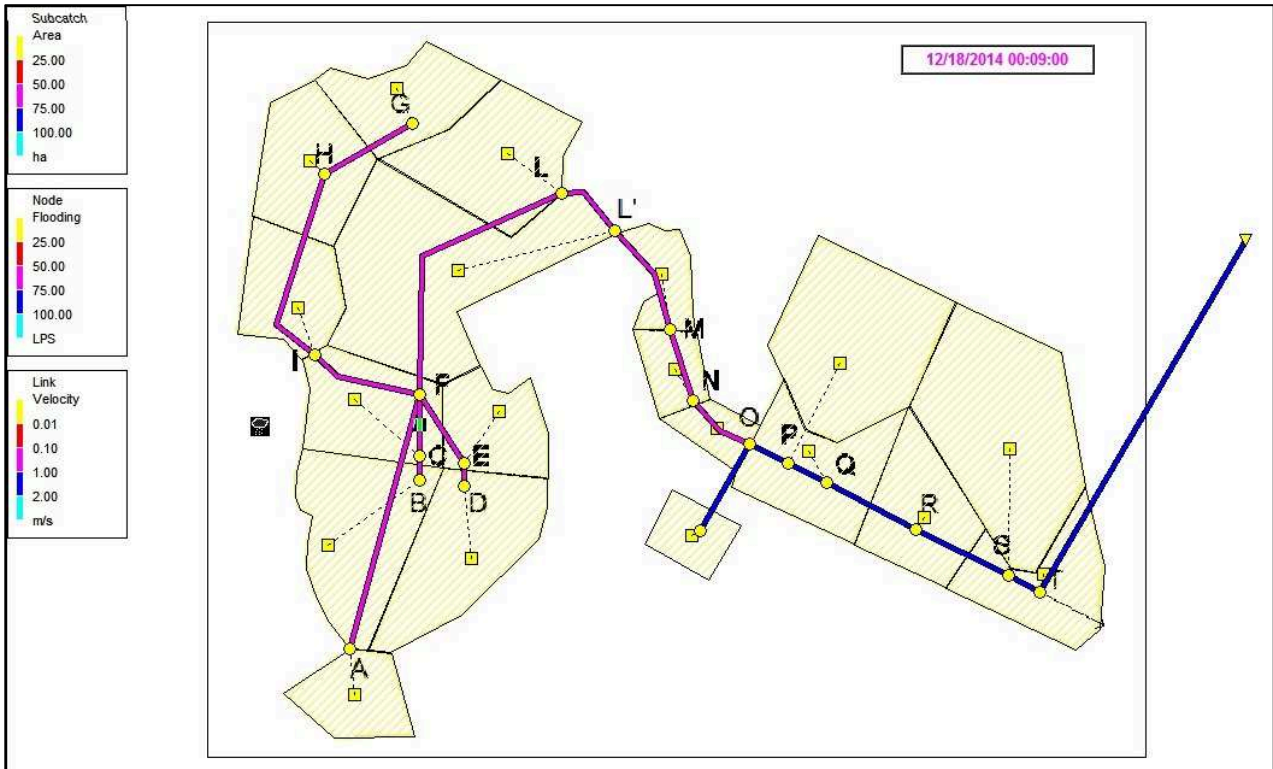


Figure 8.12 Network after 9 minutes of simulation

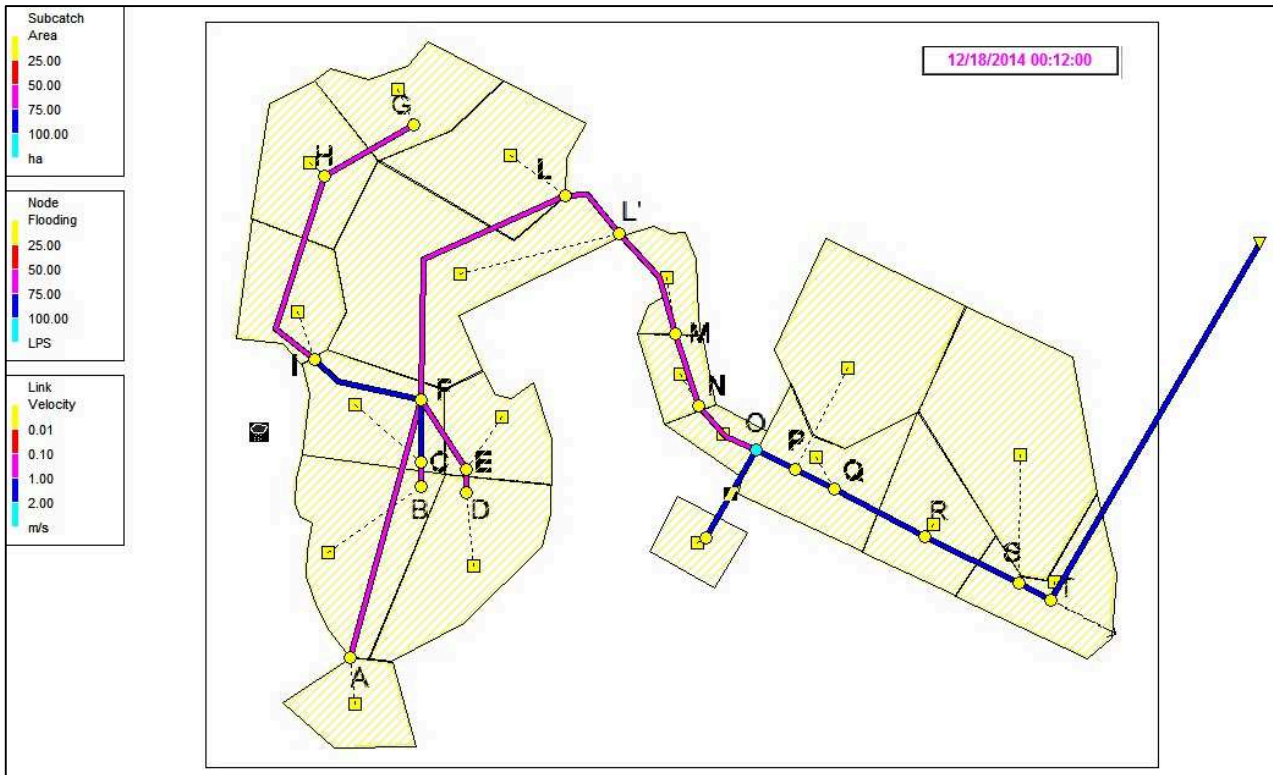


Figure 8.13 Network after 9 minutes of simulation

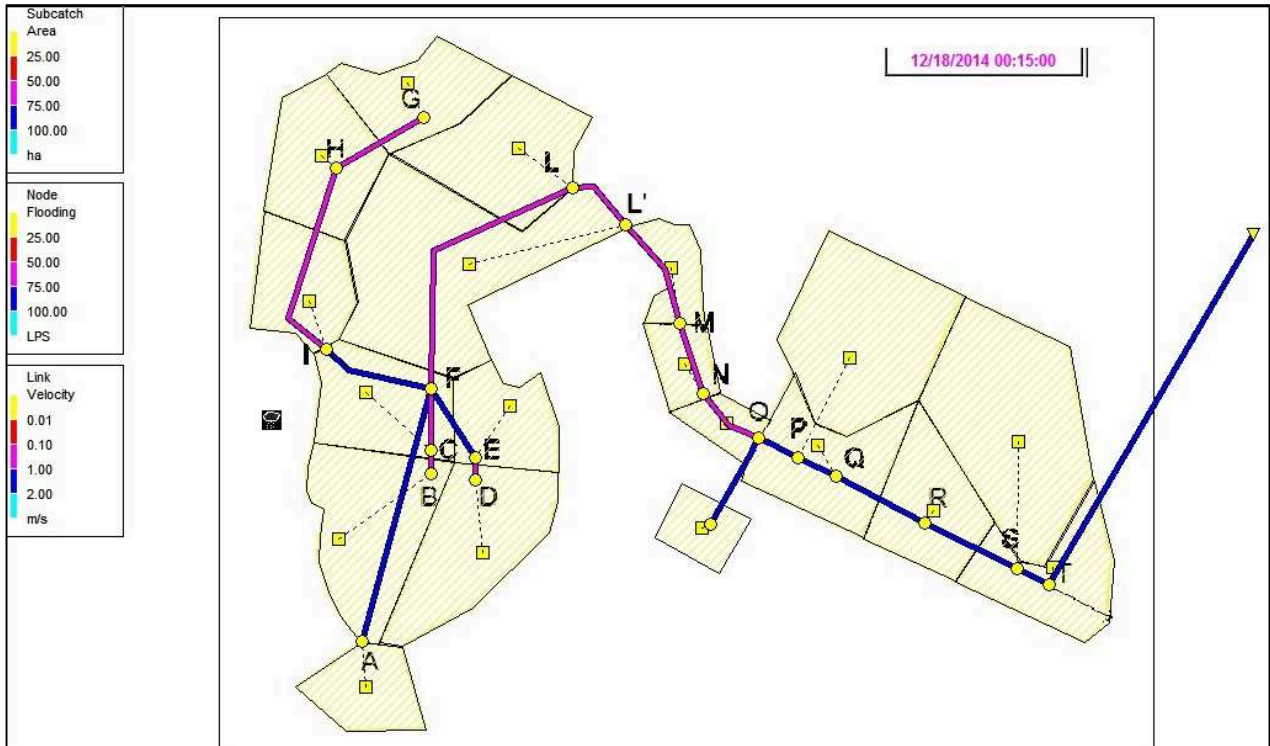


Figure 8.14 Network after 15 minutes of simulation

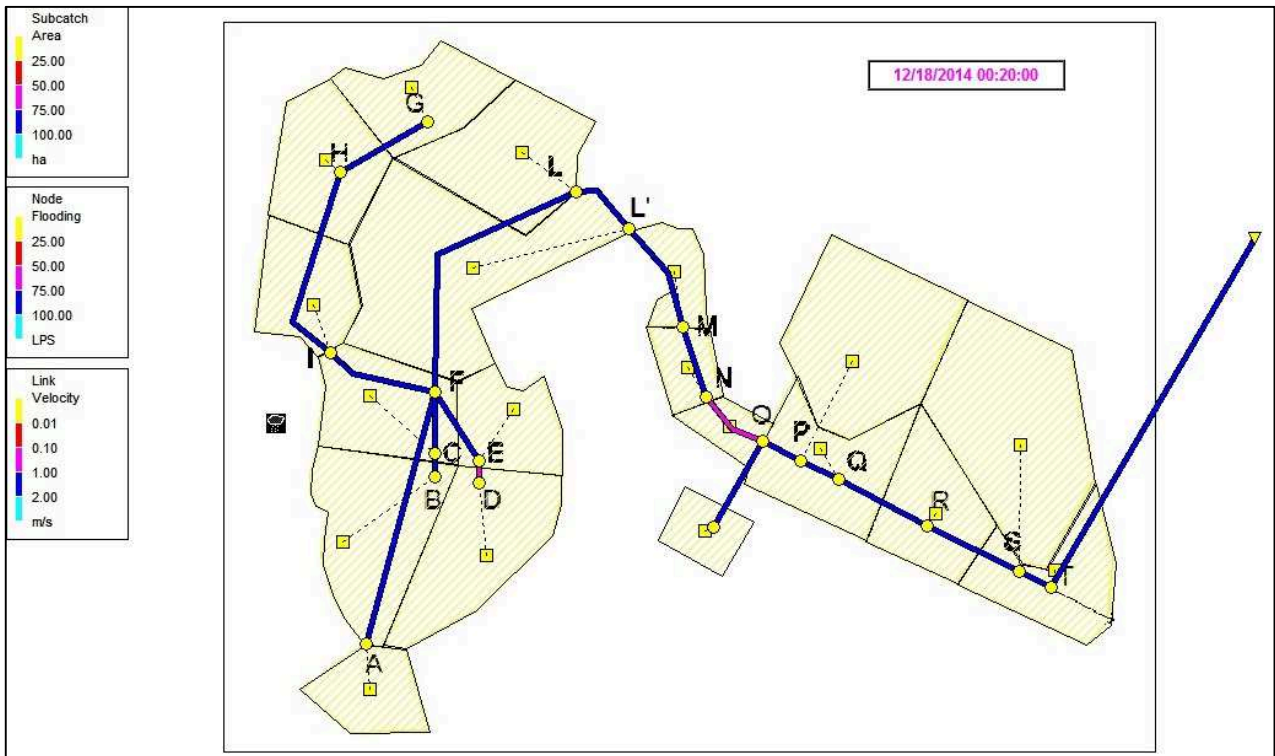


Figure 8.15 Network after 20 minutes of simulation



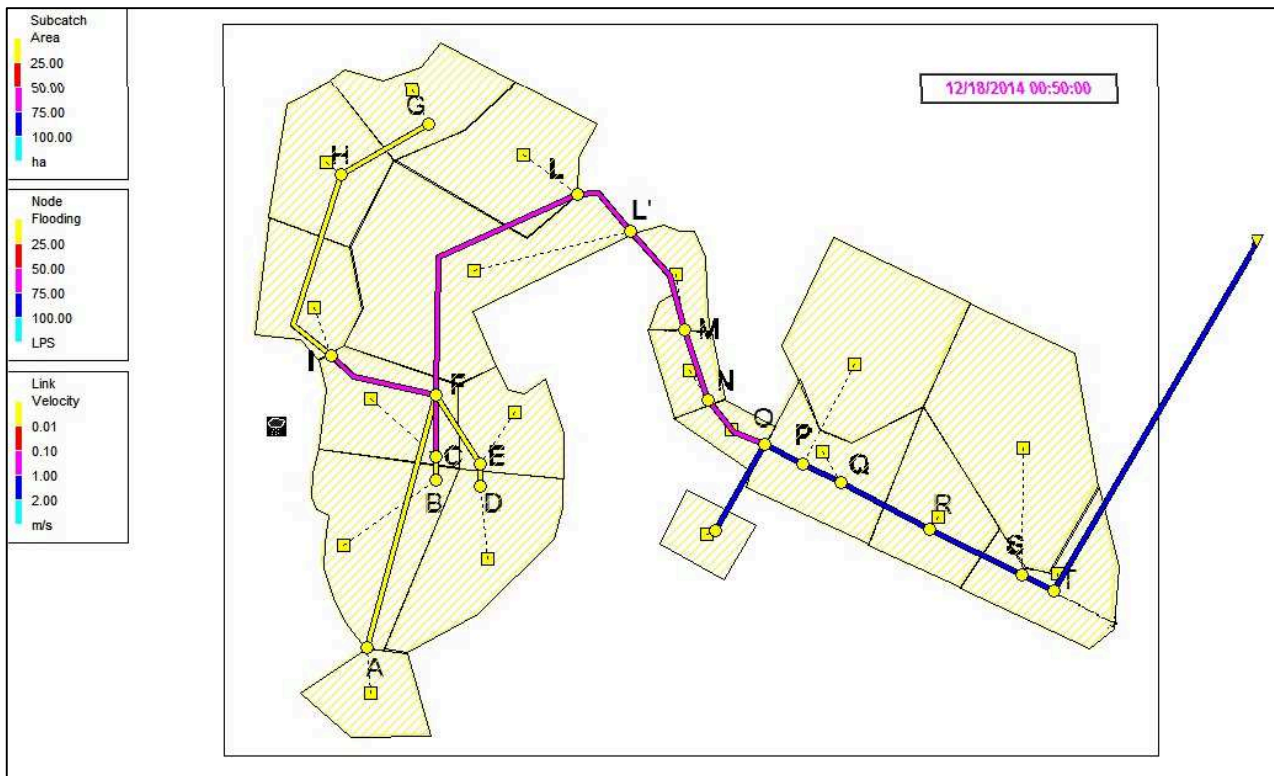


Figure 8.16 Network after 50 minutes of simulation

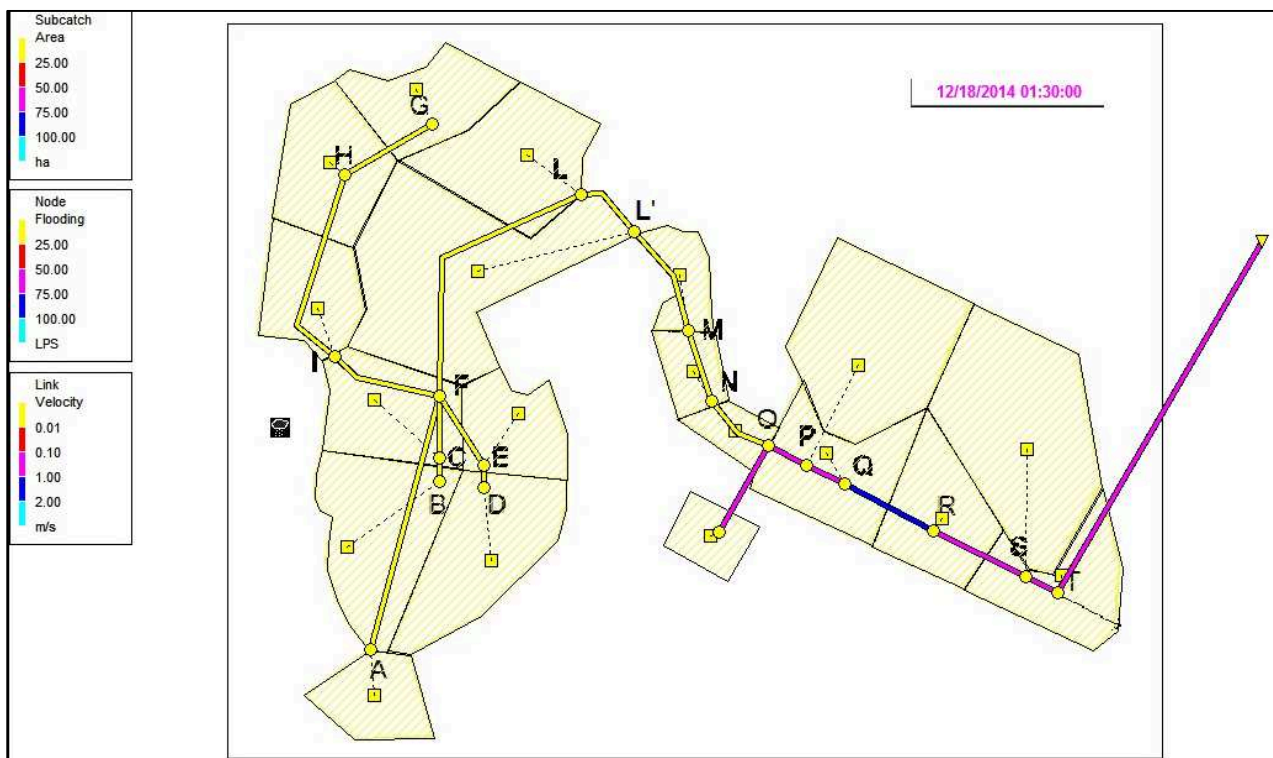


Figure 8.17 Network after 90 minutes of simulation

### 8.7 Return period of 20 years

To analyze the behavior of the network, a return period of 20 years is now considered. Such a return time is considered to analyze the weaknesses of the network, that are the points that are flooded by rain for the first hypothesized.

The SWMM program processes the evolution of the network subjected to flooding.

Table 8.7 Conduit surcharge summary - Tr 20 years

```

*****
Conduit Surcharge Summary
*****
-----
Conduit          ----- Hours Full -----      Hours      Hours
                   Both Ends  Upstream  Dnstream  Above Full  Capacity
                   -----  -----  -----  Above Full  Limited
                   -----  -----  -----  Normal Flow
DE                0.22     0.31     0.23     0.31     0.31
EF                0.01     0.01     0.01     0.01     0.01
HI                0.49     0.52     0.50     0.52     0.52
NO                0.01     0.24     0.01     0.23     0.24
    
```

Table 8.8 Node flooding summary - Tr 20 years

```

*****
Node Flooding Summary
*****

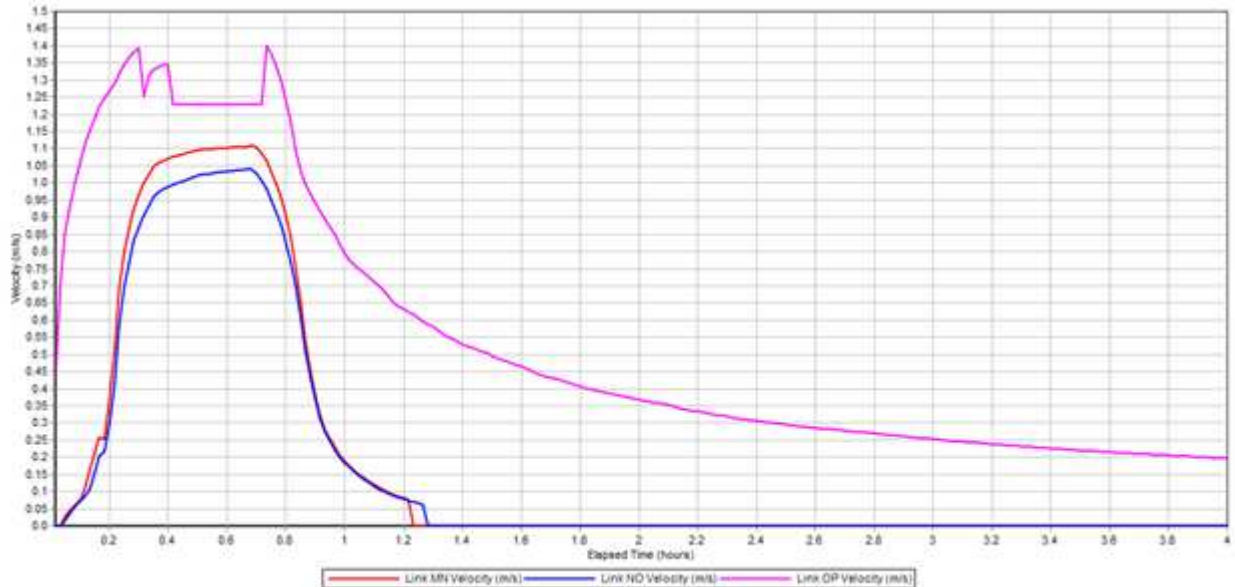
Flooding refers to all water that overflows
a node, whether it ponds or not.
-----
Node          Hours      Maximum
              Flooded    Rate
              -----  LPS
D              0.31     3.02
E              0.01     0.08
H              0.52    13.10
N              0.24    12.14
    
```

Table 8.9 Link flow summary - Tr 20 years

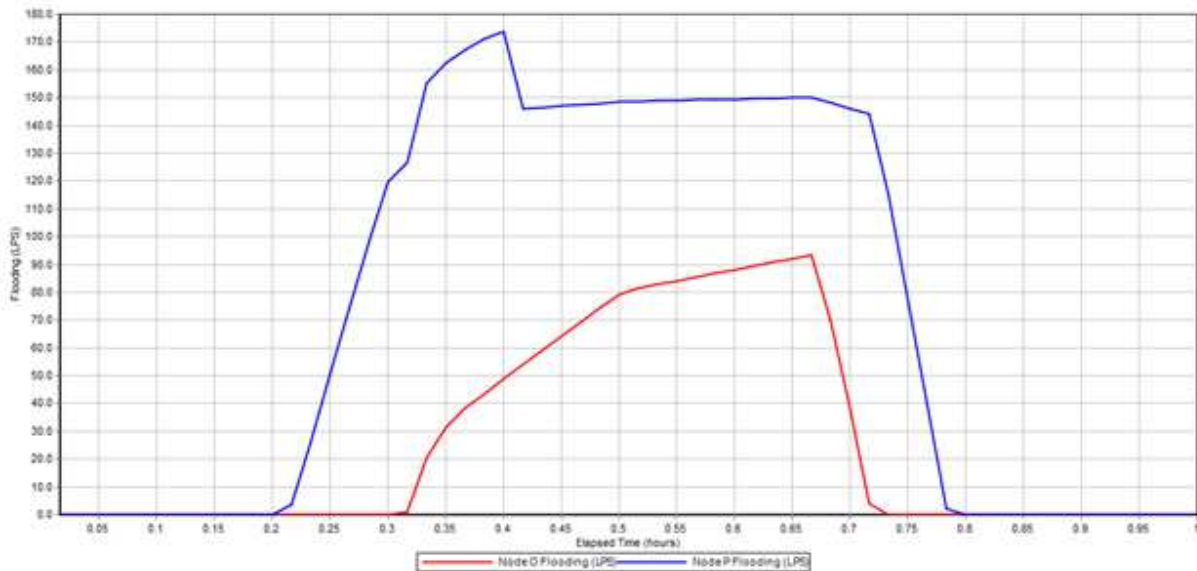
```

*****
Link Flow Summary
*****
-----
Link                                     Type                               Maximum
                                         |Flow|                               LPS
-----
AF                                       CONDUIT                             5.84
BC                                       CONDUIT                             15.50
CF                                       CONDUIT                             25.19
DE                                       CONDUIT                             11.29
EF                                       CONDUIT                             19.67
GH                                       CONDUIT                              9.71
HI                                       CONDUIT                              8.89
IF                                       CONDUIT                             15.99
FL                                       CONDUIT                             65.90
LL'                                       CONDUIT                             78.72
L'M                                       CONDUIT                             103.49
MN                                       CONDUIT                             107.22
NO                                       CONDUIT                             106.93
XO                                       CONDUIT                              6.66
OP                                       CONDUIT                             112.68
PQ                                       CONDUIT                             132.34
QR                                       CONDUIT                             145.88
RS                                       CONDUIT                             155.51
ST                                       CONDUIT                             178.41
OUT                                       CONDUIT                             188.04

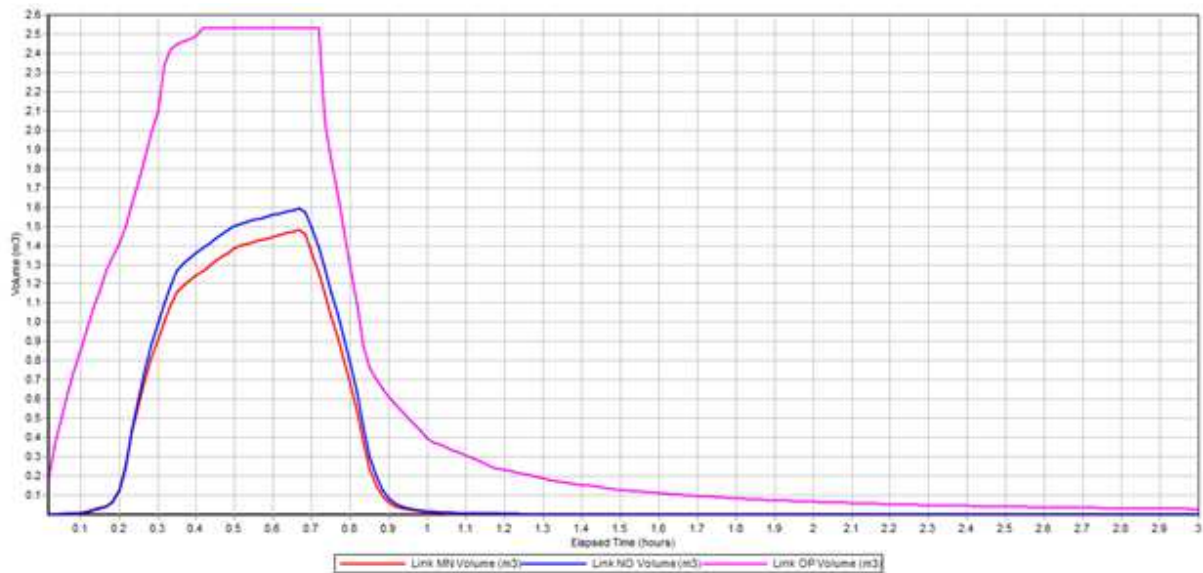
```



Graph 8.12 Velocity (m/s) measured in links MN, NO, OP - Disturbance in link OP



Graph 8.13 Node flooding (l/s) represented in node O and P - Disturbance in link OP



Graph 8.14 Water volume (m3) in links MN, NO, OP.

The area of the museum is an hectar wide and has a runoff coefficient of 0.8 because it is almost completely waterproof, so the link coming from this area is engaged in the network of the gardens of the arena, and creates a strong disturbance in motion, given the huge amount of water flowing through it. The best solution would be to discharge this water elsewhere. Considering a return time of 20 years the initial diameter of the pipes of the network must be widened to avoid flooding, because the diameter in not enough large. Fundamental is to widen pipelines that arimmediately upstream and downstream of the joint of the conduct from the museum: these are the flooding points of the network. The conduit that arrives from the museum, for a return time of 20 years, has a diameter of 0,7 m, it would be a proper solution to divide the area in two parts and discharge the volume of water coming from the museum in two different pipelines, after studying the current network shape.



## 9. Conclusions

After performing the study of this area so small but complex it is clear that many actions are required to protect a good as precious as the Scrovegni Chapel.

The first point of working is the creation of a new drainage network: through quick calculations can be easily defined and sized, and it can solve many flooding problems. In addition to expanding the network it is in a public interest to improve the current existing network, because it is insufficient and badly arranged. The most important hystorical artwork of Padua is flooded by heavy rains, the news is printed in many newspapers and articles coming from international cultural framework, does not deal to rectify the drainage network surrounding the chapel, or at least to make maintenance.

This work has demonstrated, through the use of a proper software, the effectiveness of the calculations made with the rational method to define a urban drainage network, starting from physical data of the area and rainfall time series. The assumptions made in the project have been proved consistent with the actual status of the area, thanks to the limited size of the basin which does not present too many heterogeneous features in its interior and can be easily mathematically modeled.

Various possible situations and methods of intervention have been treated: these acting phases that, overlapped, probably could preserve this weak area in an appropriate way from flood attacks.

After analyzing the problem, in theory and practice through appropriate calculations, it is considered necessary to waterproof the area, as priority intervention, and then to fix the hydraulic network, removing any possible point of flooding from the closed area of the church and installing new tactical drains, secondly it is essential to create a new network.

Once dimensioned, as calculated above, it may be discharged in the lower part of the gardens, as described in the project, or directly, and even better, discharged elsewhere. Unfortunately it was not possible to make assumptions on the extent of discharging municipal network away from the gardens due to a lack of data, which are not present in municipality database or were not provided.



# ANNEX I – Rainfall data

*Annex Table 1 Padova maximum rainfall data obtained from Annali Idrologici.*

<b>YEAR</b>	<b>1 HOUR</b>	<b>3 HOURS</b>	<b>6 HOURS</b>	<b>12 HOURS</b>	<b>24 HOURS</b>
1936	10	20	22	33,4	43,4
1937	25,3	40,8	49,8	70,4	74,4
1938	59	66	67	67	67
1939	23	23	28,6	39,6	41
1940	37	38	39,8	39,8	39,8
1941	23,2	68	90	101	104
1942	15,8	17,8	19,4	20,2	20,2
1943	12	22	24,4	25,6	29
1944	11,7	29,5	47	75	94,1
1946	28	31,2	31,2	43,8	61,2
1947	44	66,4	82	120	134,8
1948	28	30	36	52,8	87
1949	29,6	29,6	39,2	39,2	50,2
1950	24,4	24,6	38	44	57
1951	21,6	41,2	47,8	47,8	54,4
1952	23,8	31,6	49	60	73,6
1953	23,8	43,2	50,2	54,4	60,6
1954	27	29,2	29,6	36,8	37,4
1955	54	68,6	71,2	71,2	71,2
1956	19,8	27	29,2	39,6	68,6
1957	31,4	39,6	39,8	42,2	57,2
1958	56	71,8	75	79,6	82,8
1959	23	32,2	36,4	37,4	50,2
1960	25,6	31	36,2	50,4	52,6
1961	24,6	28,4	36,6	38,6	53,8
1962	12	21,8	29,2	37,8	55,4
1963	38,4	40,2	41,4	44,8	48,6
1964	26,4	27,6	41,2	42,4	42,4
1965	27	35	42,2	48,4	52
1966	22,8	36,5	46,4	60	81,5
1967	35,9	87	112,6	116,2	116,2
1968	30,4	48,8	73,8	77	77,6
1969	46,8	73,4	75,6	76,4	87
1970	32,8	38,8	39	39,2	39,2
1971	35	38	38	38	49
1972	29	43,6	47,6	48,8	48,8
1973	16,6	24	30	40,8	54,8
1985	21,2	21,2	28	45	70
1986	36,2	40,4	44,5	59,8	87,5
1987	37	50	70	86	96,6
1989	41,4	43	62,4	76	97
1990	36,2	36,4	38	65	68
1994	62	77	80,6	80,6	88,8

Annex Table 2 Padova maximum rainfall values calculated from hourly rainfall data revealed by Botanic Garden station.

<b>YEAR</b>	<b>1 HOUR</b>	<b>3 HOURS</b>	<b>6 HOURS</b>	<b>12 HOURS</b>
1993	23,4	24,4	24,4	26,6
1994	51,6	70,8	70,8	82,2
1995	31,6	39,2	39,4	40,8
1996	21,4	27,2	37,6	51,4
1997	22	22,8	22,8	33,8
1998	20	27,2	46	53,4
1999	17	18	21	33,2
2000	34	36,4	36,4	39,2
2001	26,6	39,2	48,2	59,2
2002	31,8	49,6	49,8	60,4
2003	15,4	23,2	26,4	31,6
2004	29,4	44,8	45,4	50,4
2005	35,6	35,6	70,2	71,2
2006	45,2	56,4	60,8	103,2
2007	35	35,4	35,4	42,4
2008	33,2	35,6	38,8	50,8
2009	35	63,2	92,4	134,6
2010	52,8	63,2	63,2	63,2
2011	28,4	39,4	39,4	42,8
2012	23,2	34,6	41	42,2
2013	34,8	38,8	44	44
2014	19,8	24	32,8	53

Annex Table 3 Combined rainfall data

<b>YEAR</b>	<b>1 HOUR</b>	<b>3 HOURS</b>	<b>6 HOURS</b>	<b>12 HOURS</b>	<b>24 HOURS</b>
1936	10	20	22	33,4	43,4
1937	25,3	40,8	49,8	70,4	74,4
1938	59	66	67	67	67
1939	23	23	28,6	39,6	41
1940	37	38	39,8	39,8	39,8
1941	23,2	68	90	101	104
1942	15,8	17,8	19,4	20,2	20,2
1943	12	22	24,4	25,6	29
1944	11,7	29,5	47	75	94,1
1946	28	31,2	31,2	43,8	61,2
1947	44	66,4	82	120	134,8
1948	28	30	36	52,8	87
1949	29,6	29,6	39,2	39,2	50,2
1950	24,4	24,6	38	44	57
1951	21,6	41,2	47,8	47,8	54,4
1952	23,8	31,6	49	60	73,6
1953	23,8	43,2	50,2	54,4	60,6
1954	27	29,2	29,6	36,8	37,4
1955	54	68,6	71,2	71,2	71,2
1956	19,8	27	29,2	39,6	68,6
1957	31,4	39,6	39,8	42,2	57,2
1958	56	71,8	75	79,6	82,8
1959	23	32,2	36,4	37,4	50,2
1960	25,6	31	36,2	50,4	52,6
1961	24,6	28,4	36,6	38,6	53,8
1962	12	21,8	29,2	37,8	55,4
1963	38,4	40,2	41,4	44,8	48,6
1964	26,4	27,6	41,2	42,4	42,4
1965	27	35	42,2	48,4	52
1966	22,8	36,5	46,4	60	81,5
1967	35,9	87	112,6	116,2	116,2
1968	30,4	48,8	73,8	77	77,6
1969	46,8	73,4	75,6	76,4	87
1970	32,8	38,8	39	39,2	39,2
1971	35	38	38	38	49
1972	29	43,6	47,6	48,8	48,8
1973	16,6	24	30	40,8	54,8
1985	21,2	21,2	28	45	70
1986	36,2	40,4	44,5	59,8	87,5
1987	37	50	70	86	96,6
1989	41,4	43	62,4	76	97

<b>YEAR</b>	<b>1 HOUR</b>	<b>3 HOURS</b>	<b>6 HOURS</b>	<b>12 HOURS</b>	<b>24 HOURS</b>
1990	36,2	36,4	38	65	68
1994	62	77	80,6	80,6	88,8
1993	23,4	24,4	24,4	26,6	34,80
1995	31,6	39,2	39,4	40,8	74,80
1996	21,4	27,2	37,6	51,4	81,40
1997	22	22,8	22,8	33,8	38,00
1998	20	27,2	46	53,4	60,20
1999	17	18	21	33,2	49,20
2000	34	36,4	36,4	39,2	42,40
2001	26,6	39,2	48,2	59,2	61,60
2002	31,8	49,6	49,8	60,4	60,40
2003	15,4	23,2	26,4	31,6	51,20
2004	29,4	44,8	45,4	50,4	55,40
2005	35,6	35,6	70,2	71,2	96,00
2006	45,2	56,4	60,8	103,2	98,60
2007	35	35,4	35,4	42,4	58,60
2008	33,2	35,6	38,8	50,8	77,80
2009	35	63,2	92,4	134,6	158,20
2010	52,8	63,2	63,2	63,2	63,40
2011	28,4	39,4	39,4	42,8	61,40
2012	23,2	34,6	41	42,2	60,40
2013	34,8	38,8	44	44	51,40
2014	19,8	24	32,8	53	53,40

# ANNEX II - Rainfall data analysis

Annex 2 Table 1 Whole representation of depth-duration for 1 hour rainfall

<b>i</b>	<b>hi</b>	<b>Fhi</b>	<b>yi</b>	<b>i</b>	<b>hi</b>	<b>Fhi</b>	<b>yi</b>
<b>1</b>	10	0,014	-1,45	<b>36</b>	28	0,507	0,39
<b>2</b>	11,7	0,028	-1,27	<b>37</b>	28,4	0,521	0,43
<b>3</b>	12	0,042	-1,15	<b>38</b>	29	0,535	0,47
<b>4</b>	12	0,056	-1,06	<b>39</b>	29,4	0,549	0,51
<b>5</b>	15,4	0,070	-0,98	<b>40</b>	29,6	0,563	0,56
<b>6</b>	15,8	0,085	-0,90	<b>41</b>	29,6	0,577	0,60
<b>7</b>	16,6	0,099	-0,84	<b>42</b>	30,4	0,592	0,64
<b>8</b>	17	0,113	-0,78	<b>43</b>	31,4	0,606	0,69
<b>9</b>	19,8	0,127	-0,73	<b>44</b>	31,6	0,620	0,74
<b>10</b>	19,8	0,141	-0,67	<b>45</b>	31,8	0,634	0,79
<b>11</b>	20	0,155	-0,62	<b>46</b>	32,6	0,648	0,83
<b>12</b>	20,2	0,169	-0,58	<b>47</b>	32,8	0,662	0,89
<b>13</b>	21,2	0,183	-0,53	<b>48</b>	33,2	0,676	0,94
<b>14</b>	21,4	0,197	-0,48	<b>49</b>	33,8	0,690	0,99
<b>15</b>	21,4	0,211	-0,44	<b>50</b>	34	0,704	1,05
<b>16</b>	21,6	0,225	-0,40	<b>51</b>	34,8	0,718	1,11
<b>17</b>	22	0,239	-0,36	<b>52</b>	35	0,732	1,17
<b>18</b>	22	0,254	-0,32	<b>53</b>	35	0,746	1,23
<b>19</b>	22,8	0,268	-0,28	<b>54</b>	35	0,761	1,30
<b>20</b>	23	0,282	-0,24	<b>55</b>	35,6	0,775	1,37
<b>21</b>	23	0,296	-0,20	<b>56</b>	35,9	0,789	1,44
<b>22</b>	23,2	0,310	-0,16	<b>57</b>	36,2	0,803	1,52
<b>23</b>	23,2	0,324	-0,12	<b>58</b>	36,2	0,817	1,60
<b>24</b>	23,4	0,338	-0,08	<b>59</b>	37	0,831	1,69
<b>25</b>	23,8	0,352	-0,04	<b>60</b>	37	0,845	1,78
<b>26</b>	23,8	0,366	0,00	<b>61</b>	38,4	0,859	1,89
<b>27</b>	24,4	0,380	0,03	<b>62</b>	41,4	0,873	2,00
<b>28</b>	24,6	0,394	0,07	<b>63</b>	44	0,887	2,12
<b>29</b>	25,3	0,408	0,11	<b>64</b>	45,2	0,901	2,27
<b>30</b>	25,6	0,423	0,15	<b>65</b>	46,8	0,915	2,43
<b>31</b>	26,4	0,437	0,19	<b>66</b>	52,8	0,930	2,62
<b>32</b>	26,6	0,451	0,23	<b>67</b>	54	0,944	2,85
<b>33</b>	27	0,465	0,27	<b>68</b>	56	0,958	3,14
<b>34</b>	27	0,479	0,31	<b>69</b>	59	0,972	3,56
<b>35</b>	28	0,493	0,35	<b>70</b>	62	0,986	4,26

Annex 2 Table 2 Three hours precipitation analysis

<b>i</b>	<b>hi</b>	<b>Fhi</b>	<b>yi</b>	<b>i</b>	<b>hi</b>	<b>Fhi</b>	<b>yi</b>
<b>1</b>	17,8	0,01	-1,45	<b>36</b>	35,6	0,51	0,39
<b>2</b>	18	0,03	-1,27	<b>37</b>	36,4	0,52	0,43
<b>3</b>	20	0,04	-1,15	<b>38</b>	36,4	0,54	0,47
<b>4</b>	21,2	0,06	-1,06	<b>39</b>	36,5	0,55	0,51
<b>5</b>	21,8	0,07	-0,98	<b>40</b>	38	0,56	0,56
<b>6</b>	22	0,08	-0,90	<b>41</b>	38	0,58	0,60
<b>7</b>	22,4	0,10	-0,84	<b>42</b>	38,8	0,59	0,64
<b>8</b>	22,8	0,11	-0,78	<b>43</b>	38,8	0,61	0,69
<b>9</b>	23	0,13	-0,73	<b>44</b>	39	0,62	0,74
<b>10</b>	23,2	0,14	-0,67	<b>45</b>	39,2	0,63	0,79
<b>11</b>	24	0,15	-0,62	<b>46</b>	39,2	0,65	0,83
<b>12</b>	24	0,17	-0,58	<b>47</b>	39,4	0,66	0,89
<b>13</b>	24,4	0,18	-0,53	<b>48</b>	39,6	0,68	0,94
<b>14</b>	24,6	0,20	-0,48	<b>49</b>	40,2	0,69	0,99
<b>15</b>	24,8	0,21	-0,44	<b>50</b>	40,4	0,70	1,05
<b>16</b>	27	0,23	-0,40	<b>51</b>	40,8	0,72	1,11
<b>17</b>	27,2	0,24	-0,36	<b>52</b>	41,2	0,73	1,17
<b>18</b>	27,2	0,25	-0,32	<b>53</b>	43	0,75	1,23
<b>19</b>	27,6	0,27	-0,28	<b>54</b>	43,2	0,76	1,30
<b>20</b>	28,4	0,28	-0,24	<b>55</b>	43,6	0,77	1,37
<b>21</b>	29,2	0,30	-0,20	<b>56</b>	44,8	0,79	1,44
<b>22</b>	29,5	0,31	-0,16	<b>57</b>	48,8	0,80	1,52
<b>23</b>	29,6	0,32	-0,12	<b>58</b>	49,6	0,82	1,60
<b>24</b>	30	0,34	-0,08	<b>59</b>	50	0,83	1,69
<b>25</b>	31	0,35	-0,04	<b>60</b>	56,4	0,85	1,78
<b>26</b>	31,2	0,37	0,00	<b>61</b>	63,2	0,86	1,89
<b>27</b>	31,6	0,38	0,03	<b>62</b>	63,2	0,87	2,00
<b>28</b>	32	0,39	0,07	<b>63</b>	66	0,89	2,12
<b>29</b>	32,2	0,41	0,11	<b>64</b>	66,4	0,90	2,27
<b>30</b>	34	0,42	0,15	<b>65</b>	68	0,92	2,43
<b>31</b>	34,6	0,44	0,19	<b>66</b>	68,6	0,93	2,62
<b>32</b>	35	0,45	0,23	<b>67</b>	71,8	0,94	2,85
<b>33</b>	35,4	0,46	0,27	<b>68</b>	73,4	0,96	3,14
<b>34</b>	35,4	0,48	0,31	<b>69</b>	77	0,97	3,56
<b>35</b>	35,6	0,49	0,35	<b>70</b>	87	0,99	4,26



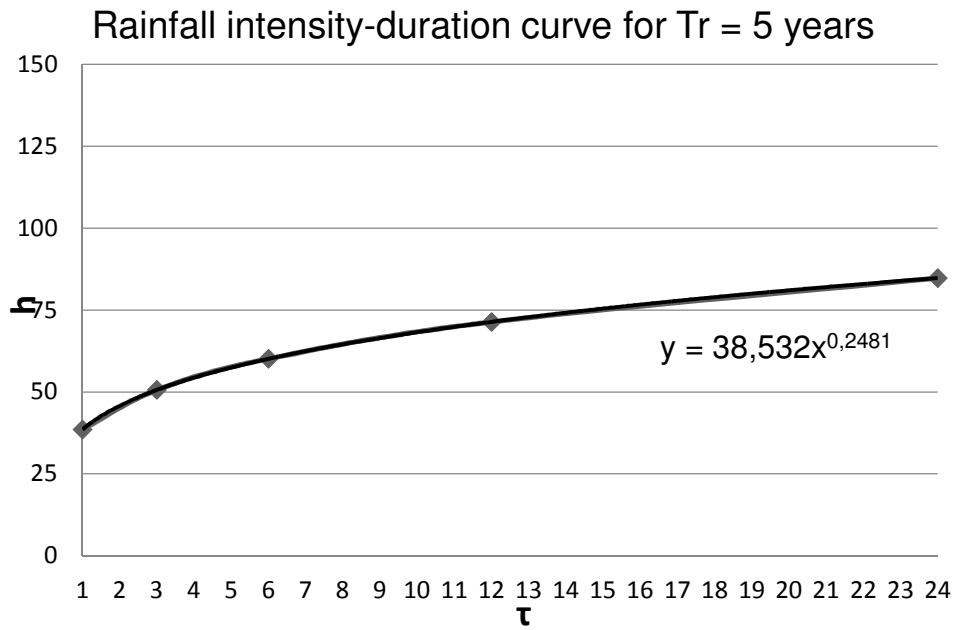
Annex 2 Table 3 Six hours rainfall data analysis

<b>i</b>	<b>hi</b>	<b>Fhi</b>	<b>yi</b>	<b>i</b>	<b>hi</b>	<b>Fhi</b>	<b>yi</b>
<b>1</b>	19,4	0,01	-1,45	<b>36</b>	39,8	0,51	0,39
<b>2</b>	21	0,03	-1,27	<b>37</b>	39,8	0,52	0,43
<b>3</b>	22	0,04	-1,15	<b>38</b>	41	0,54	0,47
<b>4</b>	22,8	0,06	-1,06	<b>39</b>	41,2	0,55	0,51
<b>5</b>	24,4	0,07	-0,98	<b>40</b>	41,4	0,56	0,56
<b>6</b>	24,4	0,08	-0,90	<b>41</b>	42,2	0,58	0,60
<b>7</b>	26,4	0,10	-0,84	<b>42</b>	43,6	0,59	0,64
<b>8</b>	26,4	0,11	-0,78	<b>43</b>	44	0,61	0,69
<b>9</b>	28	0,13	-0,73	<b>44</b>	44,5	0,62	0,74
<b>10</b>	28,6	0,14	-0,67	<b>45</b>	45,4	0,63	0,79
<b>11</b>	29,2	0,15	-0,62	<b>46</b>	46	0,65	0,83
<b>12</b>	29,2	0,17	-0,58	<b>47</b>	46,4	0,66	0,89
<b>13</b>	29,6	0,18	-0,53	<b>48</b>	47	0,68	0,94
<b>14</b>	30	0,20	-0,48	<b>49</b>	47,6	0,69	0,99
<b>15</b>	31,2	0,21	-0,44	<b>50</b>	47,8	0,70	1,05
<b>16</b>	32	0,23	-0,40	<b>51</b>	48,2	0,72	1,11
<b>17</b>	32,8	0,24	-0,36	<b>52</b>	49	0,73	1,17
<b>18</b>	34,8	0,25	-0,32	<b>53</b>	49,8	0,75	1,23
<b>19</b>	35,4	0,27	-0,28	<b>54</b>	49,8	0,76	1,30
<b>20</b>	36	0,28	-0,24	<b>55</b>	50,2	0,77	1,37
<b>21</b>	36,2	0,30	-0,20	<b>56</b>	60,8	0,79	1,44
<b>22</b>	36,4	0,31	-0,16	<b>57</b>	62,4	0,80	1,52
<b>23</b>	36,4	0,32	-0,12	<b>58</b>	63,2	0,82	1,60
<b>24</b>	36,6	0,34	-0,08	<b>59</b>	67	0,83	1,69
<b>25</b>	37,4	0,35	-0,04	<b>60</b>	70	0,85	1,78
<b>26</b>	37,6	0,37	0,00	<b>61</b>	70,2	0,86	1,89
<b>27</b>	38	0,38	0,03	<b>62</b>	71,2	0,87	2,00
<b>28</b>	38	0,39	0,07	<b>63</b>	73,8	0,89	2,12
<b>29</b>	38	0,41	0,11	<b>64</b>	75	0,90	2,27
<b>30</b>	38,8	0,42	0,15	<b>65</b>	75,6	0,92	2,43
<b>31</b>	39	0,44	0,19	<b>66</b>	80,6	0,93	2,62
<b>32</b>	39	0,45	0,23	<b>67</b>	82	0,94	2,85
<b>33</b>	39,2	0,46	0,27	<b>68</b>	90	0,96	3,14
<b>34</b>	39,4	0,48	0,31	<b>69</b>	92,4	0,97	3,56
<b>35</b>	39,4	0,49	0,35	<b>70</b>	112,6	0,99	4,26

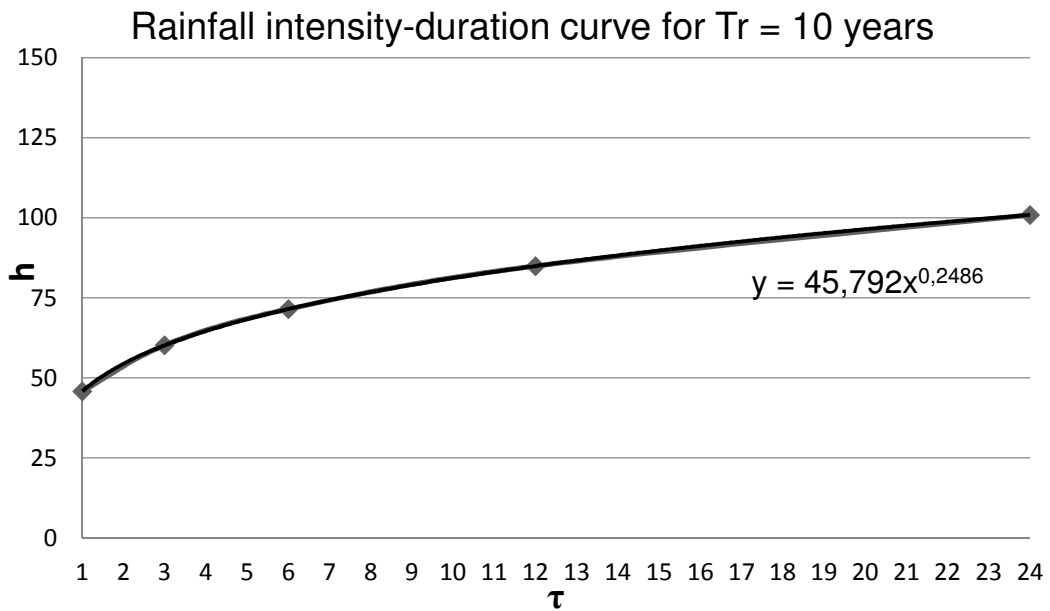
Annex 2 Table 4 12 hours rainfall analysis

<b>i</b>	<b>hi</b>	<b>Fhi</b>	<b>yi</b>	<b>i</b>	<b>hi</b>	<b>Fhi</b>	<b>yi</b>
<b>1</b>	20,2	0,01	-1,45	<b>36</b>	47,8	0,51	0,39
<b>2</b>	25,6	0,03	-1,27	<b>37</b>	48,4	0,52	0,43
<b>3</b>	26,6	0,04	-1,15	<b>38</b>	48,8	0,54	0,47
<b>4</b>	31,6	0,06	-1,06	<b>39</b>	49,6	0,55	0,51
<b>5</b>	33,2	0,07	-0,98	<b>40</b>	50,4	0,56	0,56
<b>6</b>	33,4	0,08	-0,90	<b>41</b>	50,4	0,58	0,60
<b>7</b>	33,8	0,10	-0,84	<b>42</b>	50,8	0,59	0,64
<b>8</b>	35,5	0,11	-0,78	<b>43</b>	51,4	0,61	0,69
<b>9</b>	36,8	0,13	-0,73	<b>44</b>	52,8	0,62	0,74
<b>10</b>	37,4	0,14	-0,67	<b>45</b>	53	0,63	0,79
<b>11</b>	37,4	0,15	-0,62	<b>46</b>	53,4	0,65	0,83
<b>12</b>	37,8	0,17	-0,58	<b>47</b>	54,4	0,66	0,89
<b>13</b>	38	0,18	-0,53	<b>48</b>	59,2	0,68	0,94
<b>14</b>	38,6	0,20	-0,48	<b>49</b>	59,8	0,69	0,99
<b>15</b>	39	0,21	-0,44	<b>50</b>	60	0,70	1,05
<b>16</b>	39,2	0,23	-0,40	<b>51</b>	60	0,72	1,11
<b>17</b>	39,2	0,24	-0,36	<b>52</b>	60,4	0,73	1,17
<b>18</b>	39,2	0,25	-0,32	<b>53</b>	63,2	0,75	1,23
<b>19</b>	39,6	0,27	-0,28	<b>54</b>	65	0,76	1,30
<b>20</b>	39,6	0,28	-0,24	<b>55</b>	67	0,77	1,37
<b>21</b>	39,8	0,30	-0,20	<b>56</b>	70,4	0,79	1,44
<b>22</b>	40,8	0,31	-0,16	<b>57</b>	71,2	0,80	1,52
<b>23</b>	40,8	0,32	-0,12	<b>58</b>	71,2	0,82	1,60
<b>24</b>	42,2	0,34	-0,08	<b>59</b>	75	0,83	1,69
<b>25</b>	42,2	0,35	-0,04	<b>60</b>	76	0,85	1,78
<b>26</b>	42,4	0,37	0,00	<b>61</b>	76,4	0,86	1,89
<b>27</b>	42,4	0,38	0,03	<b>62</b>	77	0,87	2,00
<b>28</b>	42,8	0,39	0,07	<b>63</b>	79,6	0,89	2,12
<b>29</b>	43,2	0,41	0,11	<b>64</b>	80,6	0,90	2,27
<b>30</b>	43,8	0,42	0,15	<b>65</b>	86	0,92	2,43
<b>31</b>	44	0,44	0,19	<b>66</b>	101	0,93	2,62
<b>32</b>	44	0,45	0,23	<b>67</b>	103,2	0,94	2,85
<b>33</b>	44	0,46	0,27	<b>68</b>	116,2	0,96	3,14
<b>34</b>	44,8	0,48	0,31	<b>69</b>	120	0,97	3,56
<b>35</b>	45	0,49	0,35	<b>70</b>	134,6	0,99	4,26

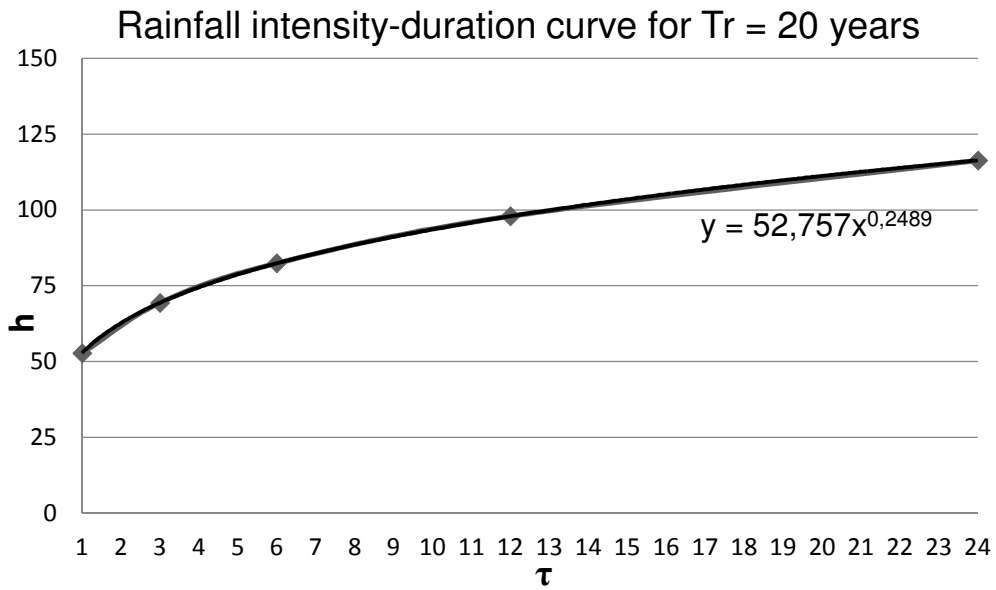
# ANNEX III - Rainfall-intensity curves



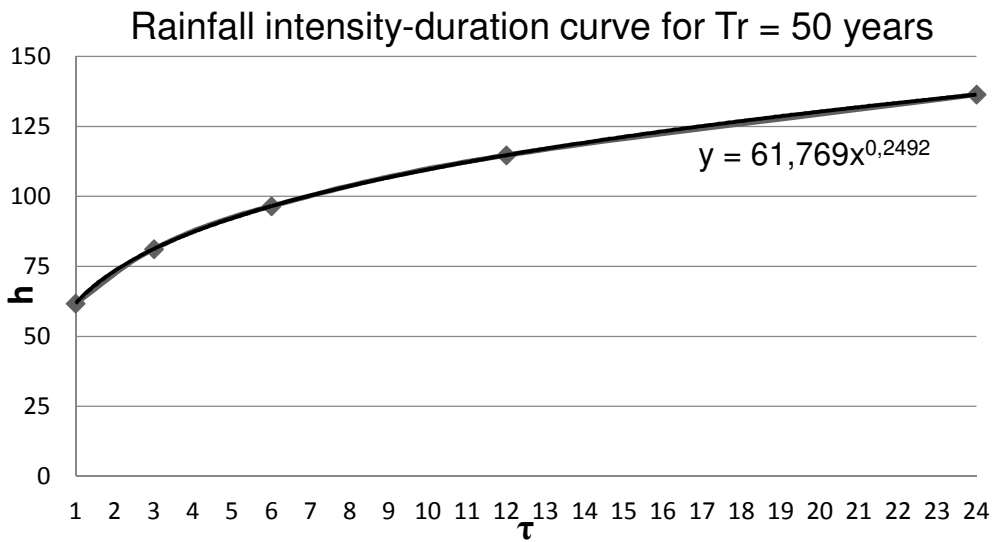
Annex III Graph 1 A.  $T_r$  5 years – Rainfall-intensity curve representation



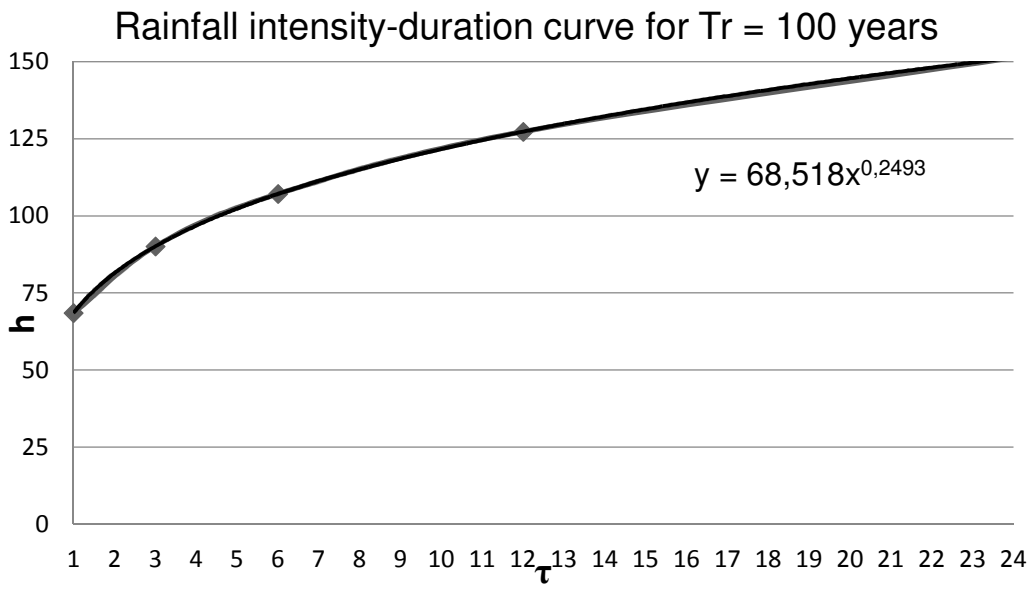
Annex III Graph 2 A.  $T_r$  10 years – Rainfall-intensity curve representation



Annex III Graph 3 A. Tr 20 years – Rainfall-intensity curve representation



Annex III Graph 4 A. Tr 50 years – Rainfall-intensity curve representation



Annex III Graph 5 A. Tr 100 years – Rainfall-intensity curve representation

# ANNEX IV - Pearson test

Pi	yi	hi	Ni
0,17	-0,58	18,95	8
0,33	-0,09	23,48	13
0,50	0,37	27,74	10
0,67	0,90	32,70	10
0,83	1,70	40,10	13
1		62,00	10

Table 0.1 Pearson test application for 1 hour rainfall

$\chi^2 = 0,89 <$  theoretical value equal to 5,99.

Pi	yi	hi	Ni
0,17	-0,58	23,69	9
0,33	-0,09	30,08	13
0,50	0,37	36,10	9
0,67	0,90	43,11	16
0,83	1,70	53,55	6
1		62,00	12

Table 0.2 Pearson test application for 3 hours rainfall

$\chi^2 = 4,44 <$  theoretical value equal to 5,99.

Pi	yi	hi	Ni
0,17	-0,58	27,52	8
0,33	-0,09	35,25	8
0,50	0,37	42,52	14
0,67	0,90	50,99	13
0,83	1,70	63,61	9
1		112,00	13

Table 0.3 Pearson test application for 6 hours rainfall

$\chi^2 = 2,79 <$  theoretical value equal to 5,99.



Pi	yi	hi	Ni
0,17	-0,58	32,69	4
0,33	-0,09	41,90	16
0,50	0,37	50,57	15
0,67	0,90	60,67	11
0,83	1,70	75,72	6
1		62,00	13

*Table 0.4 Pearson test application for 12 hours rainfall*

$\chi^2 = 4,44 < \text{theoretical value equal to } 5,99.$

# Bibliography

Berne, A., Delrieu G., Creutin J. D., Obled C. (2004), *Temporal and spatial resolution of rainfall measurements required for urban hydrology*, J. Hydrol.

Camporese M., Crestani E., Salandin P. (2012), *Assessment of local hydraulic parameters by Enkf data assimilation in real aquifers: a case study in downtown Padova (Italy)*, Università degli Studi di Padova.

D'Alpaos L., P. Salandin e P. Simonini (2011), *Studio finalizzato alla definizione degli scenari di carattere idraulico e geotecnico relativi alla realizzazione del nuovo auditorium di Padova*. Dipartimento di Ingegneria Idraulica, Marittima, Geotecnica e Ambientale (IMAGE)

Da Deppo L., Datei C. (2004), *Fognature*, Quarta Edizione. Ed. Libreria Internazionale Cortina Padova.

Da Deppo L., Datei C., Salandin P. (2010), *Sistemazione dei corsi d'acqua*, Ed. Libreria Internazionale Cortina.

Dal Maso, A. (2006), *La serie secolare di precipitazione a Padova: caratteri statistici principali e loro variazioni*, Tesi di Laurea, Università degli studi di Padova, Facoltà di Ingegneria.

Illiceto V. (2002), *Studio del sottosuolo della Cappella degli Scrovegni*, Rapporto Tecnico. Comune di Padova – Settore Edilizia Monumentale

Larry W. Mays (2001), *Stormwater collection systems design handbook*, McGraw-Hill.

Marani, M. (2003), *Processi e modelli dell'idrometeorologia*, Dipartimento IMAGE, Università di Padova.

U.S. EPA (1992), *Storm Water Management Model. User's Guide*, Athens, Georgia.

## Web sites:

<http://hydrology.usu.edu/taudem/taudem5/downloads.html>

[http://unica2.unica.it/rdeidda//studenti/Idrologia\\_A4/Cap\\_08\\_Modelli\\_Afflussi-Deflussi.pdf](http://unica2.unica.it/rdeidda//studenti/Idrologia_A4/Cap_08_Modelli_Afflussi-Deflussi.pdf)

<http://www.itl.nist.gov/div898/handbook/eda/section3/eda359.htm>

[http://www.mapwindow.org/apps/wiki/lib/exe/fetch.php?media=mapwindow\\_watershed.pdf](http://www.mapwindow.org/apps/wiki/lib/exe/fetch.php?media=mapwindow_watershed.pdf)

[http://www.padovanet.it/allegati/C\\_1\\_Allegati\\_13450\\_Allegato.pdf](http://www.padovanet.it/allegati/C_1_Allegati_13450_Allegato.pdf)